THE ROLE OF Xrel3 IN EARLY DEVELOPMENT OF Xenopus laevis

OLGA SKHIRTLADZE

The role of *Xrel3* in early development of *Xenopus laevis*.

Olga Skhirtladze B.Sc.

A thesis submitted to the School of Graduate
Studies for the partial fulfillment of the
Requirements for the degree of
Masters of Science

Faculty of Medicine
Memorial University of Newfoundland
2004

St. John's Newfoundland and Labrador

Abstract

A novel *Xenopus* gene called *Xrel3* has been recently described, which encodes a member of the Rel/NF-κB family of transcriptional activators (Yang *et al.,* 1998; Lake *et al.,* 2001). *Xrel3* mRNA is expressed during early cleavage stages, followed by a dramatic decline to undetectable levels at gastrulation. Later in development, messages localize to the prospective forebrain, dorsal mid-hindbrain, notochord, and otocyst. Overexpression of *Xrel3* by microinjecting synthetic RNA into two-cell stage embryo in the animal pole region causes embryos to develop abnormal growths, or tumours (Yang *et al.,* 1998). Ectopic expression of *Xrel3* seems to have a major effect on pre-gastrula development. Overexpressed in the dorsal region of the embryo it caused a reduction in dorsoanterior structures in embryos, with a majority of embryos having small heads, kinked backs and shortened tails. Most of them failed to initiate gastrulation movements, as compared to controls. When animal caps from embryos injected with *Xrel3* were treated with XTC-CM, *Xrel3* reduces activin-induced elongation of animal caps. *Xrel3*, however, does not reduce FGF-mediated induction of animal caps, or the expression of *Xbra* in FGF-treated embryos. The results presented here show that *Xrel3* inhibits mesoderm induction, but not by interfering with bFGF pathway, but by regulating activin A signalling.

Acknowledgements

This project would not be successfully completed without the help and assistance of faculty and staff of the Terry Fox labs, that guided me through it all with their advice and providing a nice laboratory atmosphere.

I would like to thank my supervisor Dr. Ken Kao for giving me the opportunity to work and his help and supervision, for always being there for me with his advice. His patience and support were priceless.

Special thanks to Blue Lake and Rebecca Ford for taking me under their wing, showing me around the lab, teaching me all the required techniques in molecular and developmental biology, and also providing a fun environment to work.

Finally, my love and appreciation to my parents and my brother for their support and understanding during my long educational journey.

Table of Contents

List of Figures

List of Tables

List of abbreviations

α	- alpha
AREs	- activin response elements
APS	- ammonium persulfate
ATP	- adenosine triphosphate
β	- beta
BMP	- bone morphogenetic protein
BMP-2	- bone morphogenetic protein-2
BMP-4	- bone morphogenetic protein-4
Bra	- Brachyury
bp	- base pair
BSA	- bovine serum albumin
bFGF	- basic fibroblast growth factor
Ca^{2+}	- calcium
cDNA	- complementary DNA
cm	- centimetre
DNA	- deoxyribonucleic acid
dH_2O	- distilled water
DEPC-water	- diethyl prycarbonate treated water
DNTPs	- deoxyribonucleotide triphosphates
DTT	- dithiothreitol (Cleland's reagent)
EDTA	- ethylenediamine tetraacetic acid

EF-1α	- elongation Factor-1α
eFGF	- embryonic fibroblast growth factors
FAST-1	- forkhead activin signal transducer-1
FGFRs	- fibroblast growth factor receptors
FGFs	- fibroblast growth factors
g	- gram
G1	- Gap 1 phase of the cell cycle
G2	- Gap 2 phase of the cell cycle
Gli	- glioma
Gli 1	- glioma 1
HCl	- hydrochloric acid
HCG	- human chorinonic gonadotropin
IDV	- Integrated Density Values
IKK	- Inhibitory kappa B kinase
IκB	- Inhibitory kappa B
INOS	- inducible nitric oxide synthetase
κ	- kappa
kg	- kilogram
L	- litre
M	- molar
MAP	- mitogen-activated protein
MAPK	- mitogen-activated protein kinase
MBT	- midblastula transition

MEK - mitogen-activated protein kinase kinase

MH1 - main homology1

MHC - major histocompatibility complex

mg - milligrams

mm - millimetre

mM - millimolar

min - minute

Mix 1 - mesoderm induced homeobox 1

mL - millilitre

mRNA - messenger ribonucleic acid

μm - micrometre

μL - microlitre

NAM - normal amphibian medium

NaOH - sodium hydroxide

NF-κB - Nuclear factor-kappa B

ng - nanogram

NLS - nuclear localization signal

OD - optical density

ODC - ornithine decarboxylase

P - phosphate

p53 - protein 53

PCR - polymerase chain reaction

RNA - ribonucleic acid

RHD	- Rel homology domain
Rpm	- revolutions per minute
RT	- room temperatures
RT-PCR	- reverse transcriptase-linked polymerase chain reaction
S	- sulfur
SBE	- Smad-binding element
SH2	- Src Homology 2
Shh	- sonic hedgehog
TBP	- TATA-binding protein
TEMED	- N, N ,N`,N`-tetramethylethylenediamine
TGF-β	- transforming growth factor-β
Tm	- temperature maximum
Vg1	- Vegetal 1
Xbra	- *Xenopus* Brachyury
XDnmt1	- *Xenopus* DNA methyltransferase 1
XFAST	- *Xenopus* forkhead activin signal transducer
XFD-1	- *Xenopus* forkhead 1
Xgsk-3ß	- *Xenopus* glycogen synthase kinase-3ß
Xlim- 1	- *Xenopus* Lim1
XMix.1	- *Xenopus* mesoderm induced homeobox 1
Xnr3	- *Xenopus* Nodal Related 3
XrelA	- *Xenopus* rel A
Xrel2	- *Xenopus* rel 2

Xrel3	- *Xenopus* rel 3
Xp100	- *Xenopus* protein 100
Xsna	- *Xenopus* snail
XTC	- *Xenopus* tissue culture
XTC-CM	- *Xenopus* tissue culture-conditioned medium
XWnt 8	- *Xenopus* Wnt 8
UTP	- uridine triphosphate
UV	- ultraviolet (light)
°C	- degrees celcius
%	- percent

CHAPTER 1

INTRODUCTION.

1.1 *Xenopus laevis* as a model of choice in the study of development of vertebrates.

At the molecular level, the basis of development is thought to be highly conserved between frogs and humans (Wallingford, 1999). Similar developmental pathways seem to be responsible for the induction of genes and the response to induction. This implies that the discoveries of gene product interactions found in animal models should give us a better understanding of developmental processes in humans. The research that is done all over the world by many workers brings us closer to understanding how a highly structured organism can be formed from a simple egg (Wallingford, 1999).

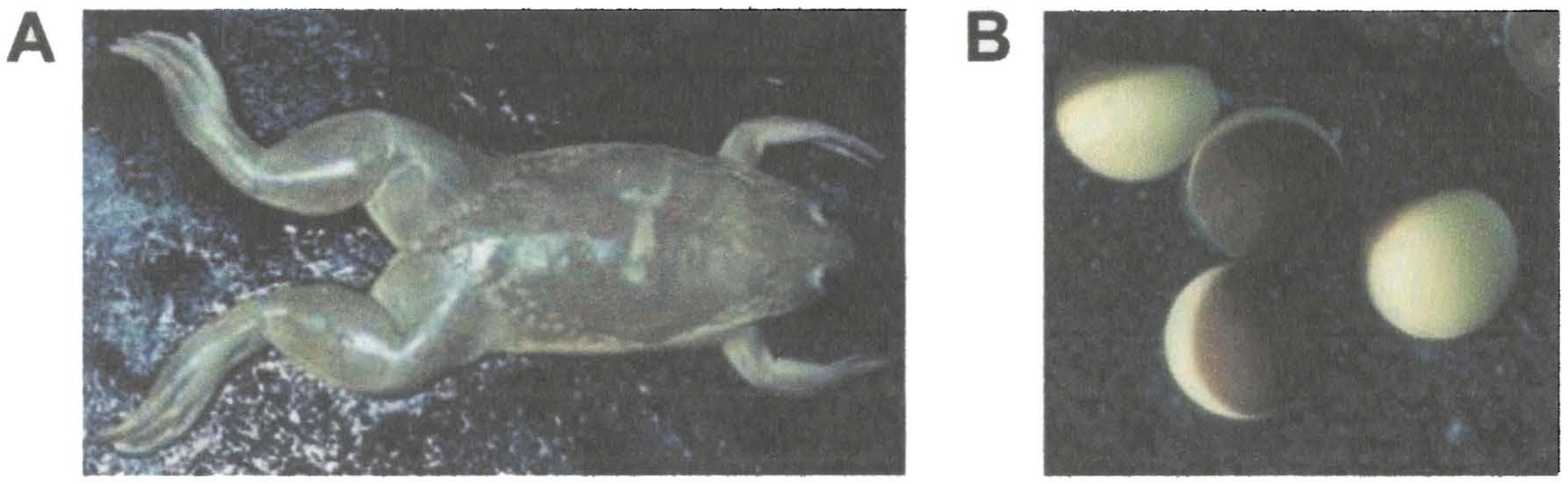

Figure 1.1 South African Clawed Frog named *Xenopus* laevis and its oocytes.
(A) Representative picture of female frog. **(B)** *Xenopus laevis* oocytes (1.0-2.0 mm in diameter), which are pigmented dark brown in one hemisphere (animal hemisphere), and show the yellow colour of the egg yolk on the other hemisphere (vegetal hemisphere).

Xenopus laevis (Figure 1.1) is used extensively for biological studies all over the world. It is perhaps the best known of the fourteen species of the Genus *Xenopus*. This

frog is native to the mountain area of South Africa and the middle of the African continent. *Xenopus laevis* live their entire lives in an aquatic environment. The term "Xenopus" is Latin for "peculiar foot," an apt description for the enormously webbed, five-toed, three-clawed rear feet typical of the group. "laevis" means "smooth" (Deuchar, 1975).

Xenopus laevis has the following taxonomic hierarchy (Nieuwkoop and Faber, 1994): Class, Amphibia; Subclass, Apsidospondyli; Order, Anura; Suborder, Opisthocoela; Family, Pipidae; Sub-family, Xenopodinae; Genus, *Xenopus;* Species, *laevis.*

One reason for *Xenopus* being so widely studied is that it is a vertebrate that undergoes external fertilization, and thus fertilized eggs of *Xenopus* are easy to obtain. Female frogs can be induced to lay eggs by injection with the human hormone, chorinonic gonadotropin, about 14 to 16 hours before egg collection. It is also easy to maintain and feed this species of frog, which can live in dechlorinated tap water while fed manufactured animal feed. Early embryos (see Figure 1.1 B) contain the yolky reserve nutrition for the initial stages of development, and can be cultured at room temperatures in simple salt solutions. The comparatively large size of eggs (about 1.2 to 1.4 mm), their hardiness and resistance to infection facilitates dissections, microinjections and other physical manipulations. The development of embryos is relatively rapid; they go from fertilization through neurulation in approximately 18 hours at 22°C (David and Sargent, 1988; Hausen and Riebesell, 1991; Jones and Smith 1999a).

Thus, *Xenopus laevis* is a popular animal model for the study of embryonic development, differentiation, cell cycle, analysis of gene function, identification of

molecules that are involved in early vertebrate development and elucidation of signalling pathways that are involved in tumourigenesis (Wallingford, 1999).

1.2 An overview of development of *Xenopus laevis.*

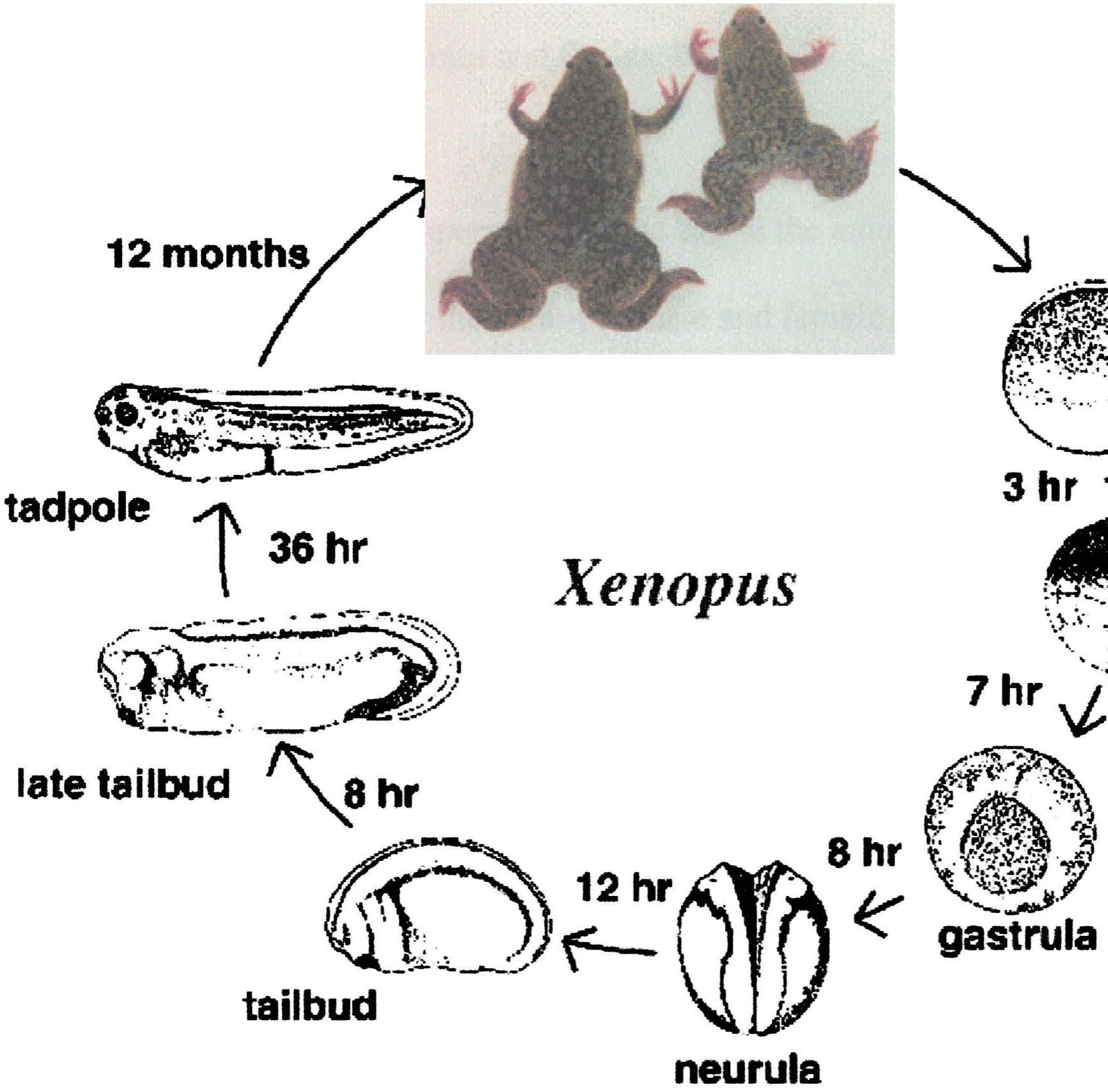

Figure 1.2 *Xenopus laevis* life cycle. Pictures were reproduced from Nieuwkoop and Faber (1994).

The basic stages in frog development are illustrated in Figure 1.2. The *Xenopus laevis* egg (Figure 1.1 B) is a huge cell (1.2 to 1.4 mm in diameter) with a single animal-vegetal axis. The animal cytoplasm of the egg usually contains the nucleus of the oocyte,

while the vegetal half of the egg is the site for the storage of yolk. The lower hemisphere (the vegetal pole), is lightly pigmented, the upper animal half is darkly pigmented (Hausen and Riebesell, 1991; Arendt and Nubler-Jung, 1999). When deposited in the water and ready for fertilization, the haploid egg is arrested at metaphase of meiosis II (Hausen and Riebesell, 1991; Jones and Smith, 1999a).

1.2.1 Fertilization.

During fertilization the sperm enters the egg at the animal hemisphere, the egg completes meiosis, followed by the fusion of male and female nuclei and the formation of a diploid zygote nucleus (Deuchar, 1975; Hausen and Riebesell, 1991). Entrance of the sperm initiates a sequence of events: re-orientation of the zygote with respect to gravity so that the less dense pigmented half of the embryo is at the top, which occurs within twenty minutes of fertilization; rotation of the egg's cortex relative to its cytoplasmic core by thirty degrees in an animal-vegetal direction within forty minutes after fertilization, which is revealed by the appearance of a light-coloured band, known as the gray crescent in other amphibian species (Jones and Smith, 1999a; Figure 1.3), opposite the point where the sperm entered. The site of sperm entry establishes a dorso-ventral axis in early embryos (Jones and Smith, 1999a). Through mechanisms that are not yet completely clear, the cortical rotation establishes a signaling centre, often referred to as the "Nieuwkoop Centre," which directs the development of the dorso-anterior region of the embryo (Gerhart *et al.*, 1989; Jones and Smith, 1999a; Arendt and Nubler-Jung, 1999).

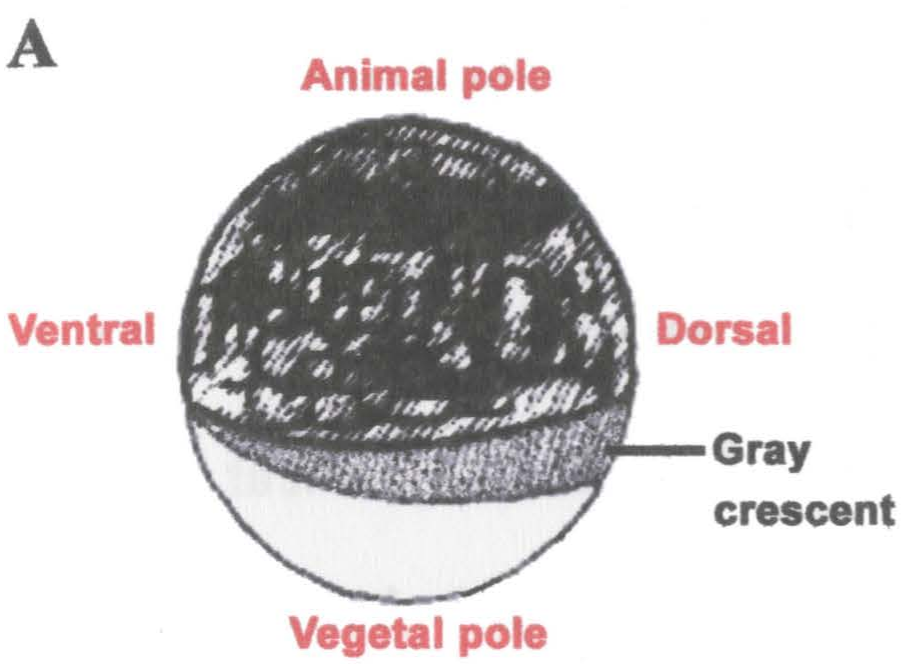

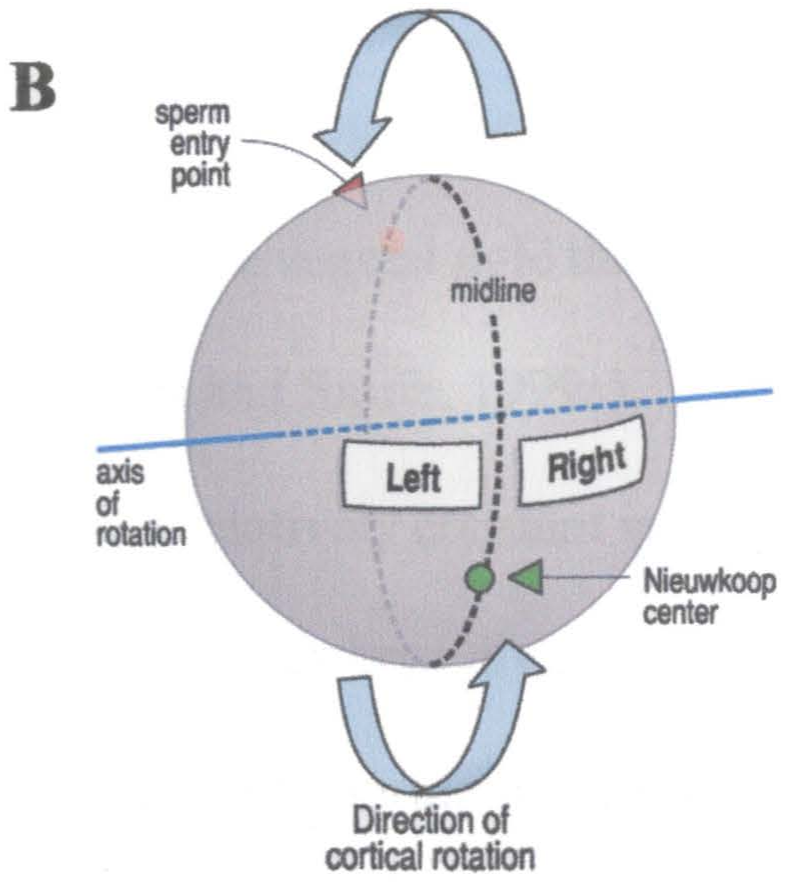

Figure 1.3 Nieuwkoop centre is established by cortical rotation.
(A) Position of the gray crescent in fertilized *Xenopus* egg, established as a result of cortical rotation.
(B) Location of the Nieuwkoop centre, which defines left and right sides in the embryo (reproduced from Wolpert *et al.*, 1998).

1.2.2 Development before the Midblastula Transition stage.

After fertilization, a series of rapid and synchronous mitotic divisions, called cleavage (Figure 1.2 and 1.4), transforms the amphibian egg into a blastula made of numerous cells called blastomeres (Deuchar, 1975). About ninety minutes (21°C) after fertilization, a furrow appears that runs longitudinally through the poles of the egg, passing through the point at which the sperm entered and bisecting the gray crescent. This divides the egg into two halves, the future left and right-hand sides of the embryo (Figure 1.3 B), forming the 2-cell stage. It is followed by a second cleavage, thirty minutes later (Figure 1.4), which runs through the poles but at right angles to the first furrow. The second cleavage forms the 4-cell stage. The furrow in the third cleavage runs horizontally but in a plane closer to the animal than to the vegetal pole and separates the animal and the vegetal poles. It produces the 8-cell stage. The next few cleavages also

proceed in synchrony, producing a 16-cell and then a 32-cell embryo. This rapid series of cleavage divisions continue beyond the 32-cell stage, resulting in the formation of progressively smaller blastomeres, which are larger at the vegetal pole than the animal pole (Hausen and Riebesell, 1991; Keller, 1991; Jones and Smith, 1999a).

The first eleven cleavage cycles in *Xenopus* are relatively constant in length. During this period of rapid cleavage most cells within the embryo divide nearly synchronously every thirty minutes. The cells are not motile during this period (Newport and Kirschner, 1982a,b; Masui and Wang, 1998) and although it is usually thought that *de novo* zygotic transcription is repressed, recent evidence indicates that transcription of some important patterning genes may be necessary as early as the 256-cell stage (Yang *et al.,* 2002). A large majority of the activities, nonetheless depend on maternal gene products (mRNA and proteins) deposited during the formation of the egg. During this entire process there has been no growth of the embryo. In a few hours at room temperature, continued cleavage has produced a hollow ball of thousands of cells called the blastula. A fluid-filled cavity, the blastocoel, forms within it (Deuchar, 1975; Hausen and Riebesell, 1991; Jones and Smith, 1999a).

Stage 1 (1-cell)
ventral view

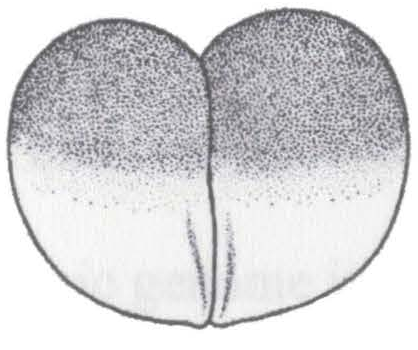

Stage 2 (2-cell)
ventral view
~90 min

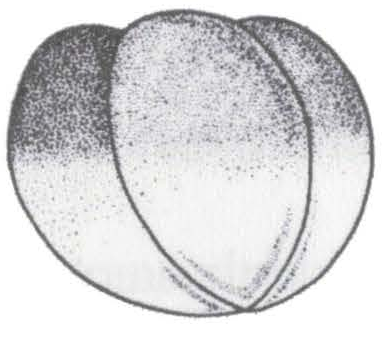

Stage 3 (4-cell)
2 hours

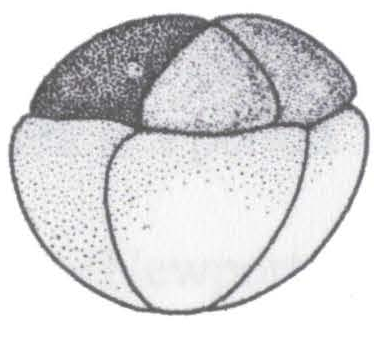

Stage 4 (8 cell)
dorso-lateral view
2 hours 15 min

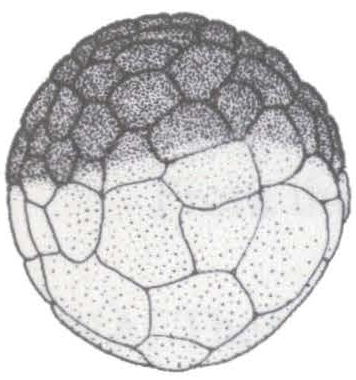

Stage 7 blastula
ventral view
4 hours

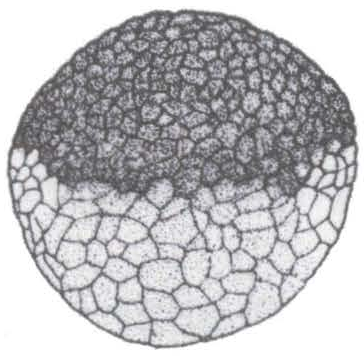

Stage 8 blastula
ventral view
5 hours

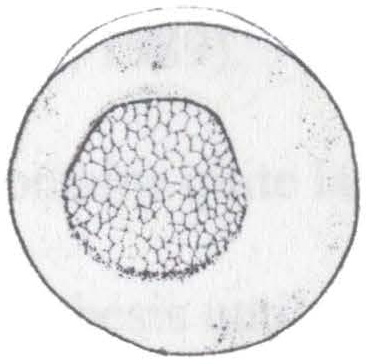

Stage 10.5
vegetal view
11 hours

Stage 14
posterior-dorsal view
16 hours 15 min

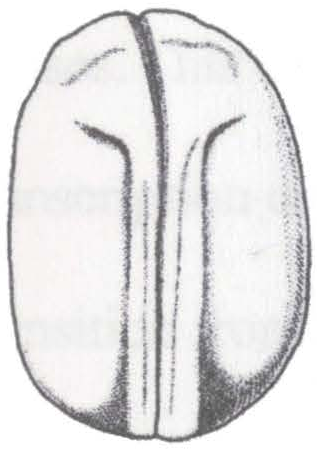

Stage 19
dorsal view
20 hours 45 min

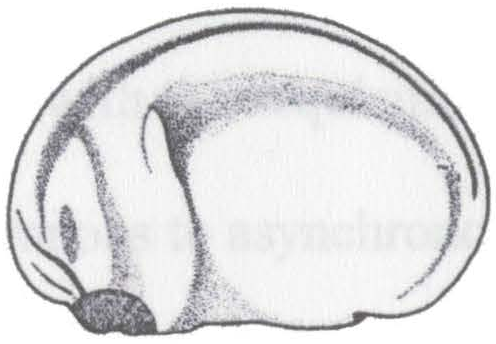

Stage 23
lateral view
1 day 45 min

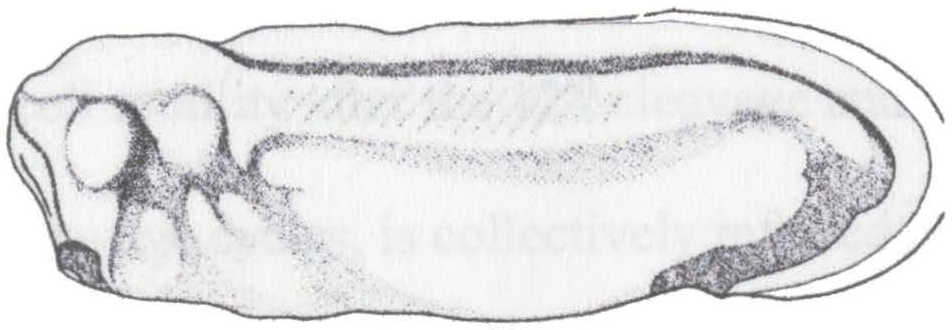

Stage 28
lateral view
1 day 8 hours

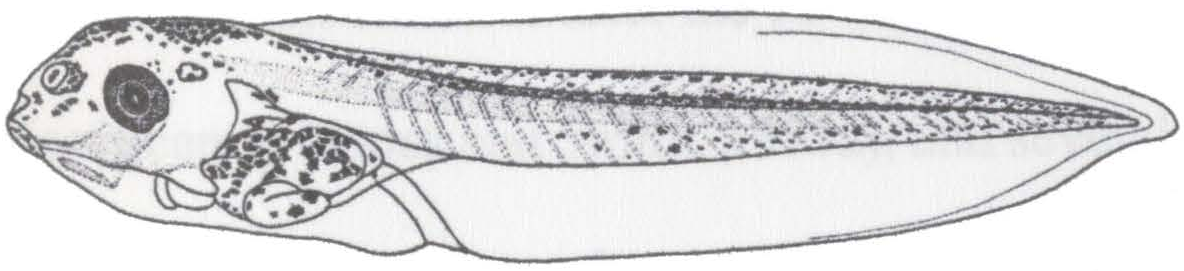

Stage 45
lateral view
4 days 2 hours

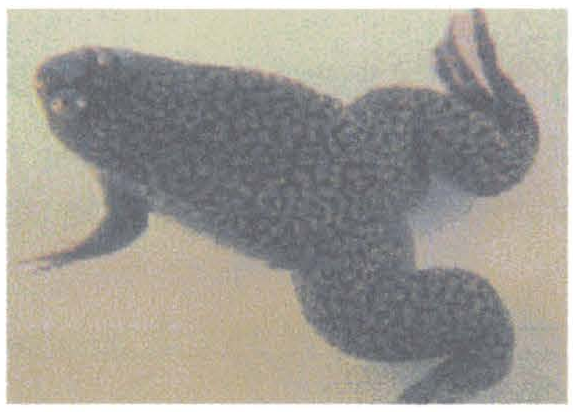

Mature frog
~ 60 days

Figure 1.4 *Xenopus laevis* development. Pictures were reproduced from Nieuwkoop and Faber (1994).

1.2.3 Midblastula transition.

During the early embryonic development of *Xenopus laevis* there is a period during which the embryonic genome is relatively transcriptionally silent (Newport and Kirschner, 1982a). This transcriptional repression is relieved at the 12 to 13th division cycle, when there is as much as a 50-fold increase in the transcription of some genes (Newport and Kirschner 1982a,b; Shiokawa *et al.*, 1989).

From the beginning, the *Xenopus* egg contains quite large amounts of maternal mRNA. There is, however, little new mRNA synthesis until 12 cleavages have taken place and the embryo contains approximately 4096 cells. The cell cycle is rapid and synchronous, oscillating between DNA synthesis and mitosis with no discernible gap (G) phases. This well-defined interval, during which the gradual activation of the embryonic transcription coincides with the acquisition of cell motility after the 12th cleavage and transition from synchronous to asynchronous cleavage cycles, is collectively referred as the midblastula transition (MBT) (Newport and Kirschner, 1982a; Stancheva and Meehan, 2000).

Within one hour after the 12th cleavage division, the rate of mitosis slows significantly (Jones and Smith, 1999a), and several new cell activities appear, including activation of RNA transcription in all cells of the embryo, acquisition of motility with the formation of lamellipodia, and the first evidence of lengthened, variable G1 and G2 phases in the cell cycle (Newport and Kirschner, 1982a). The first cleavages take place at regular 30 to 35 minute intervals in all cells, but at the 12th cleavage they become asynchronous as animal and vegetal cells take different amounts of time to complete the

next cycle of mitosis. Transcriptional activation after the 12th cleavage division coincides with the transition to mitotic asynchrony (Yasuda and Schubiger, 1992).

At the MBT there are profound changes in the cell cycle. The average cycle length progressively increases between the 12th and 16th cycles, as they acquire gap phases between DNA replication and mitosis (Newport and Kirschner, 1982a).

The MBT also marks a dramatic change in the response of the embryo to DNA damage. When ionizing radiation is administered any time before the MBT, *Xenopus* embryos initiate apoptosis by triggering different pro-apoptotic factors (Anderson *et al.*, 1997; Hensey and Gautier, 1997). However, if ionizing radiation is given after the MBT, embryos are resistant to apoptosis by multiple mechanisms, including activation of anti-apoptotic pathways, the inactivation of pro-apoptotic proteins through heterodimerization, and by promotion of cell cycle delay by an increase in the level of cyclin-dependent kinase inhibitor p27^{Xic1} (Finkielstein *et al.*, 2001).

The control of the MBT is not well known. The timing of the MBT does not depend upon rounds of cell division, upon time since fertilization, upon cell-cell interactions, upon rounds of DNA replication or upon initiation of new transcription (Newport and Kirschner, 1982a). MBT events such as maternal cyclin E degradation and sensitivity to apoptosis are regulated by a developmental timer insensitive to inhibition of DNA, RNA or protein synthesis (Maller *et al.*, 2001). Newport and Kirschener (1982b) suggested that the timing of the MBT seems to be dependent on reaching a critical ratio of DNA to cytoplasm - the quantity of DNA present per unit mass of cytoplasm. Direct evidence for this comes from the fact that transcription can be activated prematurely by

increasing the amount of DNA artificially in the egg. The amount of DNA needed to induce premature transcription is equal to the amount of nuclear DNA present after twelve cleavages, suggesting that there may be some fixed amount of a general repressor of transcription present initially in the egg cytoplasm, and that the MBT is triggered by the DNA through titration of suppressor components present in the egg. As the zygote cleaves, the amount of DNA gets larger and larger, when the amount of cytoplasm does not increase. Both cell cycle lengthening and the relief of transcriptional repression at the MBT were proposed to be regulated by stoichiometric titration of a repressor by the exponentially increasing amount of DNA in the embryo. The amount of repressor in relation to DNA gets smaller and smaller until it is insufficient to bind to all the available sites on the DNA and the repression is lifted (Newport and Kirschner, 1984).

There are probably several other separate events that regulate this developmental switch during MBT. Later models propose that other mechanisms contribute, including a decrease in the levels of the maternal DNA methyltransferase (*xDnmt1*), an enzyme involved in methylation of DNA (Stancheva and Meehan, 2000). The *Xenopus* genome, similar to other vertebrates, is methylated at the fifth position of cytosine at CpG dinucleotides. DNA methylation contributes to the transcriptional silencing during the first twelve cleavages of the zygote, and loss of this epigenetic modification is associated with premature activation of developmentally decisive genes and apoptosis of embryo cells (Stancheva and Meehan, 2000; Stancheva *et al.*, 2001). Stancheva and Meehan (2000) used antisense RNA to deplete maternal levels of *xDnmt1*, which led to hypomethylation of the genome during the first embryonic cleavages and premature gene

activation, which causes severe developmental defects in *Xenopus*. These results support a model where by the repressive effect of DNA methylation at gene promoters is utilized to regulate the precise timing of gene expression at MBT.

Veenstra *et al.* (1999) found that the transcriptional silence observed before the MBT is due to a deficiency in the transcription machinery and can be relieved by increase is translation of maternally stored components of basal transcription such as TATA-binding protein (TBP) RNA, which is strongly upregulated at the MBT (Veenstra *et al.*, 1999).

1.2.4 Gastrulation.

Before gastrulation, the *Xenopus* blastula has a thin blastocoel roof composed of small animal blastomeres, which represents prospective ectoderm, and a massive blastocoel floor of large, yolk–rich vegetal blastomeres, which will contribute to the endoderm. They enclose the blastocoel, a fluid-filled cavity (Keller, 1986; Dale and Slack, 1987a). Pre-gastrula movements in the embryo involve the increase in volume of the blastocoel by accumulation of fluid, and expansion and thinning of the blastocoel roof in a movement called epiboly (Keller, 1980). Gastrulation follows the blastula stage, and involves all the morphogenetic events between the blastula stage and the time when the three germ layers are clearly established. The movements of gastrulation involve massive rearrangements during which cells change their neighbours and environments, allowing for the interactions and inductive processes between various regions of the developing body.

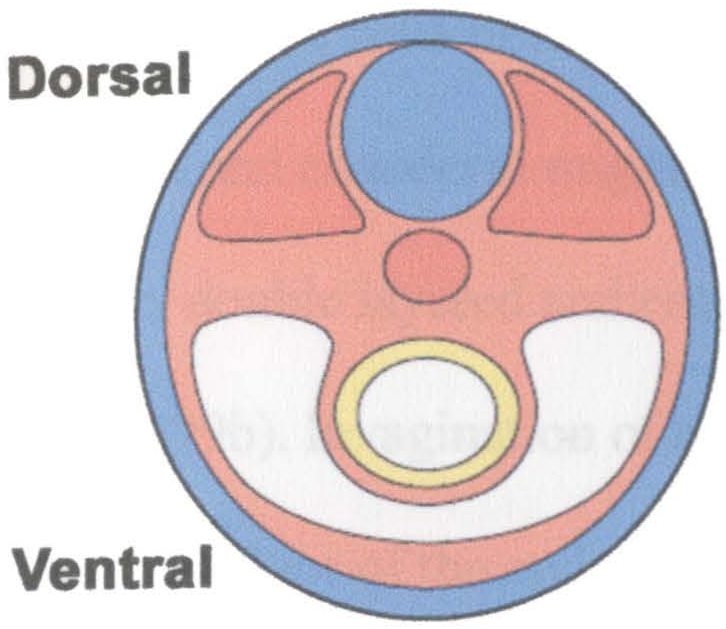

Endoderm	gut, liver, lungs
Mesoderm	skeleton, muscle, kidney, heart, blood
Ectoderm	skin, nervous system

Figure 1.5 Three germ layers. Germ layers are specified early in development: endoderm, mesoderm and ectoderm that give rise to the associated structures. Reproduced from Wolpert *et al.*, 1998.

Gastrulation transforms the amphibian blastula, a simple hollow ball of cells with radial symmetry, into a structured embryo with different cell types that can interact with each other, with a distinct body axis and three germ layers: ectoderm, endoderm and mesoderm (Figure 1.5) (Keller, 1986; Leptin, 1995). The endoderm in *Xenopus* is derived from cells located in the vegetal hemisphere of the early embryo. The cells of the endoderm contribute to the organs of the gastrointestinal and respiratory tracts, including the pancreas, liver, gall bladder, stomach, intestine, and lungs. The ectoderm is derived from the cells located in the animal hemisphere of the early *Xenopus* embryo, and gives rise to the epidermis (the outer layer of the skin) and the nervous system. Mesoderm gives rise to the connective tissue, muscles, vascular and urogenital systems (Dale and Slack, 1987a). The activities of the cells of the mesoderm drive much of the gastrulation process (Keller, 1986).

Initial stages of gastrulation (Figure 1.6) are characterized by a formation of bottle cells in the dorsal-vegetal part of the embryo, which can be visible by the appearance of a pigmented depression and the associated line of pigment. The bottle cells initiate

involution of the cells of mesoderm and endoderm through the blastopore lip. The cells of mesoderm and endoderm migrate in the direction of the animal pole, until they form a complete, double layered archenteron roof (Hausen and Riebesell, 1991; Jones and Smith, 1999b). Invagination of mesoderm and endoderm proceeds laterally and ventrally, forming the floor of the archenteron and the side-walls of the embryo. Finally the blastopore closes completing gastrulation (Deuchar, 1975).

The signals that coordinate and control the movements of gastrulation and the patterns of specialization of the tissues in its neighbourhood are located at the site where the invagination starts, the dorsal lip, which is also called the Spemann Organizer (Alberts *et al.*, 1989). The Spemann Organizer in amphibians is defined as a population of gastrula cells capable of inducing the formation of a second body axis when transplanted into a responsive environment such as the ventral side of another gastrula (Spemann and Mangold, 1924). Only 5% of cells of the gastrula located in the dorsal marginal zone make up the Spemann Organizer. At least half the cells of the gastrula require signals from the organizer for their normal development. When the organizer is absent due to early removal or interference with its formation, the embryo gastrulates but develops none of the neural or mesodermal structures characteristic of the antero-posterior axis (Stewart and Gerhart, 1990). The Spemann Organizer has a role in establishing left-right asymmetry in the developing embryo (Figure 1.3 B) (Harland and Gerhart, 1997) and also induces the nervous system of the correct size, place, and orientations, as well as dorsal axial mesoderm such as somites (Hemmati-Brivanlou and Melton, 1992). In recent years genes involved in mediating organizer function have been discovered which have greatly advanced the molecular understanding of organizer signalling.

These include genes that are involved in the bone morphogenetic protein (BMP) pathways: *noggin* (Smith and Harland, 1992), *chordin* (Sasai *et al.,* 1994), *follistatin* (Hemmati-Brivanlou *et al.,* 1994), *Xnr3* (Smith *et al.,* 1995) and *cerberus* (Bouwmeester *et al.*, 1996).

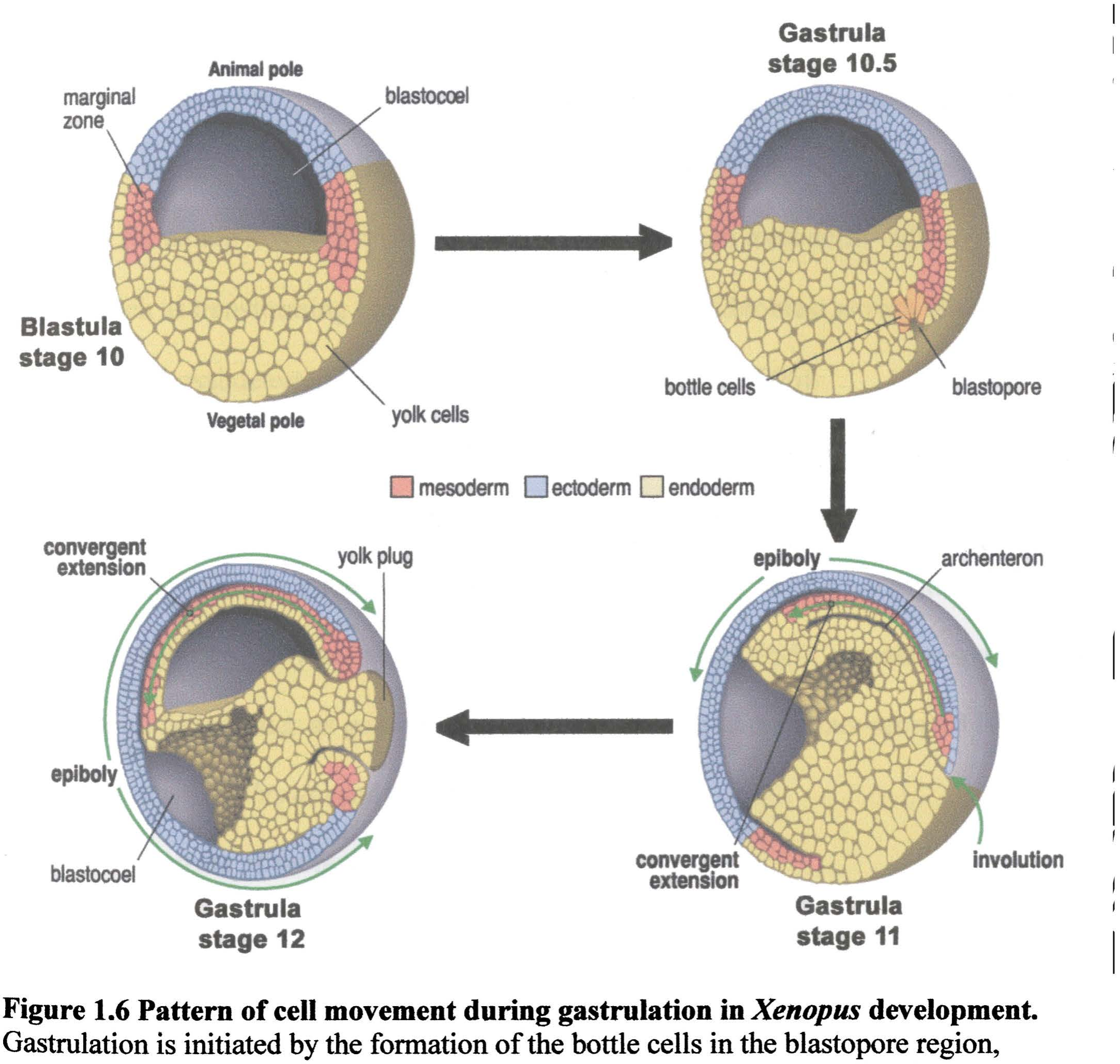

Figure 1.6 Pattern of cell movement during gastrulation in *Xenopus* development. Gastrulation is initiated by the formation of the bottle cells in the blastopore region, which is followed by the involution of mesoderm (**red**) over the dorsal lip of the blastopore. Marginal zone mesoderm and endoderm (**yellow**) move inside. At the same time the ectoderm (**blue**) of the animal cap spreads downwards. The mesoderm converges and extends along the antero-posterior axis. Reproduced from Wolpert *et al.*, 1998.

Spemann Organizer formation is initiated by activation of the early Wnt signaling pathway, which in turn activates the expression of organizer-specific genes (Harland and Gerhart, 1997; De Robertis *et al.,* 2000). Wnts are a family of secreted proteins involved in a wide range of developmental processes, and in *Xenopus* the Wnt pathway is used in mesoderm induction to specify the dorso-ventral axis, also for posterization of nervous system and subsequent patterning (Harland and Gerhart, 1997). A current model of organizer formation involves synergistic interactions between mesoderm-inducing signals, such as transforming growth factor-β (TGF-β) and fibroblast growth factors (FGFs), and dorsal determinants (Lemaire and Kodjabachian, 1996).

When Spemann Organizer genes are expressed in the ventral marginal zone, some of these genes can perform most of the organizer activities, while others perform only a limited repertoire. Among the genes that can induce secondary axis are elements of the early Wnt signaling pathway, such as *siamois* (Lemaire *et al.,* 1995), organizer-specific transcription factors such as *goosecoid* (Cho *et al.,* 1991), and organizer-secreted BMP antagonists such as *chordin* and *noggin* (Sasai *et al.,* 1994).

1.2.5 Movements of gastrulation.

During gastrulation, directed coordinated movements of large cell groups is accompanied by changes in cell morphology and cell adhesion. The behavior of cells underlying these movements, their timing and patterning are very complex and still not completely understood (Popsueva *et al.*, 2001).

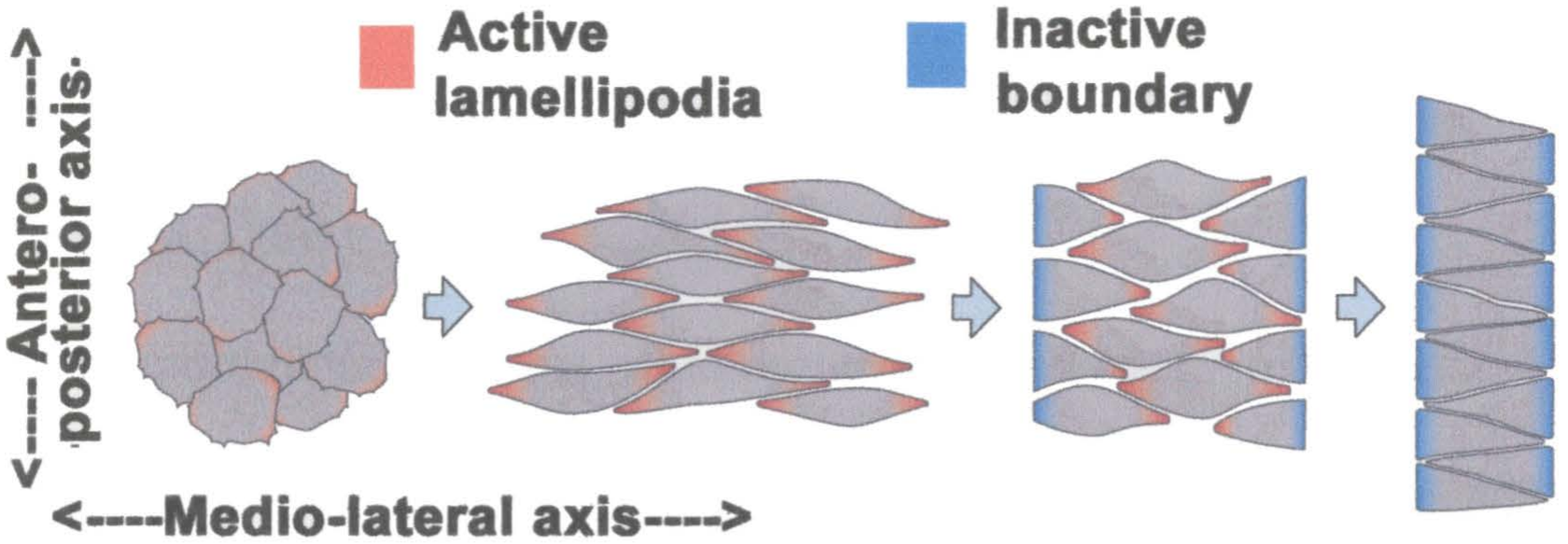

Figure 1.7. Cell movement during convergent extension of the mesoderm in amphibians. The cells have active lamellipodia (finger-like projections) and move between each other (intercalate), causing the tissue to narrow and elongate along the antero-posterior axis (reproduced from Wolpert *et al.*, 1998).

The movement of gastrulation seems to be driven by a combination of mechanisms: convergent extension (Figure 1.7) or narrowing and lengthening of the marginal zone (Gerhart and Keller, 1986); epiboly (Figure 1.6) or spreading of cells of the animal hemisphere, when the animal pole epithelium expands by cell rearrangement, becoming thinner as it spreads; involution of marginal zone cells inside embryo (Keller and Danilchik, 1988); invagination of the bottle cells (Figure 1.6) and their migration with the involuted mesodermal cells towards the animal pole over fibronectin-rich matrix lining the roof of the blastocoel (Winklbauer, 1990; Wilson and Keller, 1991; Popsueva *et al.*, 2001). Convergent extension in the marginal zone is the main driving force for gastrulation in *Xenopus* (Gerhart and Keller, 1986; Kuhl *et al.*, 2001), when cells form lamellipodia (Figure 1.7), with which they attempt to crawl over one another (Shih and Keller, 1992). Endogenous Wnt/beta-catenin signaling activity is essential for convergent extension movements due to its effect on gene expression (Kuhl *et al.*, 2001). Recent evidence suggests that intercellular calcium signaling plays an important role in

vertebrate convergent extension, and that calcium waves may represent a widely used mechanism by which large groups of cells can coordinate complex cell movements (Wallingford *et al.,* 2001).

Other important mechanisms, which contribute to these morphogenetic movements are cell adhesion to the extracellular matrix mediated by transmembrane receptors called integrins (Hynes, 1992), and cell-cell adhesion between migrating cells, which are mediated via cadherins (Ca^{2+}-dependent transmembrane adhesion proteins) (Huber *et al.*, 1996). In addition to integrins, cadherins, and extracellular matrix proteins, several other genes, such as *milk* (Ecochard *et al.,* 1998), *XRhoA* and *XRnd1* (Wunnenberg-Stapleton *et al.*, 1999), and *disheveled* (Sokol, 1996; Wallingford *et al.,* 2000) were demonstrated to affect cell movements during gastrulation.

A fine balance of spatially and temporally regulated adhesion must be maintained during gastrulation movements. Cell adhesion strength must be at intermediate level for optimal cell movements (Huttenlocher *et al.,* 1995; Palecek *et al.,* 1997). Reduction of adhesion between blastomeres is necessary for activin-induced animal cap elongation and, most likely, for gastrulation, which was demonstrated by *in vitro* experiments (Brieher and Gumbiner, 1994; Zhong *et al.,* 1999). However, excessive reduction of adhesion leads to inhibition of gastrulation (Popsueva *et al.,* 2001).

1.2.6 Mesoderm induction.

All animal tissues derive from the three germ layers and the mesoderm plays a pivotal role in organizing the body axis. Mesodermal cells lead the movement of gastrulation, are required for the patterning of the nervous system, and themselves give

rise to the muscular, skeletal, circulatory and excretory systems (Hemmati-Brivanlou and Melton, 1992). In *Xenopus*, mesoderm originates from a band of cells in the blastula embryo that make up the marginal zone. Through the processes of gastrulation and tailbud extension, the various mesoderm derivatives, including the notochord, somites, pronephros, heart, and blood islands, arrive at their proper positions along the dorsal-ventral, anterior-posterior, and left-right axis of the developing tadpole. The specification of multiple cell and tissue types within the mesoderm requires a complex interplay between localized maternal determinants and secreted maternal and zygotic inductive factors (Kessler and Melton, 1994; Harland and Gerhart, 1997; Heasman, 1997; Smith and Kumano, 2000). The timing of mesoderm induction *in vivo* is still unknown. It has been roughly estimated to occur between the 32-cell stage and the late blastula (Ding *et al.*, 1998), when signals from the vegetal hemisphere induce the equatorial region of the embryo to form mesoderm rather than ectoderm (Smith, 1993). Much of the induction and patterning of mesoderm occurs during the processes of gastrulation and tailbud extension (Smith and Kumano, 2000).

It has been shown (Figure 1.8) by fate-mapping studies (Lane and Smith, 1999), as well as with models of mesoderm morphogenesis during gastrulation (Keller, 1991), that ventral mesoderm originates from the vegetal-most portion of the blastula marginal zone, a domain called the leading edge mesoderm. Ventral mesoderm originates from the entire ring of the marginal zone (Lane and Smith, 1999; Mills *et al.*, 1999; Ciau-Uitz *et al.*, 2000), and not just from those cells furthest away from the Spemann Organizer, as it is frequently depicted (Jones and Smith, 1999b; De Robertis *et al.*, 2000).

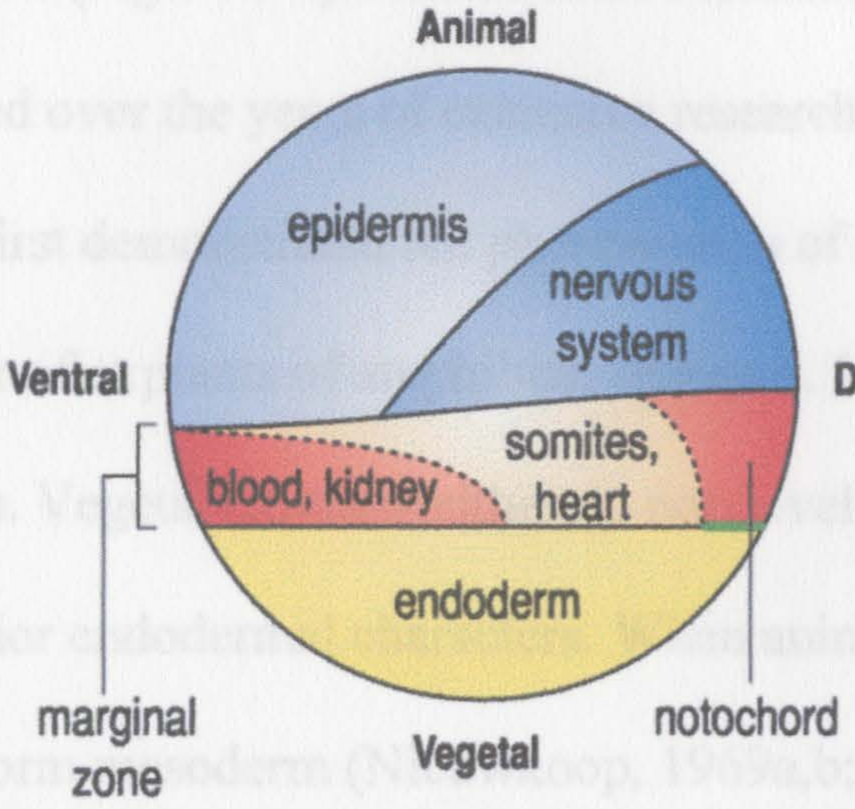

Figure 1.8 Fate map of the late Xenopus blastula, lateral view.
The normal fate of the blastula is shown. Reproduced from Wolpert *et al.*, 1998.

On the other hand, somites arise from the animal region of the blastula marginal zone, and the entire ring of the animal marginal zone, excluding the sector occupied by the Spemann Organizer, gives rise to somites (Lane and Smith, 1999).

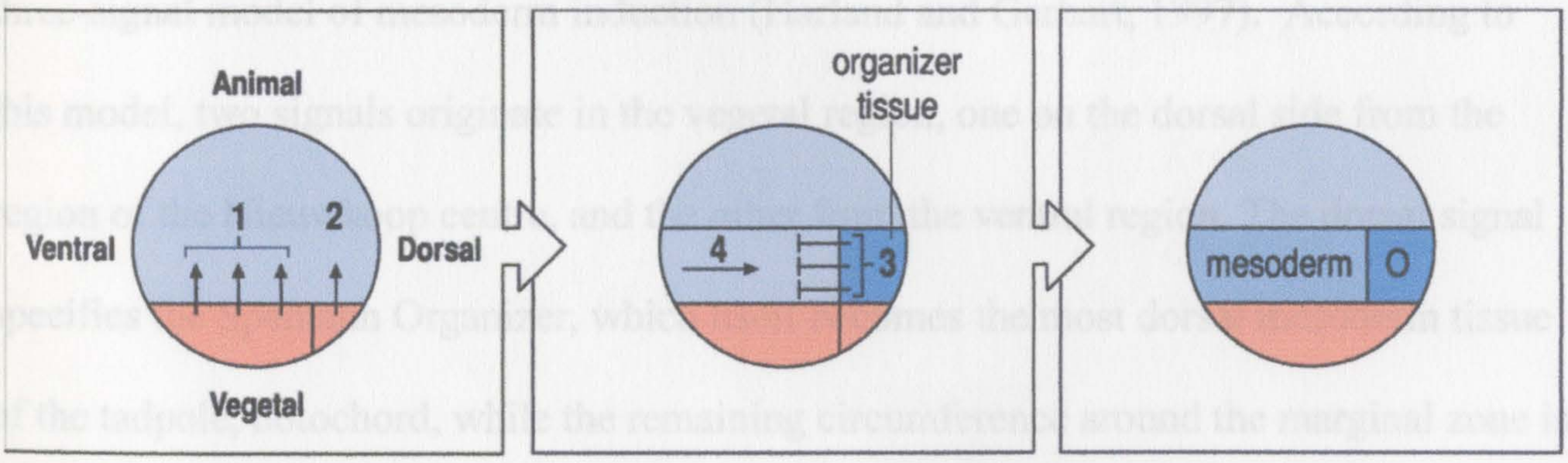

Figure 1.9 Four-signal model of mesoderm induction.
Two signals originate in the vegetal region, one **(1)** on the ventral side, which specifies ventral mesoderm, and the other **(2)** on dorsal side, which specifies the Spemann Organizer region **(O).** The third signal **(3)** from the dorsal region dorsalizes the mesoderm by inhibiting the action of the fourth **(4)** ventralizing signal. Reproduced from Wolpert *et al.*, 1998.

Four-signal model (Figure 1.9) of mesoderm induction (Slack, 1994; Wolpert *et al.,* 1998) was developed over the years of extensive research by many workers. Peter Nieuwkoop (1969a,b) first demonstrated the phenomenon of mesodermal induction, by observing the behaviour of explants of amphibian embryos. Isolated animal caps develop into a kind of epidermis. Vegetal explants either do not develop into recognizable tissues, or develop some posterior endodermal characters. When animal caps are grafted into the vegetal explants, they form mesoderm (Nieuwkoop, 1969a,b; Harland and Gerhart, 1997). Nieuwkoop concluded that the mesoderm and the head endoderm develop exclusively from the animal cap cells, which were induced by the vegetal cells (Nieuwkoop and Ubbels, 1972; Harland and Gerhart, 1997). Boterenbrood and Nieuwkoop (1973) found that explants of dorsal vegetal cells induce dorsal mesoderm, and explants of ventral vegetal cells induce ventral mesoderm (Harland and Gerhart, 1997). Slack and Smith (1983), Dale *et al.* (1985), Dale and Slack (1987b) proposed a three-signal model of mesoderm induction (Harland and Gerhart, 1997). According to this model, two signals originate in the vegetal region, one on the dorsal side from the region of the Nieuwkoop centre, and the other from the ventral region. The dorsal signal specifies the Spemann Organizer, which itself becomes the most dorsal mesoderm tissue of the tadpole, notochord, while the remaining circumference around the marginal zone is initially specified as ventral. The bone morphogenetic protein (BMP) gradient-model of mesoderm patterning attempts to explain the dorsal-to-ventral specification of mesoderm derivatives in *Xenopus* (Dale and Jones, 1999; Smith and Kumano, 2000). In this model, a gradient of BMP activity is generated in the marginal zone through the action of the

Spemann Organizer. The Spemann Organizer is the source of a number of secreted factors (Figure 1.10), including *noggin, chordin, follistatin*, and *Xnr-3*, that antagonize the activity of a uniformly expressed field of BMPs in the marginal zone (Harland and Gerhart, 1997; Heasman, 1997; Dale and Jones, 1999; Smith and Kumano, 2000). This model proposes that as a result of the antagonistic actions between BMPs and inhibitory factors, mesoderm closest to the Spemann Organizer is exposed to the lowest levels of BMPs and is thereby specified as dorsal; conversely, mesoderm farthest away from the Spemann Organizer is exposed to the highest levels of BMPs and is specified as ventral. This model has continued to be a useful interpretation of the embryological results, although it has been modified. Wolpert *et al.* (1998) proposed a four-signal model where the third signal, from the ventral region, ventralizes the mesoderm and the fourth signal dorsalizes it by inhibiting the action of the third signal (Figure 1.9).

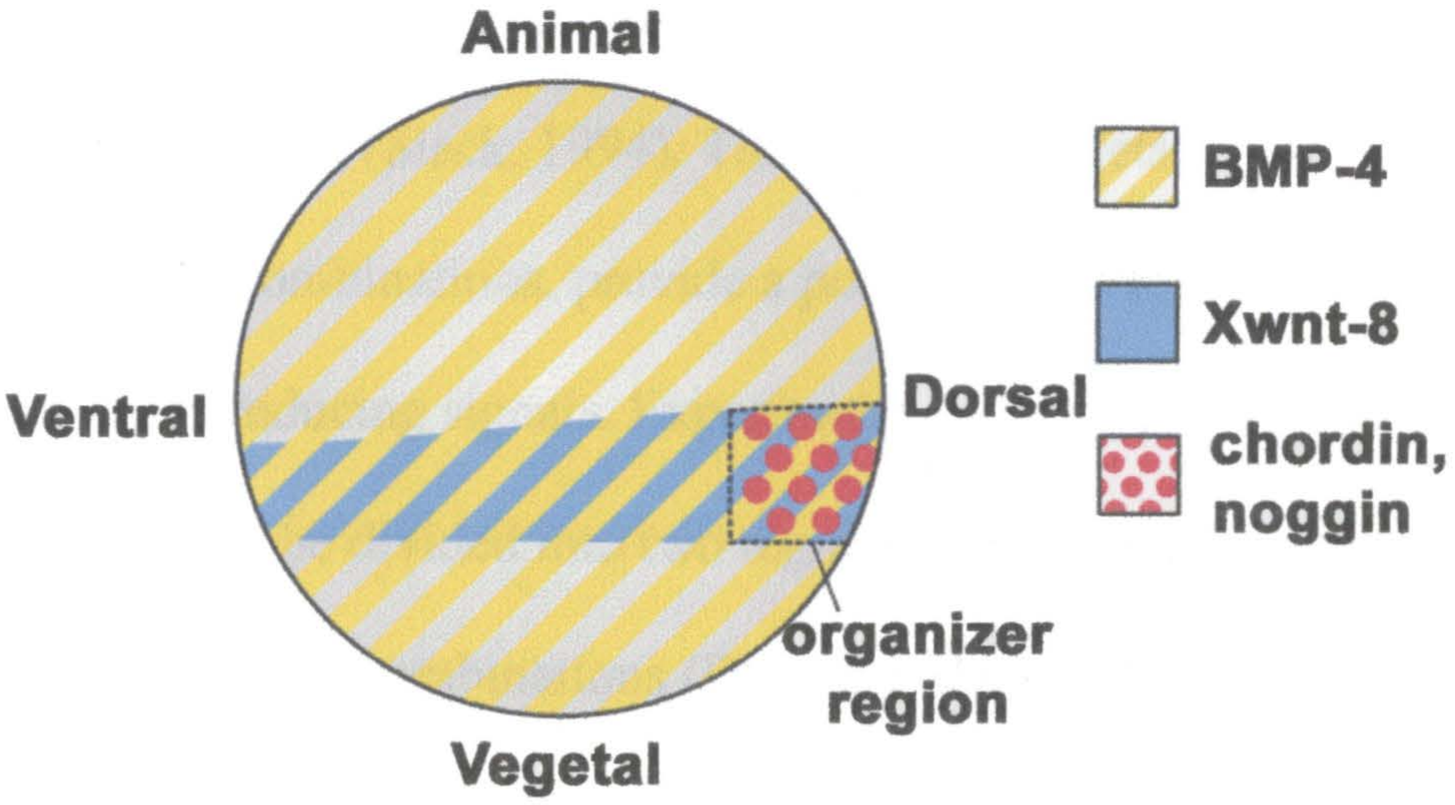

Figure 1.10 Distribution of protein signals in *Xenopus* blastula.
Modified from Wolpert *et al.*, 1998.

In many laboratories considerable research has been conducted to characterize the molecules involved in mesoderm induction and axial patterning, and it is generally agreed that mesoderm induction in the marginal zone of *Xenopus* embryos is mediated by diffusible growth factor-like molecules. Several molecules have been proposed as candidates for mesoderm-inducing signals, including members of the fibroblast growth factor (FGF) family such as basic FGF (bFGF) and embryonic FGF (eFGF), as well as members of the transforming growth factor β (TGF-β) family such as Vg1, the bone morphogenetic proteins BMP-2 and -4 and activins A and B. The use of the animal cap assay has greatly assisted in the identification and purification of candidate inducing factors. When animal cap tissue is explanted from a blastula embryo and cultured in isolation it develops into a ball of epidermis. In the presence of an inducing factor or if animal cap explants are cultured in combination with tissue taken from the vegetal hemisphere, the animal cap will differentiate into mesodermal derivatives, including notochord, muscle and blood (Slack, 1994). These animal-vegetal combinations, also known as 'Nieuwkoop' combinations, provide a powerful tool for investigating the endogenous mesoderm-inducing signals. Experiments of this type also showed that the vegetal hemisphere could be divided into two regions based upon the dorsoventral nature of inductions elicited in such combinations (Dale and Slack, 1987a).

Dorsal and ventral type mesoderm is qualitatively different and different factors induce the differentiation of specific mesodermal tissues. As tested by microinjection of RNAs and/or by animal cap assays the demonstration that FGFs and BMP-4 (Jones *et al.*, 1992; Dale *et al.*, 1992) induce ventral-type mesoderm, such as blood, mesenchyme and

mesothelium, whereas activin (Asashima *et al.*, 1990; Thomsen *et al.*, 1990) and some members of the Xwnt family (Smith and Harland, 1991; Ku and Melton, 1993; Wolda *et al.*, 1993) induce dorsal-type mesoderm such as muscle and notochord in the mesoderm induction assay quickly established them as candidates for the endogenous inducing signals. However, it is not simple, as the concentration of the factor and the determination state of the competent cells can greatly influence the type of response. For example activin A at low concentration also induces ventral type tissues (Grunz, 1983) and Xwnt-8 after MBT has a ventralizing effect (Christian and Moon, 1993).

According to the above, dorsalizing signals such as activin A should activate those genes which are preferentially expressed in the dorsal blastopore lip, like *Xlim- 1*, *goosecoid* or *XFD- 1*; ventralizing signals such as FGF should activate the genes which are transcribed in the ventral: posterior area, like *Xhox- 3*, and probably both signals should activate the genes which are initially activated throughout the marginal zone, like *Xbra* or *Xsna*. It was confirmed by several laboratories (Cho *et al.*, 1991; Smith and Harland, 1992; Taira *et al.*, 1992) that activin A and bFGF were able to activate transcription of distinct genes in isolated animal caps. Most genes (*Xsna, Mix.1, Xlim-1, Goosecoid, XFD-1*) were induced by activin A, but only some of them (*Xsna, Xhox-3, Xnot*) by bFGF. This corresponds to the fact that different threshold concentrations of activin A can induce either ventral or dorsal mesoderm. By contrast, bFGF induces only tissues of ventral or of intermediate mesoderm. However, genes like *goosecoid, XFD- 1, Xlim- 1, noggin*, which are primarily transcribed in the dorsal blastopore lip, do respond exclusively to activin A (Cho *et al.*, 1991; Smith and Harland, 1992; Taira *et al.*, 1992).

On the other hand, mesoderm induction by FGF can be modified to a more dorsal-type in a number of ways. For example, it has been shown that co-treatment with the dorsalizing agent lithium (Slack *et al.,* 1988; Kao and Elinson, 1988) and the injection of *Xwnt- 8* mRNA into animal caps results in a more dorsal-type induction following FGF treatment (Christian *et al.,* 1992). This has led to the proposal that an FGF could also be a component of the dorsal mesoderm-inducing signal.

One way to assay for inductive potential of the factors is by the "animal cap serial dilution assay". This involves exposing isolated midblastula stage animal caps to serial dilutions of the suspected inducer and cultured for up 3 days, after which mesoderm induction is assessed by either morphological or molecular criteria. A positive response is indicated by elongation of the explants and formation of vesicles. A commonly used molecular marker is *muscle-specific alpha-cardiac actin* mRNA. A more recent assay is the detection of *brachyury (Xbra)* mRNA (Godsave *et al.,*1988; Kimelman and Maas, 1992; Thompson and Slack, 1992). Members of the fibroblast growth family, in particular bFGF, and the TGF-β family, notably activins, are potent inducers in this assay. Activin protein and bFGF can be detected in the early embryo (Hemmati-Brivanlou and Melton, 1992).

1.2.7 Role of Activin A in mesoderm induction.

Activin satisfies all the requirements to be an endogenous mesoderm-inducing signal. Activin A, which is a member of the TGF-β class of growth factors, was first identified by Smith *et al.* (1990) to be an active ingredient, produced by a *Xenopus* tissue culture (XTC) cell line. Isolated animal pole regions cultured in XTC-conditioned

medium differentiate into dorsal mesodermal tissues, muscle and notochord, while controls form epidermis (Smith *et al.,* 1990). It is important to note that the XTC factor, the vegetalizing factor and a factor isolated from amniotic fluid, have been proven to be identical or closely related to activin A (Tiedemann *et al.,* 1992).

Activin protein is present in *Xenopus* oocytes and blastulae (Fukui *et al.,* 1994) and acts as a morphogen. It induces various cell types and expression of a range of mesodermal markers in a concentration-dependent manner (Green and Smith, 1991). Activin response elements (AREs*)* have been reported in several activin-inducible transcription factor genes, such as the homeobox genes *goosecoid* (Watabe *et al.,* 1995), *Mix.2* (Huang *et al.,* 1995), *HNF1 a* (Weber *et al.,* 1996), and *Xlim-1* (Rebbert and Dawid, 1997), a T-box gene *Xbra* (Latinkic *et al.,* 1997), and a *forkhead gene XFD-1* (Kaufmann *et al.,* 1996). Although the mechanisms regulating transcription of these genes remain poorly understood, molecules such as: *forkhead activin signal transducer-1 (FAST-1), Smad2, Smad3,* and *Smad4* were identified as components of activin response factors (ARFs) (Chen *et al.,* 1996, 1997; Yeo *et al.,* 1999). *Xenopus* xFAST was found to take part as an endogenous mediator of mesendoderm induction (Watanabe and Whitman, 1999).

Smad proteins are a group of recently identified family of proteins which mediate signalling for the TGF-β superfamily of cytokines, including TGF-β, activin, BMPs, and many others (Heldin *et al.,*1997). TGF-β initiates signaling through activation of type I receptor (Wrana *et al.,* 1994; Derynck and Feng 1997), which phosphorylates and activates Smad2 and/or Smad3 (Heldin *et al.,* 1997; Nakao *et al.*, 1997a). Following

phosphorylation, Smad2 and Smad3 associate and form complexes with the shared partner Smad4. These complexes then migrate to the nucleus, and regulate gene transcription through either direct DNA binding, via the MH1 domain of the Smad proteins, or association with other specific transcription factors, such as Xenopus FAST-1 in which Smad protein complexes participate in transcriptional activation of target genes (Derynck *et al.,* 1998). The expression of inhibitory Smad7, which is induced by TGF-β itself, provides an autoinhibitory feedback loop (Nakao *et al.*, 1997a). This protein inhibits TGF-β, activin and BMP signalling by interacting with the type I receptors of the TGF-β superfamily, or competing for the complex formation between pathway-specific Smads and Smad4 (Nakao *et al.,* 1997b).

1.2.8 Role of bFGF in mesodermal induction.

Members of the FGF family of secreted signalling molecules are implicated in the regulation of cell survival, proliferation, migration and differentiation in embryonic and adult life of vertebrates (Fernig and Gallagher, 1994). In later stages, FGF signalling is required for various aspects of organogenesis, including the growth and patterning of the brain, initiation and outgrowth of the limb buds and tooth morphogenesis (Thesleff and Sharpe, 1997; Reifers *et al.,* 1998). The FGF family consists of two closely related isoforms (basic and acidic FGF). The existence of at least twenty FGFs have been discovered in vertebrates that are characterized by the presence of a conserved 120 amino acid core region. FGF signaling is established by specific interactions between ligands and receptors followed by a pathway in which these signals eventually activate genes that

encode transcription factors (Galsie *et al.,* 1997; Miyake *et al.,* 1998; Klint and Claesson-Welsh, 1999).

Both *bFGF* mRNA and protein have been shown to be present in the early embryo, while *bFGF* mRNA levels are high in oocytes, they drop by 25-fold during oocyte maturation and abruptly increase at the MBT when zygotic transcription of bFGF is activated. There is evidence that bFGF is present in the marginal zone and vegetal pole of the early blastula (Shiurba *et al.,*1991; Song and Slack, 1994). However, a more recent report shows that the distribution of bFGF protein and mRNA is found predominantly in the animal hemisphere of the blastula. Basic FGF is widely expressed in later development through neurula and tailbud stages in the central nervous and somatic tissue (Song and Slack, 1994). A number of biological experiments provides further evidence that bFGF is not a component of the vegetal inducing signal and casts doubt on a major role for bFGF in mesoderm induction. Basic FGF lacks a signal peptide. Although in some systems FGFs lacking a signal peptide have been shown to be secreted by novel mechanisms (Jackson *et al.,* 1992; Mignatti *et al.,* 1992), there is good evidence that bFGF is not secreted efficiently from cells of the early *Xenopus* embryo (Isaacs *et al.*, 1994).

The receptors for bFGF are from the tyrosine kinase receptor family. Dominant negative receptor mutants obtained by microinjection of RNA encoding truncated bFGF receptors cause severe deficiencies in developing embryos. bFGF signalling was found to be an essential component of the activin pathway. Animal caps dissected from embryos injected with dominant inhibitory mutants of truncated bFGF receptors did not elongate

upon activin treatment; transcription of *Xbra, Xnot, Mix 1* and *cardiac actin* genes is greatly inhibited, while transcription of some other genes, like *goosecoid, Xlim- 1* and *Xwnt- 8* is only slightly diminished (Cornell and Kimelman, 1994; LaBonne and Whitman, 1994).

There is rapidly growing information on molecules which may act downstream of the FGF receptor. bFGF signalling may be mediated by the bFGF receptor-ras-raf-MAP kinase kinase (MEK) MAP kinase pathway. FGFs elicit their signalling through the binding to the transmembrane tyrosine kinase FGF receptor (FGFRs). The four existing FGFRs genes encode seven receptor isoforms with different binding affinities for the various FGFs (Ornitz *et al.,* 1996). Binding FGF to the receptor induces dimerisation of the FGFRs. Activation of receptor leads to the autophosphorylation of a tyrosine residue of the receptor. This modification leads to the recruitment and phosphorylation of the lipid-anchored protein FRS2, which then interacts with the Src Homology 2 (SH2) domain-containing adapter protein Grb2 (Kouhara *et al.,* 1997). Grb2 then allows the binding of the guanine nucleotide exchange factor Sos, which meditates the activation of the membrane-bound monomeric G-protein Ras (Lowenstein *et al.,* 1992). This in turn induces the activation of the kinase cascade comprising Raf, mitogen-activated protein kinase (MAPK) and MAPK kinase (MEK), the last member of which finally enters the nucleus and phosphorylates target transcription factors (Sternberg and Alberola-Ila, 1998).

Animal cap cells are competent to respond to mesoderm induction by FGFs from early cleavage stages until the late blastulae stages in *Xenopus laevis* (Slack *et al.,* 1988)

At low concentrations of FGF, inductions are of an extreme ventral character (Slack *et al.,* 1987). Such animal caps form vesicles consisting of an "outer jacket" of epidermis surrounding loosely packed mesenchyme and a layer of mesothelium, while at higher concentrations the inductions are of a more lateral character with most of the explants contain a significant number of muscle blocks. However, even at the highest doses, explants taken from the animal pole region never form notochord in response to FGF treatment. FGFs have also been shown to be implicated in the establishement of anteroposterior and dorsoventral body axis (Lamb and Harland, 1995; Furthauer *et al.,* 1997).

1.2.9 Xenopus brachyury, a marker of mesoderm induction.

Xbra is the *Xenopus* homologue of mouse *brachyury* (Smith *et al.,* 1991), which has been implicated in mesoderm formation and notochord differentiation. The corresponding gene encodes a transcription factor containing the T-box and is expressed specifically in nascent mesoderm and in the differentiating notochord (Kispert and Herrmann, 1993; Herrmann and Kispert, 1994). In *Xenopus* the gene is activated after MBT in the marginal zone; transcripts are found at gastrula stage in a ring of involuting mesoderm and later within the notochord. As shown by animal cap explants, Xbra expression occurs as a result of mesoderm induction both in response to the natural signal as well as to bFGF and activin A. The expression of Xbra defines a developmental stage at which Xbra-expressing cells can respond to dorsal-inducing factors, like Xwnt-8 and noggin (Cunliffe and Smith, 1994).

1.2.10 Neurulation and beyond.

By late gastrula (stage 12-12.5), the blastopore is nearly closed and the yolk plug is small (Figure 1.4). By this stage the three germ layers have reached their definitive position (Keller, 1991).

Neurulation is the formation of the neural tube, the early embryonic precursor of the central nervous system. The first sign of neurulation in *Xenopus* is the thickening of the inner layer of dorsal ectoderm (Jones and Smith, 1999a). As ectodermal cells elongate and become columnar, they appear on the dorsal side of the embryo as a raised plate of cells, the neural plate. Then it proceeds by the formation of the dark pigment line along the dorsal midline of the embryo and neural folds, which form on the edges of the neural plate (Papalopulu and Kintner, 1994). These rise up, fold towards the midline and fuse together to form the neural tube, which sinks beneath the epidermis. The neural plate and neural tube extend along the anterior-posterior axis of the embryo. The elongation of the neural plate and neural tube is due to convergent extension, just as is found for the involuting/invaginating cells during gastrulation. The involuting dorso-anterior mesoderm induces the adjacent mesoderm to form anterior neural tissue. As the mesoderm migrates toward the former animal pole, it contacts progressively more overlying ectoderm, which is also induced to form anterior neural tissue. The anterior neural tube gives rise to the brain; further back, the neural tube will develop into the spinal cord (Kessler and Melton, 1994; Jones and Smith, 1999a).

The most lateral part of the neural plate, which is not incorporated into the neural tube, becomes the neural crest. Neural crest cells migrate from their initial position just

dorsal to the neural tube to many different positions in the body and give rise to the neurons of the sensory and autonomous (i.e., sympathetic and parasympathetic) nervous system, as well as other, non-neural cells such as melanocytes (pigment cells) (Jones and Smith, 1999a).

Neuroectoderm can be induced by elimination of BMP signalling by signals released from dorsal mesoderm such as: noggin, chordin, and follistatin (Weinstein and Hemmati-Brivanlou, 1999). Noggin and chordin were initially identified as secreted factors that can dorsalize the mesoderm. Follistatin is an activin antagonist that can also dorsalize mesoderm when injected as mRNA. Messenger RNA for all three factors can cause induction of neural tissues from the isolated animal cap of *Xenopus*. Likewise, all three are expressed in the dorsal lip and axial mesoderm of neurulae. BMP-4, is a TGF-ß family member that has strong mesoderm ventralizing and antineuralizing activity, which is expressed throughout the gastrula of *Xenopus*, except for the dorsal lip and animal cap regions (Figure 1.10). The proposed neural inducers (noggin, chordin and follistatin) all promote the formation of anterior neural tissue. Thus, additional factors are required to produce posterior neural ectoderm. Possible factors involved in posteriorization are FGF, retinoic acid and Wnt-3a (Sasai and De Robertis, 1997).

Finally, during and after neurulation, the mesoderm becomes subdivided into different tissues along the dorsoventral axis; the most dorsal mesodermal cell type is the notochord, a rod of vacuolated cells running the length of the embryo. Lateral to the notochord, are the cells of the somites, which in *Xenopus* form predominantly muscle, and lateral and ventral to the somites are the cells of the pronephros. The lateral

mesoderm goes on eventually to form structures such as the limbs, and the most ventral mesoderm becomes blood (Jones and Smith, 1999a).

Work of Agius *et al.* (1999) suggests that double inhibition of both the *Xnr-1* and *BMP-4* transduction pathways by Cerberus is sufficient for head induction in ventral mesoderm explants (Agius *et al.,* 1999). Two homeobox genes, *Xrx1 and Xvax2*, were identified to control key aspects of eye development. In particular, *Xrx1* appears to play a role in the early specification of anterior neural regions fated to give rise to retina and forebrain structures, and in promoting cell proliferation within these territories. On the other hand, *Xvax2* is involved in regulating the eye proximo-distal and/or dorsoventral polarity, and the morphogenetic movements taking place during formation of the optic stalk and cup (Lupo *et al.,* 2000). The secreted signalling molecule Sonic hedgehog (Shh) is essential for development of organizing structures at the ventral midline and the specification of neurons and glia (Goodrich and Scott, 1998). In addition, recent evidence has indicated that *Shh* regulates the proliferation of granule neuron precursors in the cerebellum (Dahmane and Ruiz-i-Altaba, 1999; Wallace, 1999; Wechsler-Reya and Scott, 1999). Proliferative effects associated with the *Shh* pathway activation have also been described in the developing neural tube (Goodrich *et al.,* 1997, Kalyani and Rao, 1998; Rowitch *et al.,* 1999) and retina (Jensen and Wallace, 1997; Levine *et al.,* 1997).

The main vertebrate features can be recognized in a tadpole stage of the frog. At the anterior end the brain is divided up into a number of regions. There are also three branchial arches, from which the most anterior one will form the lower jaw. More posteriorly, the somites and the notochord are well developed. A transverse section

through the trunk of a *Xenopus* larva shows a characteristic vertebrate pattern along the dorsoventral axis, with the notochord occupying the dorsal midline (Wolpert *et al.*, 1998). The somites are found ventral and lateral to the notochord, followed by lateral plate and mesenchyme. The *Xenopus* tadpole gut is composed of an outer smooth muscle layer, derived from the mesoderm, and an inner epithelial layer, derived from the endoderm (Chalmers and Slack, 1998). The post-anal tail of the tadpole is formed last. After organogenesis is completed, the mature tadpole hatches out of its jelly covering and begins to swim and feed. Later the tadpole larva will undergo metamorphosis to give rise to the adult frog; the tail regresses and the limbs form (Figure 1.4, stage 45) (Wolpert *et al.*, 1998).

1.3 Role of *Rel/ NF-κB* in the early development in *Xenopus.*

1.3.1 Signal transduction by Rel/NF-κB proteins.

Rel/Nuclear factor-κB (NF-κB) is a dimeric transcription factor comprised of 50 kDa and 65 kDa subunits. NF-κB was discovered as a regulator of immunoglobulin κ light-chain transcription through the "κB" site in the intron enhancer. Consistent with its role in κ gene expression, NF-κB was found constitutively in the nucleus in B lymphocytes. The primary role of the Rel/NF-κB transcription factors is to control a variety of physiological aspects of immune and inflammatory responses (Sen and Baltimore, 1986).

In mammals, the Rel family is composed of Rel (c-Rel), RelA (p65), NF-κB1 (p50), NF-κB2 (p52) and RelB, which have sequence similarity over approximately 300 amino acids in the amino-terminal half of the protein (the Rel homology domain (RHD),

which encompasses sequences required for DNA binding, dimerization with other subunits and interaction with the inhibitor of κB (IκB) family of inhibitor proteins (Baeuerle and Henkel, 1994; Baldwin, 1996). NF-κB subunits are able to homo- or heterodimerize to form transcription factor complexes with a range of DNA-binding and activation potentials. Although all Rel members bind DNA, only RelA (p65), c-Rel, and RelB have extended carboxy-terminal transcriptional transactivating domains (Verma *et al.,* 1995).

NF-κB1 and NF-κB2, which are derived by proteolytic cleavage from the N-terminus of the precursors p105 and p100 respectively, only comprise the RHD and are devoid of intrinsic transactivating function (Baeuerle and Henkel, 1994). The predominant form of NF-κB-like DNA binding activity found in most cells is the RelA/NF-κB1 heterodimer. With the exception of RelB, which only dimerizes with NF-κB1 or NF-κB2, the remaining subunits form all possible heterodimer or homodimer combinations (Baeuerle and Henkel, 1994). Rel/NF-κB transcription factors bind to 10 base pair DNA sites (κB sites) as dimers. The activity of NF-κB is tightly regulated by interaction with inhibitory κB (IκB) proteins. In most cells Rel/NF-κB is present as a latent, inactive, IκB -bound complex in the cytoplasm (Gilmore, 1999).

Various intracellular pathways evoked by a wide range of biological factors and environmental conditions (Figure 1.11) including inflammatory cytokines, phorbol esters, bacterial toxins (such as lipopolysaccharide), viruses, growth factors, UV light, free radicals and a variety of mitogens (Baeuerle and Henkel, 1994) can activate the Rel/NF-κB dimer by signaling degradation of the Rel/NF-κB inhibitor IκB protein

(Gilmore, 1999). The IκB family members have in common a series of ankyrin repeats, which interact with the DNA-binding domain and the nuclear localization signal (NLS) of NF-κB, thus maintaining the transcription factor as an inactive complex (Zandi *et al.*, 1997). IκB degradation uncovers a NLS in each subunit of the Rel/NF–κB dimer and allows the dimer to translocate from its inactive cytoplasmic location into the nucleus (Baeuerle and Henkel, 1994).

Almost all signals that lead to activation of NF–κB converge in a high molecular weight complex that contains a serine-specific IκB kinase (IKK). The IKK is an unusual kinase in that it contains two related kinases, IKKα and IKKβ, that are active as a dimer (Figure 1.11). Upon cellular activation, these inhibitors are rapidly phosphorylated on two amino-terminal serines, then ubiquitinated, and degraded by the 26S proteasome, releasing a functional NF–κB (Zandi *et al.,* 1997). The unmasked NF-κB can then enter the nucleus to activate the expression of a variety of genes including those encoding cytokines, growth factors, acute phase response proteins, immunoreceptors, other transcription factors, cell adhesion molecules, viral proteins and regulators of apoptosis (Ghosh and Chen, 1999). One of the target genes activated by NF-κB is *IκBα*. Newly synthesized IκBα can enter the nucleus, remove NF-κB from DNA, and export the complex back to the cytoplasm to restore the original latent state (Gilmore, 1999). Rel/ NF-κB are expressed in a wide variety of tissues and transactivate genes that are involved in the immune response, apoptosis, cancer, and development.

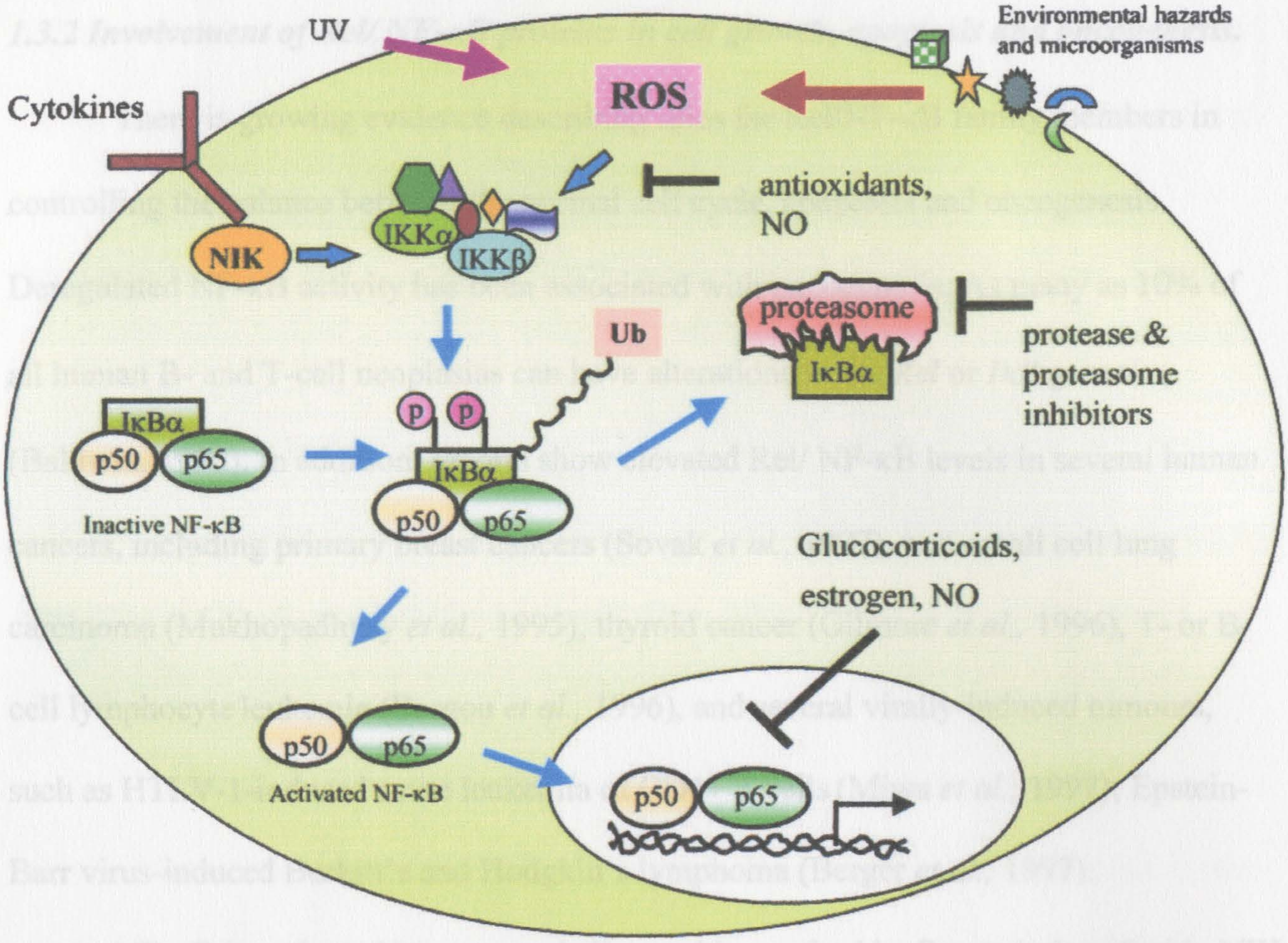

Figure 1.11 NF-κB activation and its inhibition.
Such extracellular inducers as: **reactive oxygen species (ROS), ubiquitin (Ub), ultraviolet light (UV)** can activate IκB kinase (IKK). Activated IKK can phosphorylate IκBα associated with NF-κB p50/p65 heterodimer. The activation of IKK and phosphorylation of IκBα can be blocked by antioxidants and NO. Phosphorylated IκBα then serves as a substrate for ubiquitination, which is followed by degradation of IκBα by proteasomes. The inhibitors of proteasomes or proteases can block this process. After degradation of IκBα, the p50/p65 complex translocates into the nucleus and binds to the κB-sites of gene promoters. Both glucocorticoids and NO can decrease the DNA-binding activity of NF-κB.
Activation (→); inhibition (---|).
Reproduced from Chen *et al.,* 1999.

1.3.2 Involvement of Rel/ NF-κB proteins in cell growth, apoptosis and oncogenesis.

There is growing evidence describing roles for Rel/NF-κB family members in controlling the balance between the normal cell cycle, apoptosis and oncogenesis. Deregulated NF-κB activity has been associated with oncogenesis. As many as 10% of all human B- and T-cell neoplasias can have alterations in the *Rel* or *IκB* genes (Baldwin, 1996). In addition, reports show elevated Rel/ NF-κB levels in several human cancers, including primary breast cancers (Sovak *et al.,* 1997), non-small cell lung carcinoma (Mukhopadhyay *et al.,* 1995), thyroid cancer (Gilmore *et al.,* 1996), T- or B-cell lymphocyte leukemia (Bargou *et al.,* 1996), and several virally-induced tumours, such as HTLV-1-induced acute leukemia of CD4+ T cells (Miwa *et al.,* 1997); Epstein-Barr virus-induced Burkitt's and Hodgkin's lymphoma (Berger *et al.,* 1997).

NF-κB is activated by oncogenic Ras and is required by Ras to induce foci in NIH 3T3 cells (Finco *et al.,* 1997). Hodgkin's lymphoma cells depleted of NF-κB activity revealed strongly impaired tumour growth in mice (Bargou *et al.,* 1997). The only member of this group that remains consistently oncogenic *in vitro* and *in vivo* is v-Rel, which induces oncogenic transformation in avian lymphoid cells (Gilmore *et al.,* 1996; Carrasco *et al.,* 1996). Still, the exact mechanisms by which these proteins contribute to the disregulation of cell growth remain unclear.

Members of the Rel/NF-κB protein family have been implicated in signal transduction programs to regulate apoptosis in a variety of cell types, either in positive or negative ways. The role of NF-κB in the apoptosis process is not straightforward, whether Rel/ NF-κB promotes or inhibits apoptosis appears to depend upon the specific

cell types and the type of inducer (Gilmore, 1999). The finding that NF-κB is activated during or immediately before cell apoptosis under certain stimulatory conditions has led to the suggestion that this transcription factor may function to promote apoptosis (Marianneau *et al.,* 1997; Baichwal and Baeuerle, 1997). Treatment of human thymocytes and promyelocytic leukemia cells with etoposide activates NF-κB and induces apoptosis (Bessho *et al.,* 1994). NF-κB is concomitantly activated with TNF α-induced apoptosis in certain cell types (Kitajima *et al.,* 1996). It has also been shown that inhibition of *NF-κB* gene activity by certain antioxidants prevents apoptosis (Bessho *et al.,* 1994).

Numerous recent studies have clearly demonstrated an anti-apoptotic role for NF-κB (Li and Stark, 2002). Rel/NF-κB was found to prevent cell death elicited by the cytokine tumour necrosis factor alpha (TNF-α). The ability of NF-κB to protect cells against chemotherapeutic drugs or TNF-mediated apoptosis function, demonstrates the need for NF-κB function for cell survival (Chen *et al.,* 1999). In the absence of NF-κB activation, TNF can trigger the caspase cascade by interacting with Fas-associated death domain protein, which then recruits and activates caspase-8 (Salvesen and Dixit, 1997; Green and Reed, 1998; Thornberry and Lazebnik, 1998). Active caspase-8 promotes cell death by either directly processing other downstream caspases or cleaving the cytosolic Bid protein, a proapoptotic family member of Bcl-2 (Green and Reed, 1998; Luo *et al.,* 1998). Truncated Bid translocates to mitochondria, resulting in the release of cytochrome c from mitochondria into the cytosol and the subsequent activation of apoptosis (Luo *et al.,* 1998). However, in the presence of NF-κB activation, the caspase-

8-mediated apoptotic pathway is suppressed (Wang *et al.*, 1998). Inhibition of NF-κB led to apoptosis in cells expressing oncogenic forms of Ras (Mayo *et al.*, 1997). Neiman *et al.* (1991) showed that v-Rel-transformed chicken tumour cells were resistant to apoptosis-inducing stimuli, such as radiation and dexamethasone, when grown in cell culture (Neiman *et al.*, 1991).

Recent demonstrations that cellular proliferation defects, attributed to the absence of NF-κB, are associated with a delay in cell cycle progression in G1 (Bargou *et al.*, 1997) in addition to the previously described physical association with NF-κB and CBP/p300 (Perkins *et al.*, 1997), establishes a link between NF-κB and regulators of the cell cycle. In addition, numerous studies indicate that NF-κB also functions in promoting cell growth. For instance, p50/p52 double-knockout animals fail to generate mature osteoclasts and B cells (Iotsova *et al.*, 1997), which also shows the critical roles of NF-κB in development.

1.3.3 Role of Rel/NF-κB proteins in development.

The role of NF-κB has expanded from an immune response factor for the development and function of B cells, to that regarding the development and function of many other cells, including T cells, thymocytes, dendritic cells, macrophages, and fibroblasts. Rel/NF-kappaB is also a critical factor in the embryonic development of multiple organ systems including the liver, lung, and limbs. Recent reports demonstrate the expression of Rel/NF-κB proteins in the proliferative zone of the developing avian limb bud and the requirement of NF-κB for the proper growth of this tissue. Inhibition of NF-κB activity in limb mesenchyme leads to an arrest in limb growth and a reduction in

expression of *Shh, Twist* and altered expression pattern of *BMP-4, Lhx-2, FGF-8, Msx-1* (Bushdid *et al.,* 1998; Kanegae *et al.*, 1998).

From a molecular standpoint, the development of the lung shows marked similarities to that of the limb. Both processes utilize many of the same signals to direct morphogenesis of the developing lung. Specifically, *FGFs, BMP-4*, and *Shh* regulate branching and proliferation of the lung epithelium (Hogan, 1999). NF-κB acts as a mediator of epithelial-mesenchymal interactions in the developing chick limb, directing gene expression that ultimately regulates cell growth or differentiation. High-level expression of *RelA* was found in the nonbranching lung mesenchyme but was not detected in the branching structures of the lung. Inhibition of mesenchymal *NF-κB* in lung cultures resulted in increased epithelial budding, while activation of *NF-κB* in the lung mesenchyme repressed budding. Expression patterns of several genes were altered in response to changes in mesenchymal NF-κB activity, including *FGF-10, BMP-4,* and *TGF-β1*. NF-κB represents the first transcription factor reported to direct the branching morphogenesis of the developing chick lung, functioning within the chick lung mesenchyme to limit growth and branching of the adjacent epithelium (Muraoka *et al.*, 2000).

There is evidence that *NF-κB* activates the *Shh* signalling pathway in the development of vertebrates (Bushdid *et al.,* 1998; Kanegae *et al.*, 1998). The only transcription factor shown to be directly downstream of Shh is the zinc-finger containing protein Gli, in vertebrates. In addition to normal development of limb (Bushdid *et al.*, 1998; Kanegae *et al.*, 1998) and lung (Muraoka *et al.,* 2000), Shh/Gli signalling is

required for normal patterning of the skeletal and nervous system, as well as in tumourigenesis (Matise and Joyner, 1999; Park *et al.*, 2000).

Other examples of the role of Rel/NF-κB proteins in development: in a mouse gene knockout study, disruption of the *RelA* (p65) locus led to embryonic death at 15–16 days of gestation, accompanied by massive degeneration of the liver as a result of apoptosis (Beg *et al.*, 1995). Mice with suppressed *NF-κB* reveal defective early morphogenesis of hair follicles, exocrine glands and teeth. These affected epithelial appendices normally display high NF-κB activity, the suppression of which results in increased apoptosis. Furthermore, NF-κB is required for peripheral lymph node formation and macrophage function (Schmidt-Ullrich *et al.*, 2001). Additionally, disruption of the *IKK1* locus in mice severely impairs signal activation of *NF-κB* and results in truncation of both the fore- and hindlimbs (Takeda *et al.*, 1999). In *NF-κB1 (p50)* gene knockout mice, development of immune cells was defective but these mice appeared to have normal embryogenesis (Sha *et al.*, 1995; Weih *et al.*, 1995).

Dorsal, a *Drosophila* fly homolog of NF-κB family members, is vital for the establishment of the embryonic dorso-ventral axis during development, it is localized to nuclei of blastoderm cells in a dorsal-to ventral gradient (Drier *et al.*, 2000). Genetic and biochemical studies indicate that dorsal activates body patterning genes such as *twist* and *snail* that specify mesodermal and neurogenic cell lineages. Activation of *twist* and *snail,* in ventral regions of early embryos, is the first step in the differentiation of the *Drosophila* mesoderm (Drier and Steward, 1997; Govind, 1999). In *Xenopus laevis* embryonic members of the *Toll/Spätzle* signalling pathway could induce a secondary

body axis, which suggests a possibility that a *Dorsal*-like morphogen might also exist in amphibians (Armstrong *et al.*, 1998). The exact role of NF-κB family members in the development of cell lineages and embryonic development remains to be defined.

1.3.4. Involvement of Rel/NF-kB in mesoderm induction.

In addition to acting as a mediator of epithelial-mesenchymal interactions in the developing chick lung (Muraoka *et al.*, 2000) and limb tissue (Kanegae *et al.*, 1998; Bushdid *et al.*, 1998), Rel/NF-kB proteins were also found to have a role in mesoderm induction (Beck *et al.*, 1998). Suppression of *Xenopus* RelA (XrelA) activity in early oocytes by expression of dominant inhibitor mutant of XrelA in animal caps blocks the induction of mesoderm and prevents the maintenance of Xbra expression by bFGF, showing that this mutant inhibits gastrula stage FGF signaling downstream of MAP kinase and Xbra expression. In addition, this mutant also prevents activin-generated elongation movements in animal caps (Beck *et al.*, 1998).

1.3.5 Interaction of NF-kB in activin signalling pathway.

Several studies show that NF-κB and TGF-β signaling pathways were found to interplay and oppose each other in coordinating cellular physiological responses. TGF-β was found to antagonize the activation of important target genes of proinflammatory stimuli of NF-κB in macrophages and lymphocytes, such as inducible nitric oxide synthetase (iNOS) and major histocompatibility complex (MHC) class I and class II antigens (Geiser *et al.*, 1993; Vodovotz *et al.*, 1996). Conversely, several stimuli of NF-κB inhibit activities of TGF-β in matrix synthesis, inflammation, apoptosis, and hematopoiesis (Oberhammer *et al.*, 1992; Snoeck *et al.*, 1996). Bitzer *et al.* (2000) report

a mechanism of suppression of TGF-β signaling by NF-kB/RelA-dependent pathways. Their results suggest that activation of NF-κB/RelA by a variety of pathogenic and proinflammatory stimuli inhibits TGF-β signaling at the level of TGF-β type I receptor function through increase of transcription of the *Smad7* gene and elevation of intracellular levels of Smad7 protein (Bitzer *et al.,* 2000). Smad7 is a regulatory protein which is able to inhibit TGF-β and activin signalling in a negative-feedback loop, mediated by a direct regulation by Smad3 and Smad4 via a Smad-binding element (SBE) in the Smad7 promoter. Interestingly, it was found that the Smad7 promoter was also regulated by nuclear factor κB (NF-κB). Expression of the NF-κB p65 subunit was able to inhibit the Smad7 promoter (Nagarajan *et al.,* 2000). Activin A was also found to induce growth arrest of rat hepatocytes *in vitro* and *in vivo*. It was also demonstrated that the induction of Smad7 by the α1-adrenergic agonist, norepinephrine, enhances epidermal growth factor-stimulated DNA synthesis and inhibits activin A-induced growth inhibition) is dependent on NF-κB (Kanamaru *et al.,* 2001). These observations indicate that there exists an intrinsic interaction between these two signalling pathways that might be dependent on the cellular context, as well as the nature of gene expression.

1.3.6 Rel/NF-κB proteins in Xenopus laevis development.

In *Xenopus laevis,* a number of Rel/NF-κB proteins have been identified that are known to be expressed in the early stages of *Xenopus* development: Xrel2 (Tannahill and Wardle, 1995), XrelA (Kao and Hopwood, 1991; Richardson *et al.,* 1995; Kao and Lockwood, 1996), and XrelB (Suzuki *et al.,*1995), Xp100 (Suzuki *et al.,* 1998) and Xrel3 (Yang *et al.,* 1998).

Wild type *XrelA* has a role in dorsoventral patterning. *XrelA* mRNA is present throughout oogenesis and during early embryogenesis. The mRNA is relatively evenly expressed over the whole embryo during the early embryonic stages (Kao and Hopwood, 1991; Richardson *et al.,* 1995), but the protein becomes localized to the nuclei of animal and marginal zone cells at MBT stages (Bearer, 1994). The presence of Rel-related factor in the nuclei of these cells prior to MBT suggests that XrelA may be involved in programming animal cells to respond to vegetal-inducing factors (Bearer, 1994).

XrelA overexpression experiments have suggested its involvement both in patterning of the head and tail of the embryo (Richardson *et al.,* 1995) and also in dorsal-ventral development (Kao and Lockwood, 1996). High levels of overexpressed XrelA causes gastrulation arrest while lower levels resulted in embryos that appeared to gastrulate normally but show exogastrulation to variable degrees with a split posterior axis made up of a duplicated notochord and nervous system in tail. If these embryos were left to develop up to the stage 30 they show little evidence of a dorsal axis, head or tail and look similar to UV ventralized embryos (Scharf and Gerhart, 1980). They also lack visible segmentation or somites but seem to have nervous tissue. The least affected embryos have a kink in the mid-axial region, which is associated with the locally disrupted segmentation and a small, poorly organized spinal cord in the mid-body. In all embryos the affected regions are characterized by disruption of tissue organization, poor segmentation and reduction in size of the nervous system. The most normal tissue is the notochord.

The expression of early markers of dorsal and mesodermal-specific genes were not affected by XrelA (Richardson *et al.,* 1995). Kao and Lockwood (1996) extended the findings of Richardson *et al.* (1995) and showed that XrelA has a significant effect on dorsoventral patterning. Embryos injected with *XrelA* RNA only in the dorsal marginal zone reduces dorsal development and attenuates *in vitro* dorsal morphogenetic movements. XrelA alters normal dorsoanterior patterning by altering gastrulation movements, specifically delaying blastopore lip formation, attenuating convergent extension, and reducing notochord formation. XrelA strongly reduces the strong axis duplication-producing effects caused by overexpression of a dominant negative mutant of *Xenopus* glycogen synthase kinase-3ß, (Xgsk-3ß). Overexpression in dorsal regions of XrelA reduces dorsoanterior development in a dominant manner, while overexpression of dominant negative Xgsk-3ß mutants in ventral regions induces a complete secondary axis (Kao and Lockwood, 1996).

Xenopus XrelB appears to have a different role in development from the XrelA. XrelB transcripts are present at all stages of oocyte maturation and in adult tissues examined. However, in staged embryos XrelB is undetectable from neurula to stage 28 and resumes expression at stage 47 (Suzuki *et al.,* 1995).

Xp100 transcript expression patterns suggest the possibility that Xp100 could be involved in the late-stage development of *Xenopus laevis*, especially in the maturation of somites. Xp100 transcripts are present at all stages of oocyte maturation and in all adult tissues examined; they decrease at the gastrula stage and resume their expression at the neurula stage. Xp100 is highly expressed in somitogenic mesoderm at the neurula stage,

while in the gastrula and tailbud stages Xp100 transcripts are not localized to restricted regions (Suzuki *et al.*, 1998).

Xenopus Xrel2 also seems to have key functions in early vertebrate development, since it is expressed throughout development but with higher levels in pre-gastrula embryos. Ectopic expression of Xrel2 disrupts normal morphogenesis at the early gastrula stages suggesting that the NF-κB /Rel family has developmental functions at stages earlier than previously thought. It does not seem to be involved in diversion of animal caps from an ectodermal to a mesodermal cell fate (Tannahill and Wardle, 1995).

1.3.7 Xrel3, a novel member of the c-rel proto-oncogene sub-family.

Xrel3 is the first and only *rel* gene that was found to be expressed in a spatio-temporally restricted manner in an early vertebrate embryo. *In situ* hybridization analysis indicates that *Xrel3* mRNA is expressed in two phases of early development. *Xrel3* mRNA is present in early cleavage stages of the embryos up to the late blastula, and then the message levels decline at gastrulation to undetectable levels. In later neurula and larval stage embryos the messages accumulate in the forebrain, dorsal aspect of the mid- and hindbrain, the otocysts and notochord of forebrain and otic placode and in the dorsal part of the mid-hindbrain. Protein analysis indicate that it shares only 64% sequence similarity to Xrel2 and none of the non-coding sequence is shared between *Xrel3* and any of the *Rel* genes (Yang *et al.*, 1998).

The significant finding about this gene is that when *Xrel3* is overexpressed in early embryos by microinjecting synthetic mRNA into two-cell stage embryo in the prospective ectodermal region (animal pole), the embryos develop abnormal growths, or

tumours, after neurula stages (Yang *et al.,* 1998; Lake *et al.*, 2001), similar to tumours induced by overexpression of *Gli1* gene (Dahmane *et al.,* 1997), a zinc-finger transcription factor that is also involved in neural differentiation in *Xenopus* and is an oncogene that is up-regulated in human gliomas, sarcomas (Kinzler *et al.,*1987; Roberts *et al.,* 1989) and basal cell carcinoma (Dahmane *et al.,* 1997). These tumours were actually observed as "warty patches" caused by overexpression of XrelA, described previously by Richardson and colleagues (Richardson *et al.*, 1995). Larger tumours are produced with *Xrel3* as compared to with *Gli1* and lower doses of *Xrel3* mRNA (~200-500 pg) are necessary to induce tumour formation as compared to *Gli1* mRNA (2000 pg; Dahmane *et al.,* 1997).

The size of the tumours is proportional to the dosage of RNA injected, and their position on the embryo depends on the location of injection: epidermal tumours develop from animal pole injection (prospective ectoderm) while tumours in the endoderm (digestive system) develop from vegetal pole injection (Yang *et al.,* 1998). The *Xrel3*-induced epidermal tumours were found to express *Otx2, Shh* and *Gli1*, as well as high levels of *Xrel3* mRNA, but not in unaffected skin or uninjected embryos (Lake *et al.,* 2001), demonstrating a possible correlation between *Xrel3, Shh* and *Gli1* expression. Shh protein is secreted from the notochord during embryonic development. One of its functions is to impart dorsal-ventral pattern to the spinal cord (Pownall, 1994). Similarly, abnormal upregulation of *Gli1* expression of uncontrolled and inappropriate stimulation of the *Shh* signalling pathway, which leads to *Gli1* upregulation, results in basal cell carcinoma (Hahn *et al.,* 1999; Britto *et al.*, 2000).

When embryos were injected into the dorsal side of a zygote with a dominant interference mutant of *Xrel3*, the C-terminal deletion mutant, *Xrel3delta58*, which dimerizes with endogenous Xrel3 and prevents its binding to DNA (Lake *et al.,* 2001), the embryos developed normally until neurulation, when they failed to develop head structures and lacked expression of *Shh, Gli1* and *Otx-2* (Lake *et al.,* 2001), genes that are required for head development (Hynes *et al.,* 1997; Acampora *et al.,* 2000). These results demonstrate that *Xrel3* is required for *Xenopus* head development and for the transcriptional activation of genes of the *Shh/Gli1* pathway in the embryonic tumours (Lake *et al.,* 2001). Still the relationship between the initiation of tumours by *Xrel3* and *Shh/Gli1* signaling remains to be established. Because *Xrel3*-induced tumours express neural patterning genes (Lake *et al.*, 2000), and *Xrel3* is expressed in the developing brain (Yang *et al.,* 1998), it is likely to have a role in neural development.

Given that *Xrel3* is expressed in two stages of development (before and after gastrulation) I predicted that *Xrel3* might have distinct functions in both pre- and post-gastrula development. It is possible to assume that tumour formation could result from Xrel3 activation of oncogenic genes such as *Shh* and, subsequently *Gli1*, or since Xrel3 caused larger tumours to form than *Gli1, Xrel3* might be acting as a regulator of tumourigenesis. *Shh* and *Gli1* mRNA were detected in tumours at a time when their endogenous expression is activated, that is during late gastula or early neurula. This event is long after the injection of *Xrel3* in the two-call stage embryos, and by the neurula stage the effects of the initially injected RNA will have turned over by late gastrulation, it is likely that Xrel3 initiates a series of events that lead to hyperproliferation of the injected

cells. The tumours developed from an event that occurred before activation of these oncogenes. Also, since *Xrel3* mRNA overexpression induced tumours when it was injected into the vegetal pole (prospective digestive system) (Yang *et al.,* 1998), suggests that *Xrel3* may have a more generalized role in tumour formation.

1.4 Objectives.

The purpose of this research was to determine a possible role of *Xrel3* in pre-gastrula embryos, specifically what happens in *Xrel3*-expressed embryos before and after the MBT, and also further investigate the origin and cause of tumours with respect to *Xrel3* overexpression.

1.4.1 Objective 1.

I wanted to gain further insight into the role of Rel/NF-κB in regulating cell growth and development, with the particular emphasis on the timing in development of the requirement for proliferating-promoting activity of *Xrel3*. I observed and analysed the early events in development before MBT stage that lead to tumour formation later in neurula stages. I investigated possible mechanisms that trigger tumour formation that occur before the MBT.

I propose that ectopic *Xrel3* expression does affect pre-gastrula development. I wanted to extend the findings by Yang *et al*. (1998) on what morphological and phenotypical effects would be on the embryo development if *Xrel3* was overexpressed in different concentrations, or in different sites of the two-cell stage embryos.

1.4.2 Objective 2.

Xrel3 regulates cell differentiation during embryogenesis and can be explained if we propose that at least one of its cellular effects is to delay the onset of MBT. As mentioned above (see section 1.2.3), the MBT is an early developmental event characterized by loss of embryonic cell division synchrony, slowing of DNA synthesis, activation of zygotic transcription and activation of cell differentiation (Newport and Kirschner, 1982a,b). There are several testable possibilities that can be explored to determine if this is the case. These are to determine whether *Xrel3*:

1. Delays the start of embryonic transcription of zygotic genes;

2. Inhibits the expression of molecular markers of the MBT;

3. Inhibits growth factor-induced differentiation.

In 1999, it was demonstrated (Kao, unpublished data) that *Xrel3*-injected animal caps are composed of more cells than control animal caps, resulting in a thickened blastocoel roof. I would like to determine how *Xrel3* regulates the MBT.

I propose that overexpression of *Xrel3* delays the entry of embryos into the MBT stage. The cells delay initiation of transcription of zygotic genes by a few hours, and/or will fail to migrate normally, which will result in more cells that abnormally accumulate in one region, failing to spread. I propose that the function in the pre-gastrula development of *Xrel3* is to maintain cells in the pre-MBT, proliferative state.

1.4.3 Objective 3.

I would like to determine if *Xrel3* overexpression delays the expression of markers of the MBT. Markers of embryonic transcription, *Ornithine Decarboxylase*

(ODC) and *Elongation Factor 1 α (Ef-1α)* become expressed in all cells after the MBT (Krieg *et al.*, 1989; Amaldi *et al.*, 1993), and the expression of their mRNA will be assayed using reverse transcriptase-linked polymerase chain reaction (RT-PCR). ODC levels normally increase at gastrulation while Ef-1α levels increase immediately at the MBT (Krieg *et al.*, 1989; Amaldi *et al.*, 1993). If these genes are expressed later than usual in *Xrel3*-injected embryos, then I will conclude that *Xrel3* delays MBT.

1.4.4 Objective 4.

In addition to loss of cell division synchrony and activation of embryonic transcription, the cells at MBT become responsive to factors that induce them to form mesoderm. To test whether *Xrel3*- expressing cells lose their ability to respond to mesoderm inducing factors, they will be treated with the potent mesoderm inducers, activin A and /or FGF and assayed for mesoderm marker expression using RT-PCR. I would like to determine *Xrel3* involvement in mesoderm formation. I will examine the effect of *Xrel3* expression on mesoderm induction, differentiation, and expression of mesodermal markers, such as *Xbra* (Smith *et al.*, 1991) described above (see section 1.2.9). I propose that *Xrel3* may be an important regulator of the initiation of cell differentiation in development, and causes tumours by preventing differentiation.

1.4.5 Objective 5.

To determine possible involvement of *Xrel3* in FGF or activin pathways. To determine the role of *Xrel3* in regulation of FGF- and/or activin-mediated mesoderm induction. Although activin plays a role in dorsal and anterior mesoderm formation

(McDowell and Gurdon, 1999), its activity is dependent on FGF induction (Schulte-Merker *et al.,* 1994), and, unlike FGF (Beck *et al.,* 1998) there has been no direct link between Activin and Rel protein activity. This area is still nonetheless certainly worthwhile to investigate for future consideration.

CHAPTER 2.

MATERIALS AND METHODS.

2.1 Animals and embryos.

Mature wild-type and albino *Xenopus laevis* adult males and females were obtained from Nasco Co., (WI, USA). They were kept in dechlorinated tap water at room temperature (RT) between 18°C and 22°C, and fed Purina Trout Chow twice a week. Females were induced to ovulate by injection of 500 I.U. (0.5 mL) of human chorionic gonadotropin (HCG, Sigma Chemical Co., MO, USA) into their dorsal lymph sacs, and placed in dechlorinated water and kept overnight in the dark at RT. Embryos were usually available after 14 to 16 hours.

To obtain testes, a male *Xenopus* was killed by heavy anesthesia using 3-aminobenzoic acid ethyl ester (methanesulfonate salts, MS222, Sigma). The testes are pale, curved structures about 1 cm long, which are positioned on either side of the spine. They were removed by making an incision in the ventral surface of the animal and they were stored in normal amphibian medium (NAM) (See Appendix A Table 1; Slack, 1984) at 4°C for up to one to two weeks.

Xenopus females start laying eggs in the morning after injection (Jones and Smith, 1999b). Embryos were obtained by *in vitro* fertilization as follows: a sperm suspension was made by macerating 1/8 of a testis in NAM solution in the Petri dish (Fisher). The sperm suspension was spread evenly over the entire bottom of a Petri dish (35 mm in diameter). Eggs squeezed from a gravid female by gentle peristasis of their ventro-lateral surfaces were spread over the sperm suspension, and 0.9 mL of distilled water was

immediately added. After five minutes the eggs were flooded with more water. After about fifteen minutes the eggs rotate so that their heavily pigmented animal hemisphere is uppermost (see Figure 2.1). This is a reliable sign of successful fertilization (Jones and Smith, 1999b).

Embryos were "dejellied" in 2% cysteine hydrochloride (Sigma Chemicals Co), pH adjusted to 7.8-8.1 with 1% sodium hydroxide (NaOH) (Fisher), and rinsed in distilled water and then in NAM/20 solution (Appendix A, Table 1B). Embryos were cultured in NAM/20 solution in Petri dishes at 14°C, 18°C and 23°C (RT), and staged (see Introduction Figure 1.5) according to Nieuwkoop and Faber (1994). Eggs began to cleave about ninety minutes after fertilization, which is when the RNA injections were carried out (Jones and Smith, 1999b).

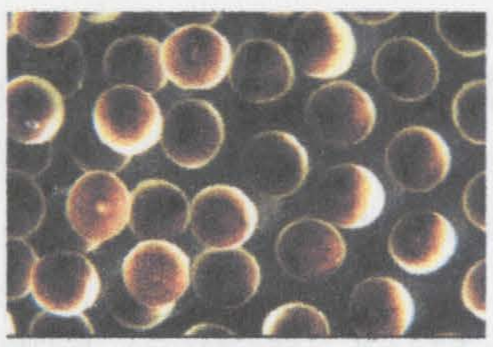

Figure 2.1 Fertilized wild-type oocytes, rotating so that their pigmented animal side is uppermost, view from above.

2.2 Microinjection equipment.

Microinjection needles were prepared from capillary tubing (# 3-000-203-G/X made by Drummond Scientific Company; USA) using a needle electrode puller (PB-7, Narishige, USA, Inc.). The diameter of the needles I made were no more than 15 μm. Needles were baked to 180°C to destroy RNAse activity, and stored in a dust-free

atmosphere. Needles were sharpened using a Pipette grinder (Model EG-4, Narishige USA, Inc; settings: speed 50, angle 20°) for thirty seconds and viewed with an Olympus SZ40 stereomicroscope.

2.3 Embryo microinjection and manipulation.

Two-cell stage embryos were microinjected with mRNA (Introduction Figure 1.5 for stages) in 4% Ficoll (Fisher) in NAM/2 (Appendix A, Table 1B) solution. Embryos to be injected were positioned within a plastic mesh grid.

Injections of RNA were carried out using a Drummond microinjection system (Nanoject II, Drummond Scientific Co., USA) under a dissecting stereomicroscope. The injection needle was attached to the Drummond micromanipulator injection system. About 2 μL of the injection sample was dispensed onto a small piece of parafilm and pulled up into the needle. Injection volumes ranged from 5-10 nL of the sample into a fertilized egg. Microinjection of embryos was done as described by Kao and Lockwood (1996) using 500-1000 *p*g capped, synthetic *Xrel3* mRNA made using the Ribomax RNA production kit (Promega). Dilutions prior to injections were performed using Diethyl Pyrocarbonate (DEPC, Sigma)-treated water. For controls equal volumes of DEPC-water were injected. Injected embryos were left to develop until the desired stage at 14°C, 18°C and 23°C (RT).

2.4 Preparation of synthetic RNA.

Synthetic mRNA was transcribed and capped as per Krieg and Melton (1987), using the SP6 RiboMAX Large Scale RNA production systems (Promega Co.,WI, USA)

and 7-methyl guanine cap analogue (New England Biolabs, Inc., Missisauga, Ontario). Template DNA was linearized using the restriction endonuclease *NotI* (Pharmacia Biotech, PA, USA) prior to *in vitro* transcription. Purified linear DNA was examined by 1% agarose gel electrophoresis prior to transcription to verify complete linearization and to ensure the presence of a clean (non-degraded) DNA fragment of the expected size. Digested and undigested DNA was compared. The reaction was phenol/chloroform extracted and precipitated in 100% ethanol and $1/10^{th}$ volume of 3M sodium acetate (pH 5.3) to purify. DNA was re-suspended in 10 μL of dH_2O and run on a gel to estimate the concentration of the pure DNA from the intensity of the band (compared with the intensity of 1650 of kb ladder, which corresponds to the 80 ng/μL of DNA). For the RNA transcription procedures we used ~5 μg of DNA. Template, rNTPs, cap analogue and RNA polymerase were assembled at room temperature in an 1.7 mL Eppendorf centrifuge tube to a total volume ~50 μL (see Appendix B, Table 2 for solutions and amounts used). The reaction mixture was then gently pipetted up and down; centrifuged briefly using Micromax centrifuge (International Equipment Company, USA); incubated at 37°C in a Fisher water bath for tow to four hours prior to the addition of a 5 μL (5U) of RQ1-RNase-free DNase (1U/μL; Promega) and continued incubation at 37°C for twenty minutes. Following transcription the DNA template was removed by adding ~100 μL of nuclease-free H_2O and then phenol/chloroform extracted with equal volumes of buffer saturated phenol and water saturated chloroform (155 μL each). The remaining top aqueous layer from the extraction was then ethanol precipitated as follows: 1/10 of 3M sodium acetate (pH 5.2) plus 2.5 x volume of absolute ethanol for 2-5 minutes on ice,

centrifuged full speed (13,200 rpm) for 5 minutes, washed pellet with 70% ethanol and then re-suspended. The newly synthesized RNA was ethanol precipitated further two times prior to re-suspension in 50 μL of nuclease-free H_2O and stored in -70°C. Purity of the RNA was determined through a comparison of optical density readings at the wavelengths of 260 and 280 (OD_{260} and OD_{280}). An OD_{260} /OD_{280} ratio of greated that or equal to 2.0 indicated that the RNA was pure. Concentrations were determined through the comparison of OD_{260} readings (quantify the RNA by UV light absorbance at 260 nm using Spectrophotometer DU-64 (Beckman, USA); OD_{260} unit = 40 μg/mL of RNA), and by electrophoresis of the RNA on 0.8-1% agarose gel. The presence of a single band of about 850 to 1000 bp in size indicated that the RNA was intact.

2.5 Embryo manipulations and analysis.

To start the investigation of the effect of *Xrel3*-overexpression on the phenotypical and morphological changes that can occur in the early development of *Xenopus laevis*, different concentrations of *Xrel3* mRNA (0 ng; 0.5 ng; 1.0 ng; 2.0 ng and 4.0 ng) were injected into the animal pole region of pigmented two-cell-stage embryos. Embryos were cultured in 4% Ficoll. The development was monitored using Nieuwkoop and Faber (1994) and about thirty embryos per each stage were fixed in Smith's fixative: a mixture of one part formalin and nine parts Smith's reagent, consisting of 2.5 mL glacial acetic acid, 0.5 g potassium dichromate and 100 mL double-distilled water; and left overnight in a dark place to prevent light penetration. The next day embryos were washed with tap water and stored in 4% formaldehyde at RT. Fixed embryos were analyzed at stages: 11, 20, and 25 (Nieuwkoop and Faber, 1994), scored for abnormalities

and photographed using an Olympus U-PMTVC camera (RS-Photometrics, Japan) attached to an Olympus SZ-PT stereomicroscope (Japan). Lights were provided by Eco-Light 20 Fiber Optic light source (Applied Scientific Devices Corp, USA).

Wild-type embryos were injected with 0.5 ng of *Xrel3* mRNA or DEPC-treated water as controls into different zones of two-cell stage embryos (100 embryos each): animal, marginal and vegetal regions (Figure 2.2). As controls the same volumes of DEPC-treated water were used. Representatives from control and injected embryos were collected, fixed at stages 9, 11.5-12, 20, and 32 in Smith's fixative (as above) and left overnight in a dark place to prevent light penetration. The next day embryos were washed with tap water and stored in 4% formaldehyde at room temperature. Fixed embryos were scored for abnormalities and photographed.

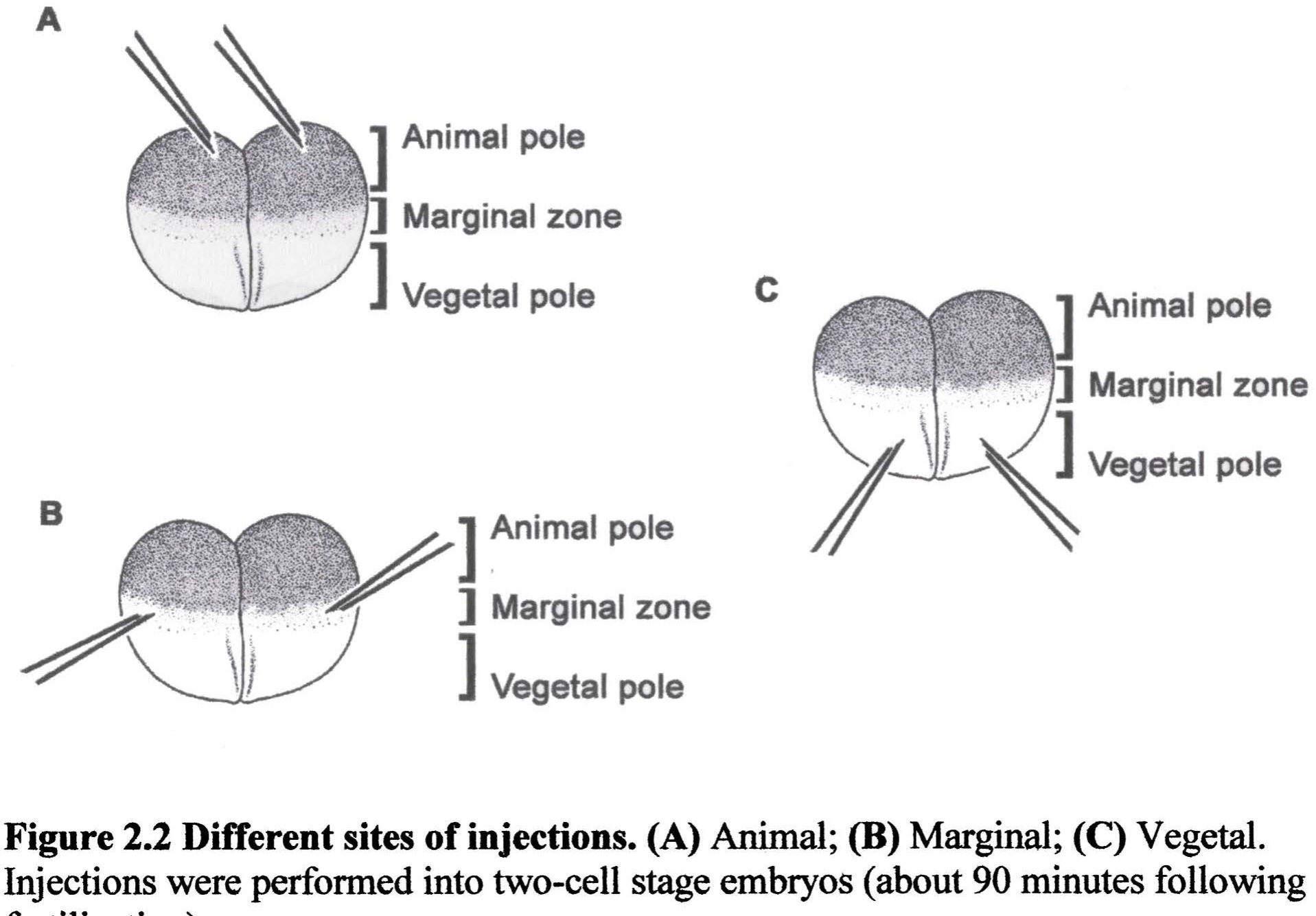

Figure 2.2 Different sites of injections. (A) Animal; **(B)** Marginal; **(C)** Vegetal. Injections were performed into two-cell stage embryos (about 90 minutes following fertilization).

For the assessment of the effects that the injection site at the marginal zone has on the development, wild-type embryos were injected with 0.5 ng of *Xrel3* mRNA or control RNA in the dorsal or lateral (Figure 2.3) marginal zone (>100 embryos each). To fix the position of the dorsal side, fertilized eggs were immersed in agarose wells in 4% Ficoll solution and tilted with the sperm entry point facing gravity as described previously (Gimlich, 1986; Kao and Lockwood, 1996). RNA was injected at the animal-vegetal pigment border at the two-cell stage on either side of the cleavage furrow for dorsal injections. For lateral injections, embryos were allowed to start second division and were injected on either side of the forming cleavage furrow, when it reached the marginal zone (Figure 2.3). The development was monitored and about 30 embryos per each stage were fixed in Smith's fixative (as above) and analyzed at stages: 10.5, 20, and 32. Embryos were scored for abnormalities and photographed. Each of these experiments was performed at least three times.

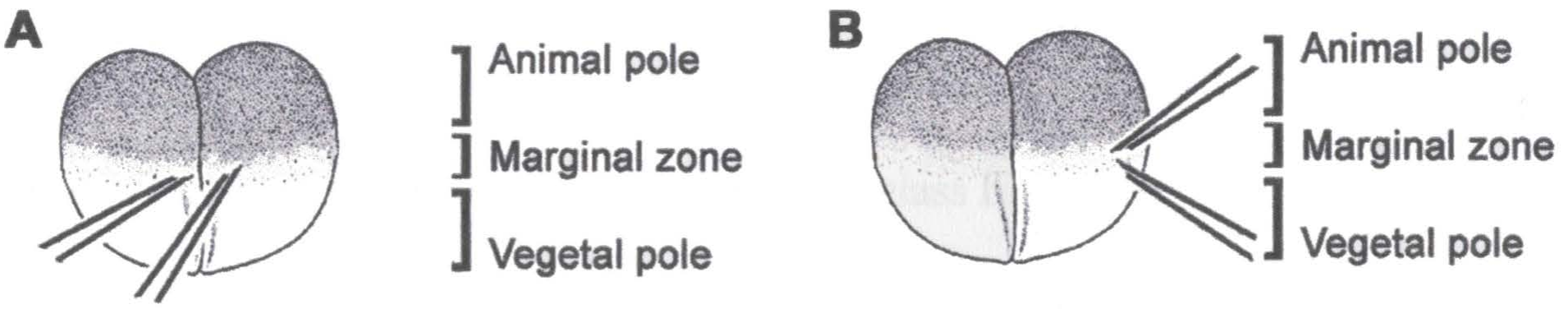

Figure 2.3 Different sites of injections. (A) Dorsal marginal zone; **(B)** Ventral marginal zone. Injections were performed into two-cell stage embryos (about 90 minutes following fertilization).

To continue with the investigation of the morphological changes that can occur in the early development of *Xenopus laevis* as a result of *Xrel3* overexpression, different

concentrations of *Xrel3* mRNA were injected into pigmented two-cell-stage embryos into the animal pole region. Embryos were cultured in 4% Ficoll solution. Two whole embryos from each stage were collected at stages 7, 9 and 11 for RT-PCR analysis (Hopwood *et al.*, 1989) with such primers as: *Histone, ODC, EF-1α, Xbra, Chordin* and *Xrel3* to check if overexpression of *Xrel3* will have any effect on activation of these markers (see below sections 2.9-2.14). The expression of these transcripts was analyzed on 2% agarose gel and normalized by histone.

2.6 ^{35}S-UTP incorporation experiment.

Pigmented two-cell-stage embryos were coinjected with 1000 pg of *Xrel3* mRNA and 50 nCi [α-^{35}S] UTP (400 Ci/ mmole, Amersham) and cultured in 4% Ficoll, in parallel with the control siblings injected with 50 nCi [α-^{35}S] UTP only and non-injected controls. Starting from stage 7, samples of 15 injected and control embryos were collected at each time point (stages 7, 8, 9, 10 and 11) and frozen at -20°C prior to being processed. Total RNA was purified by the use of NETs RNA extraction method (Hopwood *et al.*, 1989) adjusting the volumes accordingly for 15 embryos, and 20 μL of total RNA from each sample were immobilized on glass fiber filters (GF/A) (Whatman).

The filters were washed subsequently with ice-cold 20%, 10%, and 5% trichloroacetic acid (Fisher). Incorporated label was detected by a Liquid Scintillation Analyzer (Beckman LS-3801, USA) (Stancheva and Meehan, 2000).

2.7 Animal Conjugates

Vitelline membranes were removed (Figure 2.4) from stage 7-8 embryos using sharpened forceps in 50% NAM solution. Animal pole regions (caps) were dissected from the centre of the pigmented regions of the embryos. This was done using a pair of forceps as scissors, while keeping the embryos still using a pair of forceps held in the other hand. Dissected animal caps were placed with their originally outer surface down and cultured in NAM/2 in Petri dishes coated with 2% agarose at 18-22°C, allowing them to heal slightly. Explants were then either cultured in NAM/2 or for experiments involving explants and mesodermal induction, the NAM/2 medium also contained 0.1% BSA (albumin, bovine; Sigma) plus different concentrations of *basic fibroblast growth factor (bFGF*; a gift from Laura Gillespie; Health Sciences Center, St. John's, NF) or *activin*-producing *Xenopus* tissue culture conditional medium XTC-CM (a gift from Laura Gillespie).

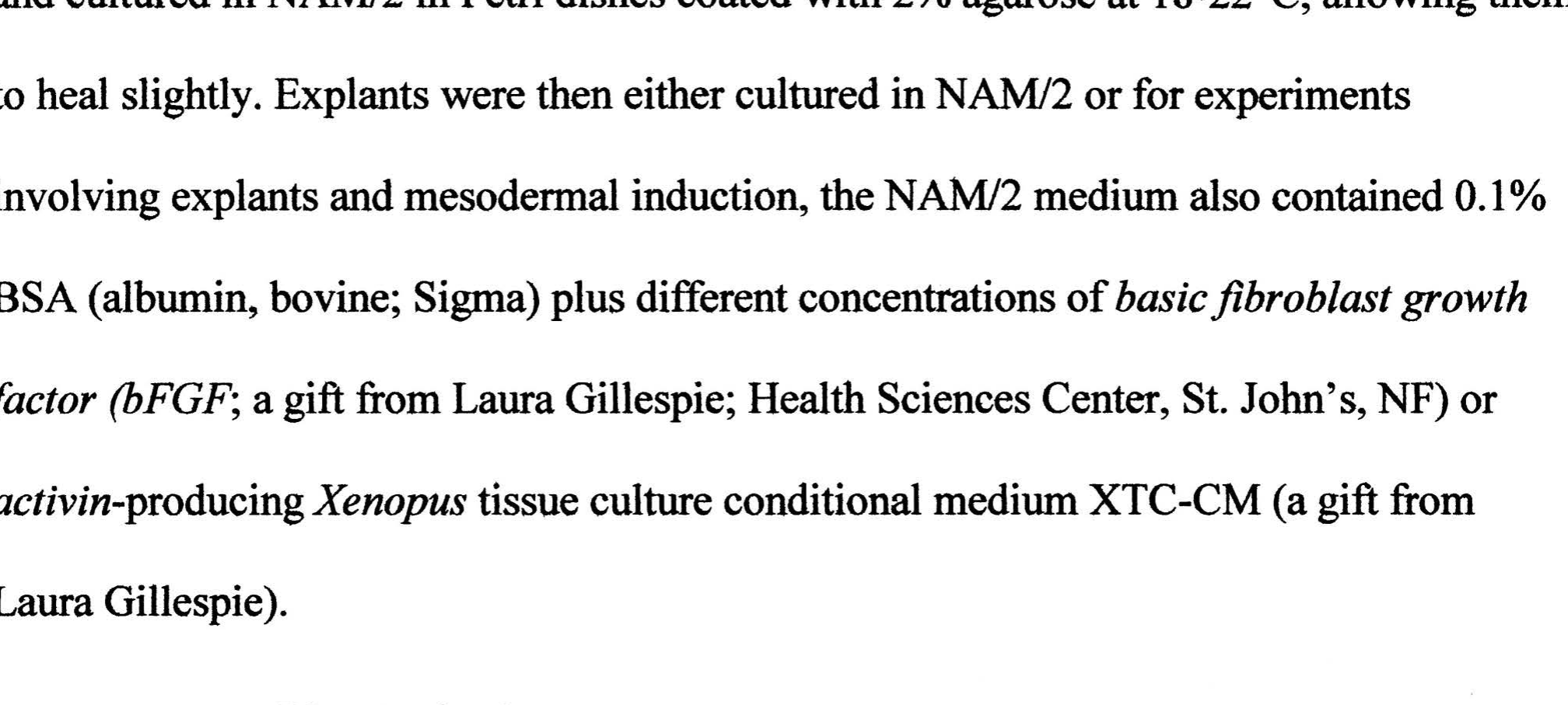

Figure 2.4 Dissection of animal caps from stage 7-8 embryos, which were cultured in NAM/2 or in the case of mesoderm induction experiment NAM/2 medium also contained 0.1% BSA plus factors: bFGF or activin.

2.7.1 Analysis of the expression levels of markers of MBT.

For the analysis of the MBT markers in *Xrel3*-injected embryos, ~200 wild-type embryos were injected into the animal pole at the two-cell stage with 1.0 ng *Xrel3* RNA or injected with control and let develop until stage 7 at room temperature. Animal caps (five caps at each time point) were isolated from control and *Xrel3*-injected embryos starting at stage 7. Samples were collected every thirty minutes initially until stage 9, and then collected at such stages as 10 and 11. Total RNA was extracted from collected animal caps according to NETs/LiCl protocol (Hopwood *et al.,* 1989). Reverse transcription was performed with random primers (see below sections 2.9-2.14). PCR was performed with ^{32}P-ATP trace labelling and gene-specific primers for *EF-1α, ODC* and *histone*. The expression of these transcripts was analyzed on 6% polyacrylamide sequencing gel. Levels of *EF-1α* and *ODC* were normalized by *histone*. Levels of each marker on the gel were assessed by spot densitometry analysis (see section on quantitation of PCR products in section 2.14).

For the analysis of the expression levels of DNA methyltransferase (Dnmt1*)* enzyme in *Xrel3* and control embryos, ~100 wild-type embryos were injected into the animal pole at the two-cell stage with 1.0 ng *Xrel3* RNA or injected with control and let develop until stage 7 at room temperature. Animal caps (five caps at each time point) were isolated from control and *Xrel3*-injected embryos starting at stage 7. RT-PCR (Hopwood *et al.,* 1989) was performed with gene-specific primers for *XDnmt1* and *histone* (see below sections 2.9-2.14). The expression of these transcripts was analyzed on 2% agarose gel. Levels of *XDnmt1* were normalized by *histone* and assessed by spot densitometry analysis.

2.8 Induction of mesoderm in Xrel3-injected animal caps using bFGF or activin.

Animal caps were dissected at stage 8 (Figure 2.4) from embryos injected in the animal pole region with 0.5 ng either *Xrel3* or control, treated with varying concentration of recombinant *Xenopus* bFGF or with XTC-CM, which was heated to the temperature of 95°C for five minutes prior to use. Explants were left to develop overnight in NAM/2 medium also contained 0.1% BSA and photographed for elongation characteristics of mesoderm induction at stage 13. About 8-10 animal caps were harvested at stage 10.5 for RT-PCR analysis using primers for *Xbra, Xrel3* and *Histone*. Levels of these markers were normalized by *histone* levels.

2.9 Scoring the results of Animal Caps assay

The results of the mesoderm induction assay were scored in several ways:

1. Observation of gastrulation-like movements. Normally, isolated animal pole tissue heals by rounding up after being dissected from the embryo, and it forms a sphere. Treatment with a mesoderm-inducing factor causes the animal pole cells to undergo gastrulation-like movements. The animal caps elongate in a characteristic fashion. Activin cause more dramatic gastrulation movements than do members of the FGF family. Elongation movements are visible after approximately four hours of culture.

2. Observation of later morphology. After three days of culture, when sibling embryos are at tadpole stages, animal caps treated with mesoderm-inducing factors form characteristic structures. In the case of *activin*, these have been termed "embryoids" (Jones and Smith, 1999b).

2.10 RNA extraction

Total RNA from *Xenopus* embryos was prepared as follows:

Two to four embryos or eight to ten animal caps, at the appropriate stage, were transferred to 1.7 mL Eppendorf tubes and homogenized with a pipette in 200 μL of NETS (100 mM sodium chloride; 10 mM ethylenediamine tetraacetic acid (EDTA), pH 8.0; 10 mM Tris-HCl, pH 8.0 and 0.2% sodium dodecyl sulfate) plus 10 μL of Proteinase K (20 mg/mL) (Boehringer Mannheim Canada, Quebec). The homogenates were then transferred to a Fisher water bath and incubated at 50-60°C for thirty minutes, after which 200 μL buffer saturated phenol and 20 μL 2M sodium acetate (pH 5.2) were added. The tubes were then vortexed and centrifuged at RT for 5 minutes at 13,200 revolutions per minute (rpm) using a IEC Micromax Digital microcentrifuge. The top aqueous layer was extracted, put in a fresh tube, and 200 μL ice-cold isopropanol plus 1 μL glycogen (Boehringer Mannheim Canada, Quebec) were added to it. The tubes were then placed for at least thirty minutes at -70°C for precipitation. The pellet of nucleic acids was obtained after centrifugation at 4°C at highest speed for ten minutes in a Fisher Scientific Model 235C Microcentrifuge. The pellets were washed with ice cold 70% ethanol, centrifuged again for five minutes, then vacuum dried briefly. In order to remove DNA present in the samples, the dried pellets were resuspended in 50 μL of DEPC-treated water plus 50 μL of 5M lithium chloride (LiCl). The mixtures were vortexed (S/P American Scientific products, USA) briefly and left to incubate on ice for 1 hour, after which they were centrifuged at 4°C at highest speed for fifteen minutes to obtain the pellet. The supernatant was carefully removed and the pellet was washed again with ice

cold 70% ethanol, re-centrifuged at 4°C for five minutes, vacuum dried briefly in BEL-ART Desiccator and resuspended in 39 μL DEPC-treated water on ice. To remove remaining traces of DNA, 0.1U (1 μL) RNAguard RNAse inhibitor (Pharmacia Biotech, PA, USA), 5 μL 10 X transcription buffer (400 mM Tris-HCl, pH 7.5; 20 mM Spermidine (Gibco BRL); 60 mM magnesium chloride) and 5U (5 μL) RQ1 RNAse free DNAse (Promega Corporation, WI, USA) were added. The tubes were vortexed, centrifuged at room temperature briefly and incubated at 37°C for twenty to thirty minutes at a Fisher water bath. The final volume was brought up to 100 μL by adding 50 μL of DEPC-treated water and phenol/chloroform extracted with an equal volume of a 1:1 mixture of phenol/chloroform (100 μL each). The samples were vortexed briefly and centrifuged at room temperature for two to three minutes at 13,200 rpm. The remaining aqueous layer was then precipitated with 2.5x volumes of ice cold 95-100% ethanol, $1/10^{th}$ volume of 3M sodium acetate (pH 5.2) and 0.02 mg (1 μL) glycogen for at least two hours at -70°C. Tubes were centrifuged at 4°C for ten minutes. The ethanol supernatants were removed and the pellets washed in ice-cold 70% ethanol. Once air-dried, the pellets were re-suspended in10 μL DEPC·treated water and stored in -70°C freezer. Concentrations were determined through a comparison of OD_{260} readings (quantify the RNA by UV light absorbance at 260 nm; OD_{260} unit = 40 μg/mL of RNA), and by electrophoresis of the RNA on 0.8-1% agarose gel. The presence of two distinct bands on an agarose gel around 850 bp and 1650 bp corresponds to the 18S and 28S subunits respectively and indicates that the RNA has not degraded.

2.11 Reverse transcriptase-linked polymerase chain reaction (RT-PCR)

Approximately 1 μg of isolated embryo RNA was diluted in a total volume of 10 μL DEPC-treated water in 0.5 mL Eppendorf tubes. If the RNA was stored at -70°C before use, it was thawed on ice first. Once resuspended, the RNA was left to denature at 65°C in a water bath. After ten minutes of incubation, the RNA was removed and immediately placed on ice to prevent internal pairing of RNA strands. To each tube of RNA, a reverse transcription mixture of RNAguard RNAse inhibitor (Pharmacia), 5x first strand buffer (Gibco BRL), deoxyribonucleotide triphosphates (dNTPs, Pharmacia), random hexanucleotide primers (Boehringer Mannheim), DTT (Gibco BRL) and Reverse Transcriptase enzyme (M- MLV, Gibco BRL) were added (see Table 3 for volumes and reagents added). The reaction mixtures were then incubated for one hour in a 37°C water bath, followed by ten minutes incubation at 95°C in order to inactivate the reverse transcriptase enzyme. The prepared complementary DNA (cDNA) was stored at –20°C (Figure 2.5).

2.12 PCR

Primer sequences for *Xrel3, Histone, Dnmt1*, were taken from such gene sequences (see Appendix A, Table 4 for references) and for *EF-1α, Chordin, Xbra, ODC* primers were designed from the gene sequences (see references in Table 4, Appendix A), using Macintosh OLIGOS 4.01 Primer Analysis Software (Copyright, 1993, National Biosciences, Inc., MN, USA). This computer program scanned random 19-20 bp

stretches of the gene and analyzed them for duplex formation, hairpin formation, GC content, melting temperatures (Tm) and internal stability. From the analysis it was possible to determine two appropriate 19 to 20 bp regions that flanked a reasonably sized region (~250 bp) of the gene. The sequences of these two regions were then sent to Oligos Etc., where the primers were manufactured (see Appendix A, Table 4 for specific sequences).

Amplification reactions were assembled into 0.5 mL Eppendorf tubes, according to Table 5 (Appendix A), using the following components: 10 x PCR buffer (Gibco BRL), magnesium chloride (50 mM, Gibco BRL), dNTPs (Pharmacia), cDNA sample, distilled water and gene-specific primers for: *Xrel3, Histone, Dnmt1, EF-1α, Xbra, Chordin, ODC*. For hot RT-PCR [α-^{32}P] dATP trace labeling (Dupont Canada, Inc., Biothechnology Systems, Mississauga, Ontario) was added. The last step was the addition of *Platinum Taq* DNA polymerase (Gibco BRL) and the remaining sterile water to make the final volume of 50 μL in each sample tube (Appendix A, Table 5). Each reaction mixture was vortexed briefly and 50 μL of light mineral oil added as a layer on top of the reaction mixture to prevent evaporation during the thermocycling program.

Each reaction mixture was assembled into a Perkin Elmer Cetus DNA Thermal Cycler 480. The cycling parameters were as follows: 94 °C hot incubation for five minutes, to eliminate primer dimers and to allow for more specific primer annealing, followed by 23 cycles for histone, *ODC, EF-1α, XDnmt1*, primers; 30 cycles for *Xbra, Chordin* and *Xrel3*, with the program: 60°C for 1 min for annealing of primers; 72°C for one min for primer extension, 94°C for 1 min for denaturation. Reactions were then

extended at 72°C for 7 min. Tm for primers was 60°C (Figure 2.5). The number of cycles in the thermocycling program above was determined for primers by testing a range of cycles from 15 to 35 (Figure 2.6). This was done to determine the linear range of amplification and at which cycle number the amplification reaction reaches its plateau (Figure 2.6 B). Once the program was completed the PCR products were stored at 4°C until run on 2% agarose gel or on a polyacrylamide gel for hot RT-PCR.

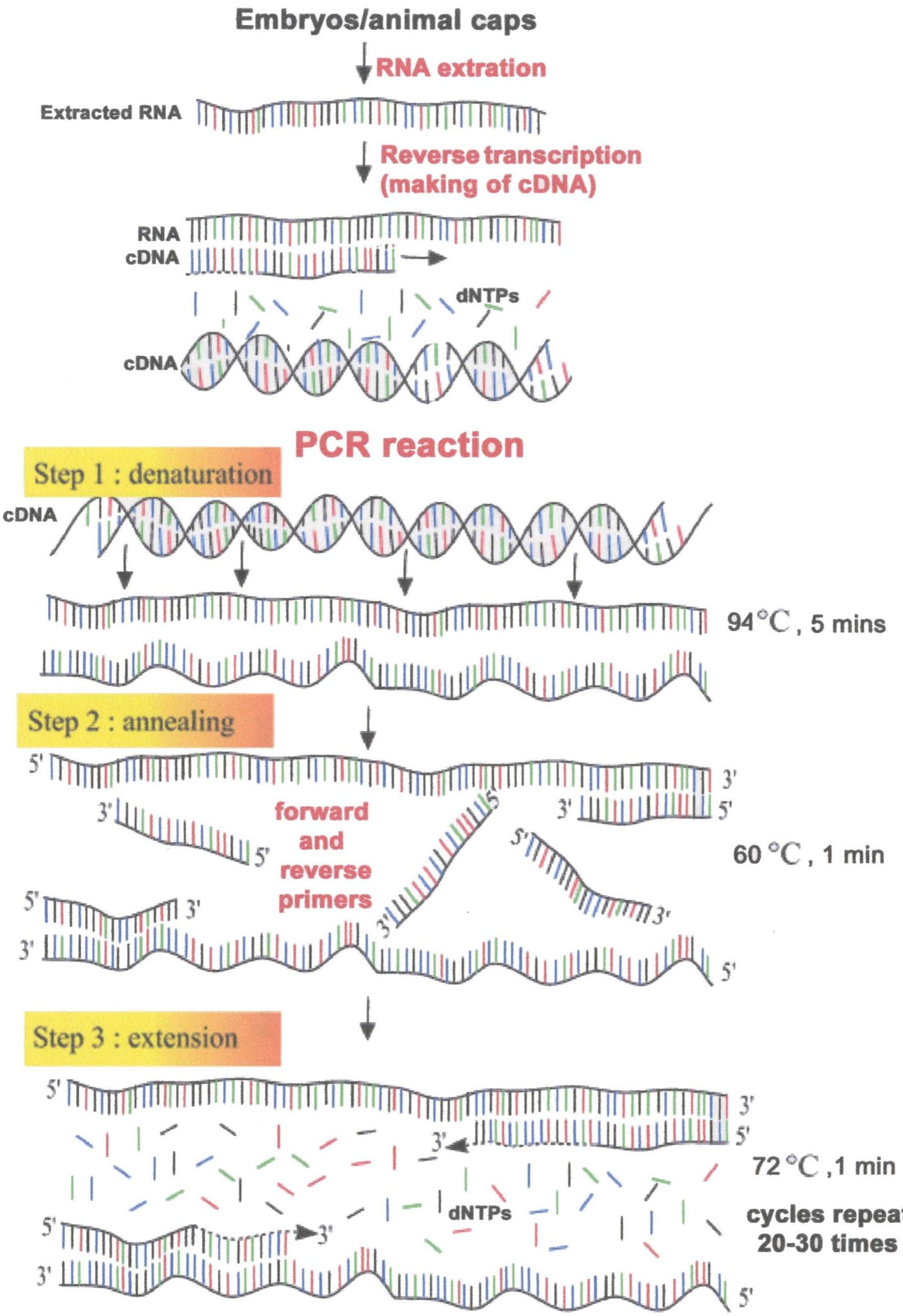

Figure 2.5 Outline of the RT-PCR reaction.

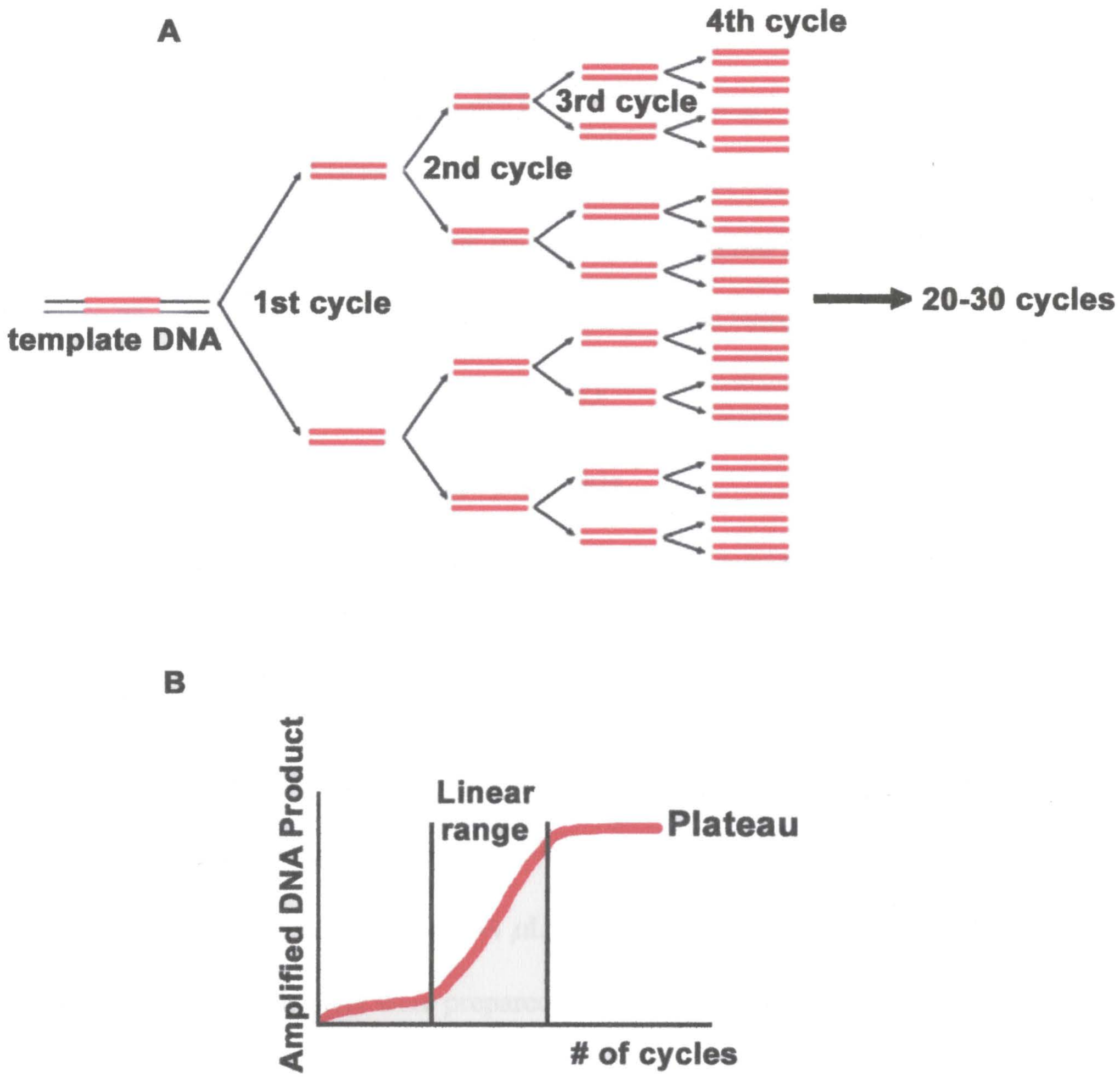

Figure 2.6 (A) Schematic diagram of amplification of DNA during PCR reaction. **(B)** A standard graph of PCR reaction follows a S-shaped curve with optimal amplification of product at linear range and saturation at the plateau.

2.13 Agarose gel electrophoresis

The PCR product were run on 2% agarose gel in 1xTBE buffer (89 mM Tris base, 89 mM boric acid and 2 mM EDTA, pH 8.0). The agarose gel was loaded in Bio-Rad SUBtm Cell (Fisher) and were run at a constant power of 104 Watts using Electrophoresis Power Supply FB 105 (Fisher) and left to run for approximately 30-40 minutes. The gels were then visualized and photographed using an agarose gel illuminator (Transilluminator 4000, Stratogene).

2.14 Polyacrylamide gel electrophoresis

The radiolabelled PCR products were run on 6% acrylamide/bisacrylamide, 8M urea denaturing sequencing gels. For 100 mL of sequencing gel mix, 48 g Urea, 15 mL 40% acrylamide/bisacrylamide (BioRad, Mississauga, Ontario), 10 mL 10xTBE and distilled water up to the 100 mL is required. Polymerization of the gels was initiated by the free radicals supplied by ~450 μL of 10% ammonium persulfate (APS; 0.1 g in 1 mL of distilled water) and stabilized by ~44 μL N, N ,N`,N`-tetramethylethylenediamine (TEMED; BioRad). The gels were prepared three hours ahead of the reactions and were run at a constant power of 60 Watts with 1xTBE buffer (89 mM Tris base, 89 mM boric acid and 2 mM EDTA, pH 8.0) and left to run for approximately 1.5 hours. The gels were then fixed with 10% glacial acetic acid/10% methanol and transferred onto 3 MM Whatman paper (Millipore, Missisauga, Ontario). The gels were dried on a Bio-Rad Model 583 gel dryer at 80°C for approximately one hour, packed in a Fisher Biotech Autoradiography Cassette-FBXC 810, containing an intensifying screen, with Dupont REFLECTION Autoradiography Film and left at -70°C for about one day.

2.15 Quantitation of PCR products

Exposed films were developed with a Kodak RP X-OMAT Processor within the Radiology Department of the Health Sciences Centre (St. John's, NL) and the relative amounts of each gene expressed were quantitated using an Ultrascan XL enhanced laser densitometer. The PCR product bands on each autoradiograph were scanned with a laser that passed vertically through their centres. The gelscan XL computer program (version 2.1, Copyright 1989, Pharmacia LKB Biotechnology Graphic Software Systems, Inc., Bromma, Sweden) generated integration curves from the scans, with the areas under the curves representing the intensities of the darkened DNA bands from the autoradiographs. The area values were recorded and the relative amounts of the PCR products calculated.

CHAPTER 3.

RESULTS.

3.1 Analysis of phenotypes and morphological features of embryos injected with different concentrations of *Xrel3* mRNA.

Xrel3 mRNA is expressed in two phases of early development in *Xenopus laevis*. Initially, messages accumulate during early stages up to the late blastula followed by a dramatic decline to undetectable levels at gastrulation. Messages then appear again during neurula stages. Because *Xrel3* overexpression is known to develop tumours (Yang *et al.,* 1998) that appear in the neurula stage, I wished to identify what factors might contribute to the formation of tumours in the earlier stages of development, in particular before the onset of embryonic transcription and gastrulation. I started by investigating the morphological changes that occured in the early development of *Xenopus laevis* when different concentrations of *Xrel3* mRNA were injected. The minimum concentration that gave any indication of tumour formation is 0.1 ng (Yang *et al.*, 1998).

Pigmented two-cell-stage embryos were injected in the animal pole region with different concentrations of *Xrel3* mRNA: 0 ng; 0.5 ng; 1.0 ng; 2.0 ng; 4.0 ng, and cultured in 4% Ficoll. The development was monitored and about thirty embryos per stage were fixed and analyzed at stages: 11, 20, and 25. The effect of overexpression of increasing concentrations of *Xrel3* in embryos is shown in Figures 3.1-3.4. The first observable abnormality is during gastrulation when the gastrulation movements of the majority of *Xrel3*-injected embryos seems to be retarded as determined by slowing in the rate of the blastopore closure at stage 11 (Figure 3.1a and 3.2). Embryos injected with

lower concentrations of *Xrel3* (0.5-1.0 ng) developed as controls (0 ng). While it took more time to gastrulate, they nonetheless complete gastrulation and neurulation. Darkly pigmented tumour-like spots on the ventral surface were observed in all embryos injected with *Xrel3* mRNA of 0.5 ng and higher (Figure 3.1 b-c, 3.3) on the epidermis in the ventral or lateral regions, consistent with previously published results (Yang *at el.*, 1998; Lake *et al.*, 2001). Very high concentrations of *Xrel3* (2.0-4.0 ng) arrested the development of embryos at gastrula or neurula stages (Figure 3.1b-d, 3.3).

The consequences of the gastrulation problems were clearly seen at the tailbud stages since virtually all the *Xrel3*-injected embryos showed a defect (Figure 3.1d, 3.4). The phenotypes are somewhat variable and the representative examples of stage 25 embryos are shown in Figure 3.1d. At later stages of development *Xrel3*-injections of 0.5 to 1.0 ng seemed to have caused the formation of microcephaly, shortened and bent trunks as well as tumours. In some cases tumours were so large they inhibited normal development of these embryos (Figure 3.1d).

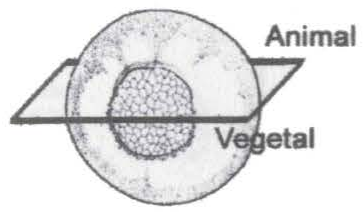

Stage 11
vegetal view

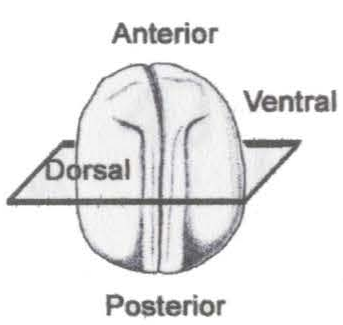

Stage 20
anterior dorsal
view

Stage 20
ventral view

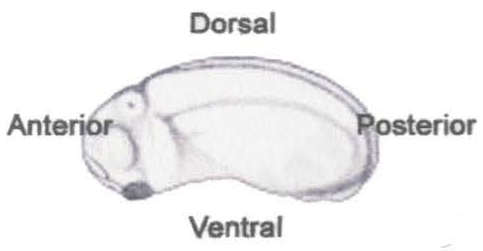

Stage 25
lateral view

Concentrations of Xrel3 mRNA injected into
the animal pole region

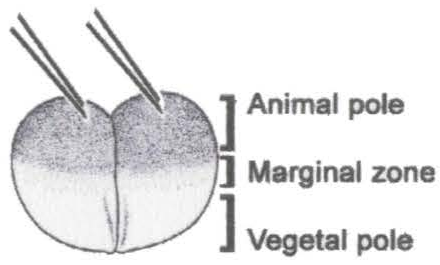

0 ng 0.5 ng 1.0 ng 2.0 ng 4.0 ng

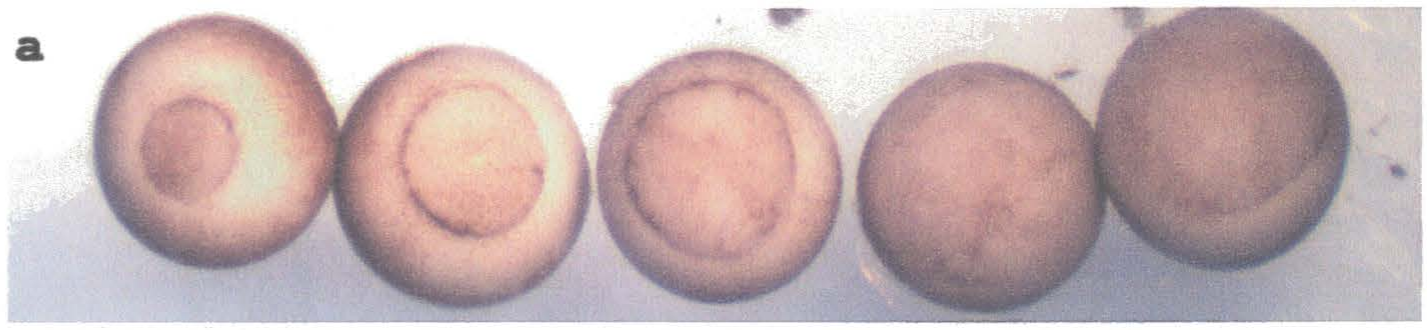

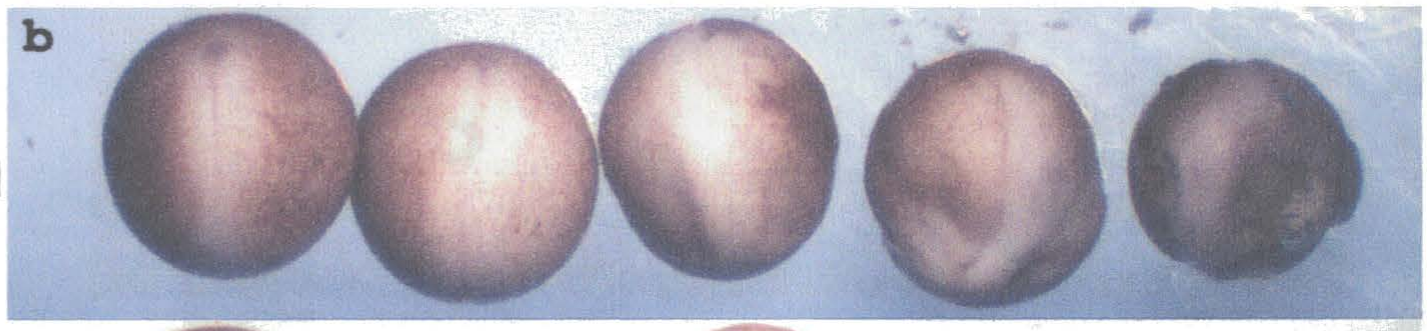

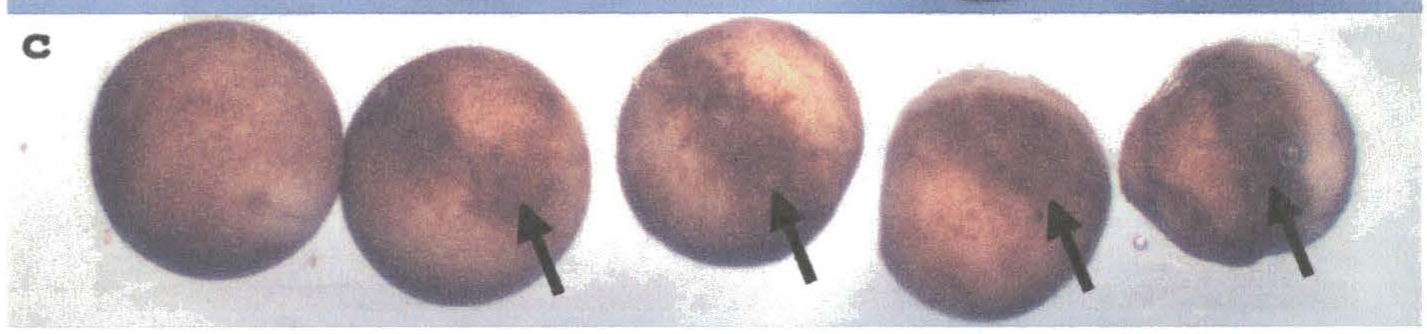

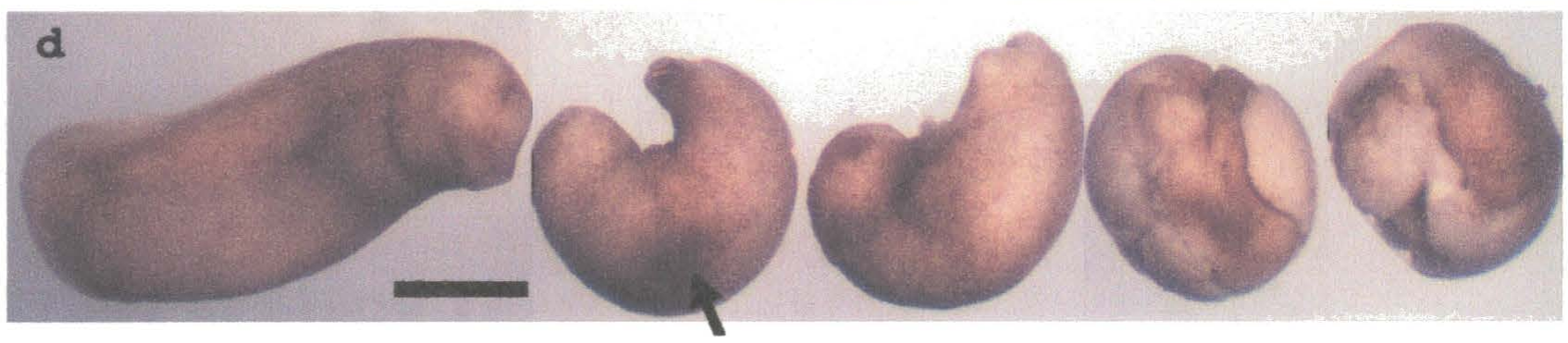

Figure 3.1. Developmental abnormalities in *Xenopus laevis* when different concentrations of *Xrel3* are overexpressed in the animal region of early embryos. Embryos were injected at the two-cell stage in the animal pole region with different concentrations of *Xrel3* mRNA: 0 ng; 0.5 ng; 1.0 ng; 2.0 ng; 4.0 ng. Embryos were fixed and photographed at stage 11 (**a**), 20 (**b-c**) and 25 (**d**). Formation of tumours as dark pigmented spots are visible in the Xrel3-injected embryos (arrows), starting with concentration 0.5-4.0 ng. No dark spots are seen in the control embryos (0 ng). High concentrations of *Xrel3* arrested the development of embryos. Scale bar, 1 mm.

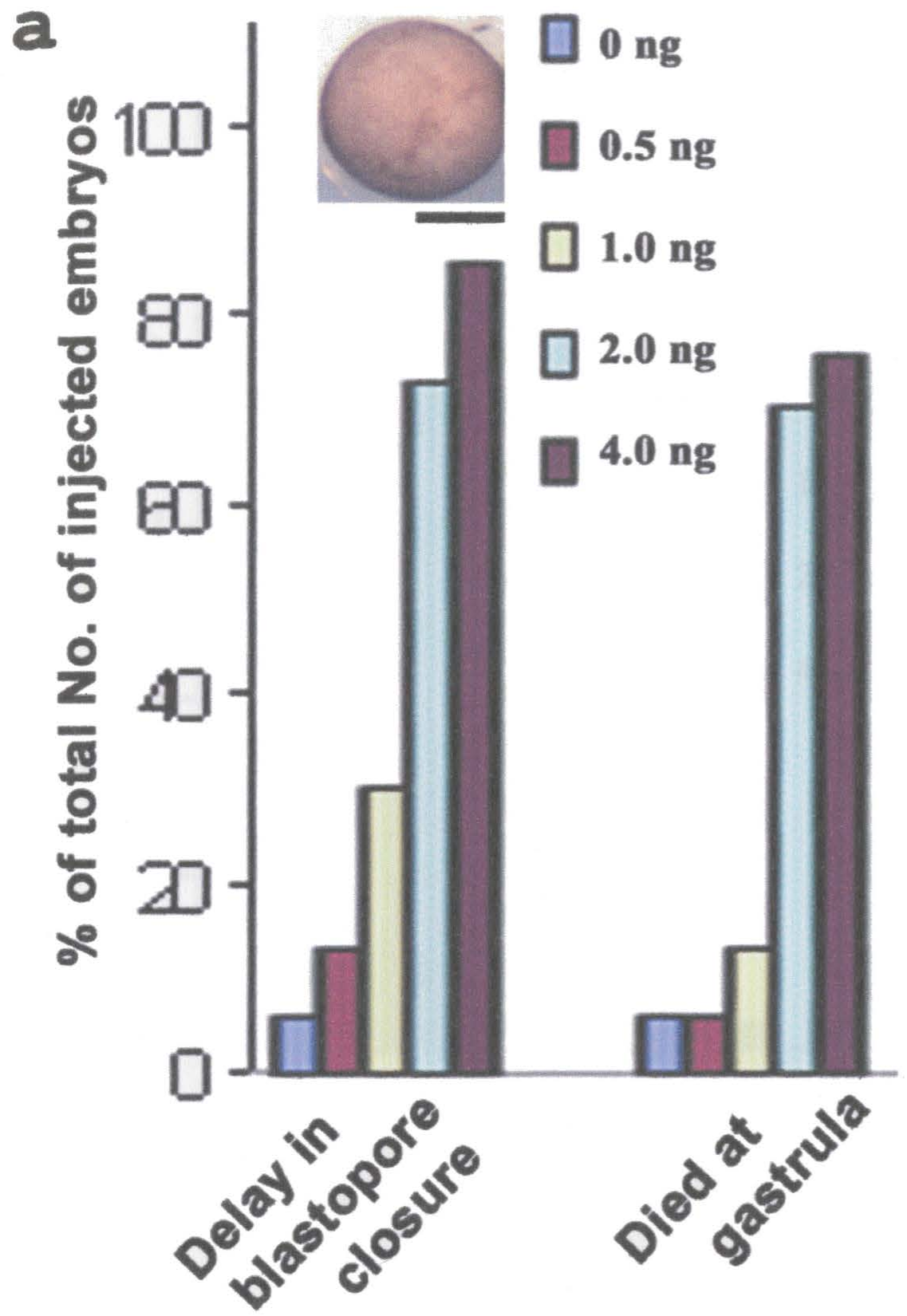

Figure 3.2. Stage 11 phenotypes observed upon overexpression of different concentrations of *Xrel3* mRNA at the animal pole regions of two-cell stage embryos.

a Embryos were injected at the 2-cell stage in the animal pole with different concentrations of *Xrel3* mRNA: 0 ng, 0.5 ng, 1.0 ng, 2.0 ng and 4.0 ng. Embryos were fixed and assessed at stages 11. Horizontal axis represents the phenotypes obtained. Pictures of representative phenotypes are shown on top of histograms. Vertical axis represents the percentage of embryos relative to a total number of embryos injected and scored in three separate experiments (for values see Appendix Table 1).

b Representative scheme and picture of normal embryo at stage 11. Scale bar, 1 mm.

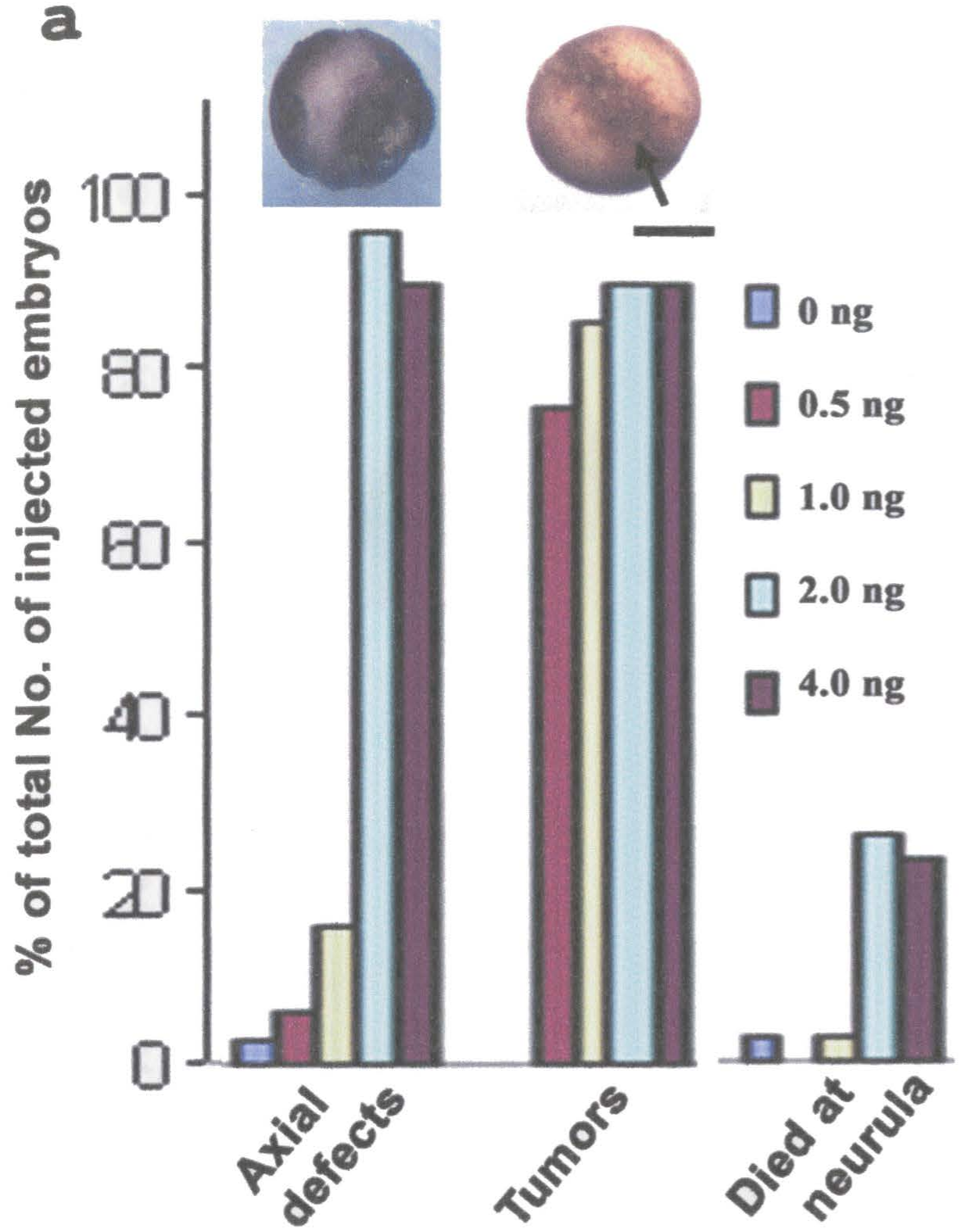

Figure 3.3. Stage 20 phenotypes observed upon overexpression of different concentrations of *Xrel3* mRNA at the animal pole regions of two-cell stage embryos.

a Embryos were injected at the 2-cell stage in the animal pole with different concentrations of *Xrel3* mRNA: 0 ng, 0.5 ng, 1.0 ng, 2.0 ng and 4.0 ng. Embryos were fixed and assessed at stages 20. Horizontal axis represents the phenotypes obtained. Pictures of representative phenotypes are shown on top of histograms. Vertical axis represents the percentage of embryos relative to a total number of embryos injected and scored in three separate experiments (for values see Appendix Table 1).

b Representative scheme and picture of normal embryo at stage 20. Scale bar, 1 mm.

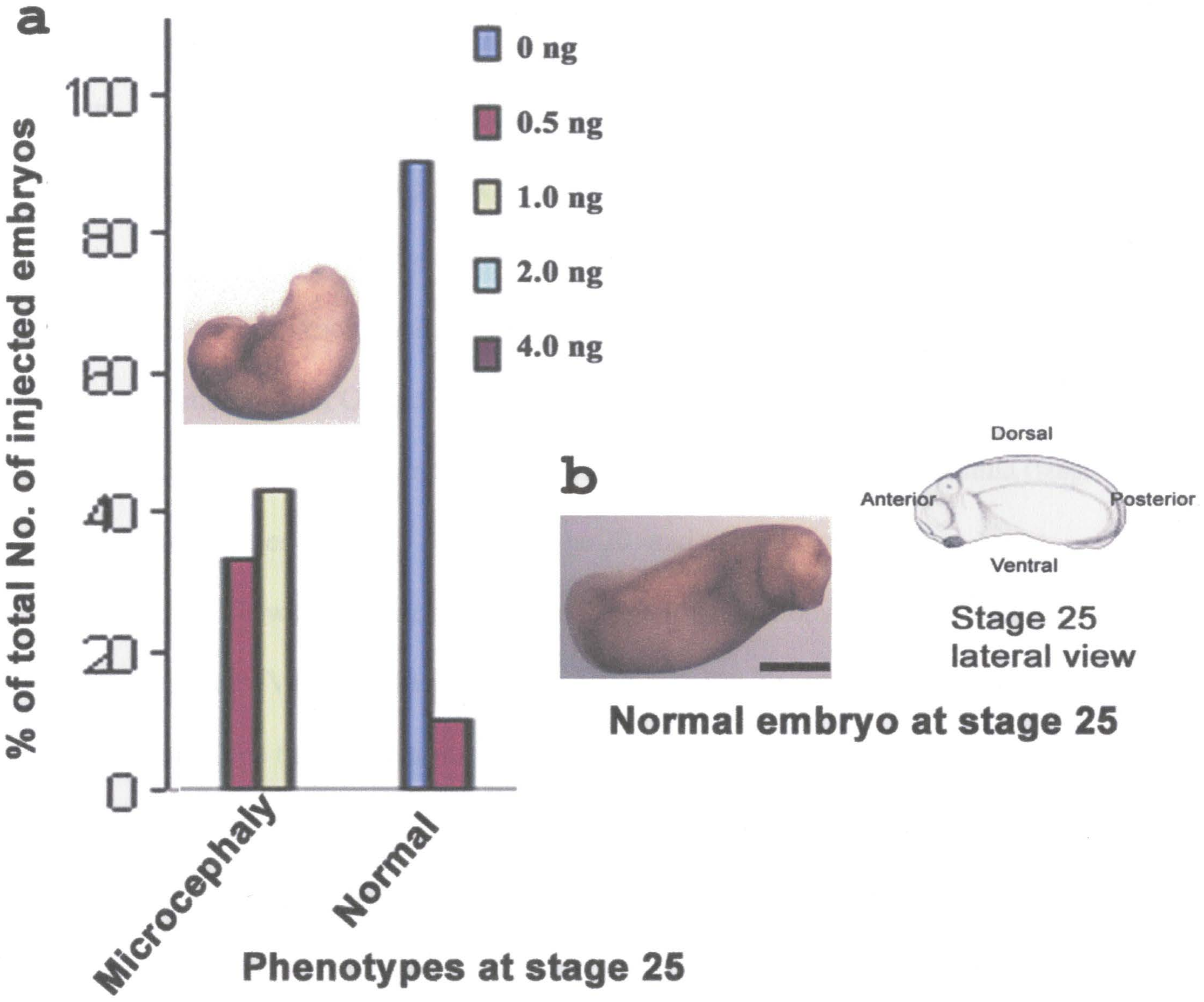

Figure 3.4. Stage 25 phenotypes observed upon overexpression of different concentrations of *Xrel3* mRNA at the animal pole regions of two-cell stage embryos.

a Embryos were injected at the 2-cell stage in the animal pole with different concentrations of *Xrel3* mRNA: 0 ng, 0.5 ng, 1.0 ng, 2.0 ng and 4.0 ng. Embryos were fixed and assessed at stages 25. Horizontal axis represents the phenotypes obtained. Pictures of representative phenotypes are shown on top of histograms. Vertical axis represents the percentage of embryos relative to a total number of embryos injected and scored in three separate experiments (for values see Appendix Table 1).

b Representative scheme and picture of normal embryo at stage 25. Scale bar, 1 mm.

3.2 Analysis of phenotypes and morphological features of *Xrel3*-injected embryos in animal, marginal or vegetal regions.

To determine if the site of injection is important in phenotypes of embryos produced, I followed the development of wild-type embryos injected with 0.5 ng of *Xrel3* mRNA or DEPC-treated water as control into different zones of two-cell stage embryos (one hundred embryos each): animal, marginal and vegetal regions. As controls, I used the same volumes of DEPC-treated water. Representatives from control and injected embryos were collected, fixed and photographed at the following stages: blastula (stage 9-10), gastrula (stages 11.5-12), neurula (stage 20) and tadpole (stage 32).

Figure 3.5 shows the phenotypes of animal region injections. The phenotypes are somewhat variable. Variable phenotypes are often noted in *Xenopus* overexpression experiments and are thought to arise, in part, from inadequate diffusion or differential stability of the injected mRNA. At stage 10 no noticeable differences were observed between controls and injected (Figure 3.5a-d). Most of the injected embryos appeared to gastrulate normally (Figure 3.5e-h), while ~26% (Figure 3.6, stage 12) exhibited delays in blastopore closure. As the development proceeded to neurula stage, injected embryos appeared to have dark pigment accumulations on the ventral side, which preceeded the dark tumour-like formations observed at later stages (Figure 3.5g-h, k-l, n) described previously (Yang *et al.*, 1998; Lake *et al.*, 2001). Abnormal head and facial development was also associated with animal pole injections (Figure 3.5o). In some cases the tumours were so large that they inhibited normal development of embryos. Tumours appeared on the surface of most of the injected with *Xrel3* embryos at stage 20 (~57%; Figure 3.5n)

only on the epidermis in the ventral or lateral regions. At later stages the embryos began to display a variety of phenotypes (Figure 3.5n-o). The mildest phenotype displayed was a distinct kink in the trunk that may have resulted from a failure of the anteroposterior axis to extend properly during gastrulation. The most severe phenotype is complex, often with the appearance of the microcephaly (Figure 3.5o), and in some cases accompanied by axis truncation. The anteroposterior axis is often warped and can be split with yolk cells bulging through an open neural tube. A phenotype intermediate between the mild and severe cases can be seen in which the head and tail are relatively normal but the trunk is more severely affected. At later stages tumour-like epidermal outgrowths persisted in only ~24% of embryos (Figure 3.6) in the ventral surface and lateral surfaces (Figure 3.5n). Control embryos injected with the same volumes of DEPC-treated water developed normally (Figure 3.5m).

An even more severe effect was caused by the injection of 0.5 ng *Xrel3* mRNA into marginal zone, where 96% of the embryos at stage 32 (Figure 3.7-3.8) either exhibited severe developmental defects or arrested at gastrula and neurula stages. Figure 3.7 shows the phenotypes of marginal zone injections. At stage 9 no noticeable differences were observed between control and *Xrel3*-injected embryos (Figure 3.7a-d). As the development proceeded to gastrulation (stage 11.5) noticeable delays in gastrulation were observed in *Xrel3*-injected embryos as compare to controls, such as delays in closure of blastopore (Figure 3.8). Embryos injected with *Xrel3* RNA seemed to undergo neurulation but exhibited developmental abnormalities compared to controls (Figure 3.7k-l, stage 20), which seemed to directly result from the defects in gastrulation. Later

stages show variable phenotypes (Figure 3.7n,o), from a distinct kink in the trunk to the appearance of microcephaly (Figure 3.7o), axis truncation (Figure 3.7n, Figure 3.8) and neural tube defects with yolk cells bulging through. In intermediate cases a comparatively normal head is formed (Figure 3.7n) indicating the involution of the dorsal mesoderm has occurred, but trunk structures are absent or severely diminished (Figure 3.7n-o). A considerable number (~34%) of the injected embryos died during gastrulation and neurulation (Figure 3.8). A few embryos also developed tumour-like outgrowths at a time later in development (~7% at stage 32; Figure 3.8) on the ventral surface, below the surface of the embryo, covered by epidermal layer of cells (Figure 3.7o). Histological analysis is needed to determine the nature of these outgrowths. Control embryos injected with the same volumes of DEPC-treated water developed normally (Figure 3.7m).

Figure 3.9 shows the phenotypes of vegetal region injections. No noticeable differences between injected and controls were observed at stage 9 (Figure 3.9a-d). Embryos injected with *Xrel3* (~38%; Figure 3.10) at the vegetal region seemed to have a delay in closure of the blastopore (Figure 3.9h) during gastrulation at stage 12 as compared to control-injected embryos, but nonetheless embryos injected with *Xrel3* appeared to proceed to neurula stages (Figure 3.9k-l). Injections into vegetal pole also caused some tumour-like outgrowths, but as with marginal-injections these tumours were below the surface of the embryos covered over by ectoderm in the ventral region (Figure 3.9n). Control embryos injected with the same volumes of DEPC-treated water developed normally (Figure 3.9m).

In conclusion, the site of injection seemed to play a major role in the phenotypes of embryos produced. Before gastrulation, as early as stage 9, different injection sites did not produce any noticeable differences between *Xrel3*-injected and controls. Overexpression of *Xrel3* into the animal region of the two-cell stage embryos showed that most of injected embryos appeared to gastrulate normally and developed normal axial structures, but some exhibited delays in blastopore closure. Tumours appeared on the surface of most of the embryos injected with *Xrel3* mRNA at stage 20 on the epidermis in the ventral or lateral regions. These embryos also show abnormal head and facial development, and in later stages often with the appearance of the microcephaly, in some cases accompanied by axis truncation. The anteroposterior axis is often warped and can be split with yolk cells bulging through an open neural tube.

Marginal zone injections with *Xrel3* either exhibited severe gastrulation defects or arrested at gastrula and neurula stages, as compared to controls. Later stages show variable phenotypes from a distinct kink in the trunk to the appearance of microcephaly, axis truncation, and neural tube defects with yolk cells bulging through. In intermediate cases a comparatively normal head is formed, indicating the involution of the dorsal mesoderm has occurred, but trunk structures are absent or severely diminished. A considerable number of injected embryos died during gastrulation and neurulation. A few embryos also developed tumour-like outgrowths later in development on the ventral surface, but these tumours were below the surface of the embryo, covered by epidermal layer of cells, as compared with the epidermal outside tumours of embryos with animal

pole injections. Histological analysis would be necessary to determine the nature of these outgrowths.

Embryos injected with *Xrel3* into the vegetal region seemed to have a delay in closure of the blastopore, during early stages of gastrulation, but the majority of them gastrulated or/and neurulated. Injections into vegetal pole also caused some tumour-like outgrowths, but as with marginal-injections these tumours were below the surface of the embryos covered over ectoderm in the ventral region.

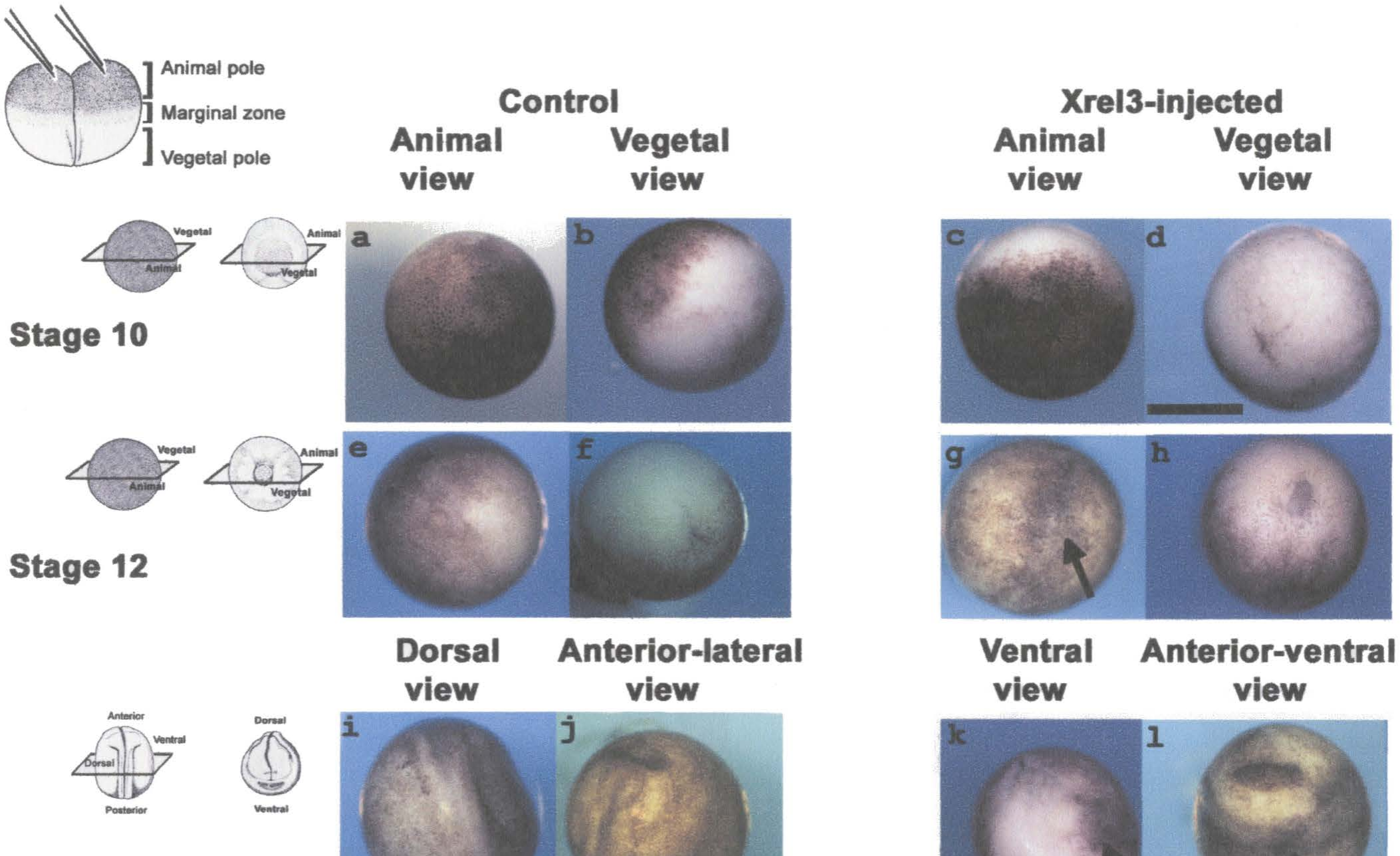

Figure 3.5. Tumour formation in *Xenopus laevis* when *Xrel3* is overexpressed in the animal region of early embryos.
Embryos were injected at the 2-cell stage in the animal pole region with either 0.5 ng *Xrel3* mRNA (**c-d, g-h, k-l, n-o**) or DEPC-treated water as control (**a-b, e-f, i-j, m**). Embryos were fixed and photographed at stage 9-10 (**a-c**), 12 (**e-h**), 20 (**i-j**) and 32 (**m-o**). Formation of tumours as dark pigmented spots (arrows) are visible in the *Xrel3*-injected embryos (**g-h, k-l, n-o**). No dark spots are seen in the control embryos. In spite of the formation of tumours, most of the *Xrel3*-injected embryos gastrulated normally and developed normal axial structures (**h, n**). Scale bar, 1 mm.

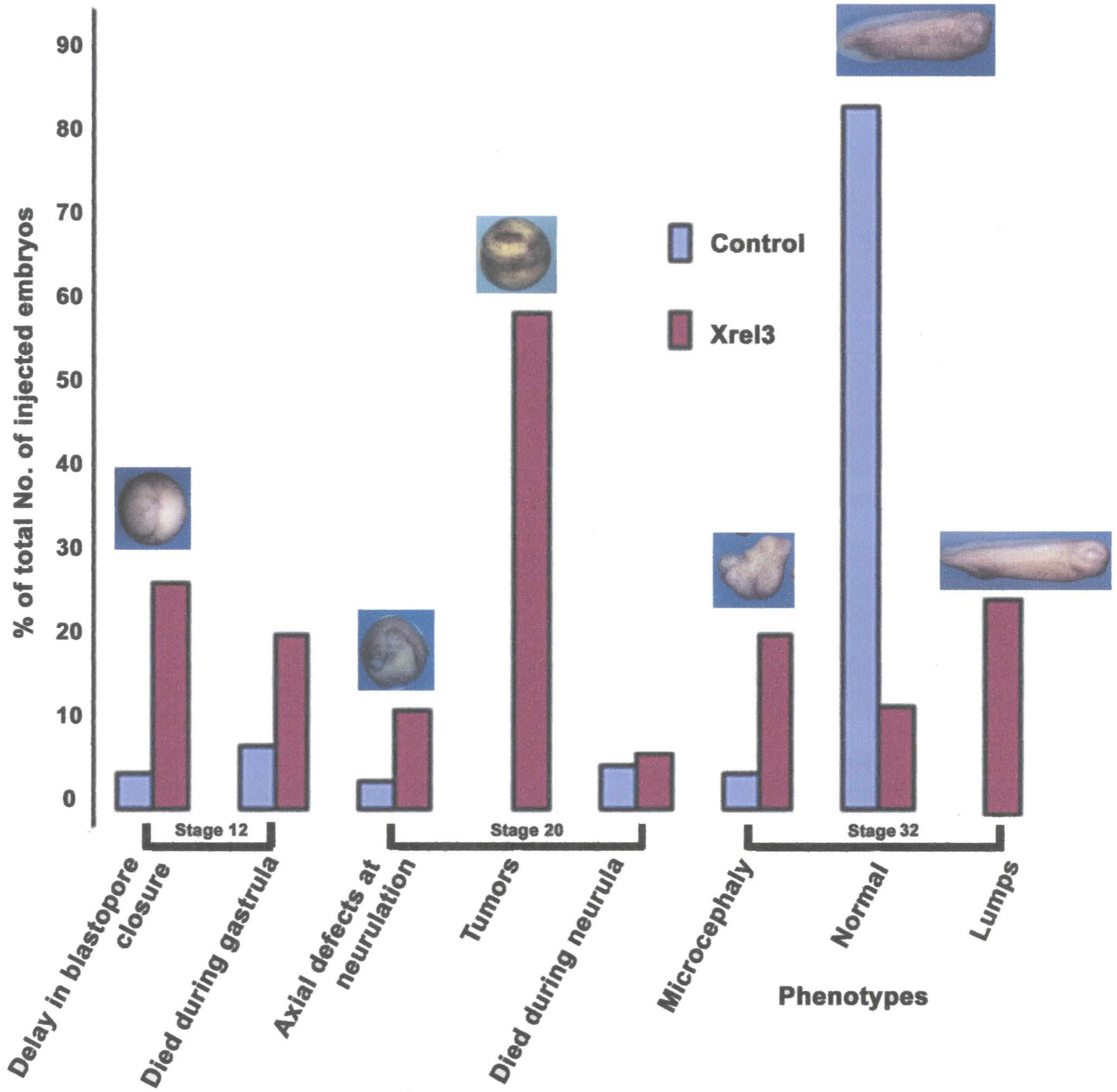

Figure 3.6. Phenotypes observed upon overexpression of *Xrel3* mRNA at the animal regions of two-cell stage embryos.
Embryos were injected at the 2-cell stage in the animal pole region with either 0.5 ng *Xrel3* mRNA or DEPC-water as control. Embryos were fixed and assessed at stages 12, 20 and 32. Horizontal axis represents the phenotypes obtained. Pictures of representative phenotypes are shown on top of histograms.
Vertical axis represents the percentage of embryos relative to a total number of embryos injected and scored in three separate experiments (for values see Appendix Table 2).

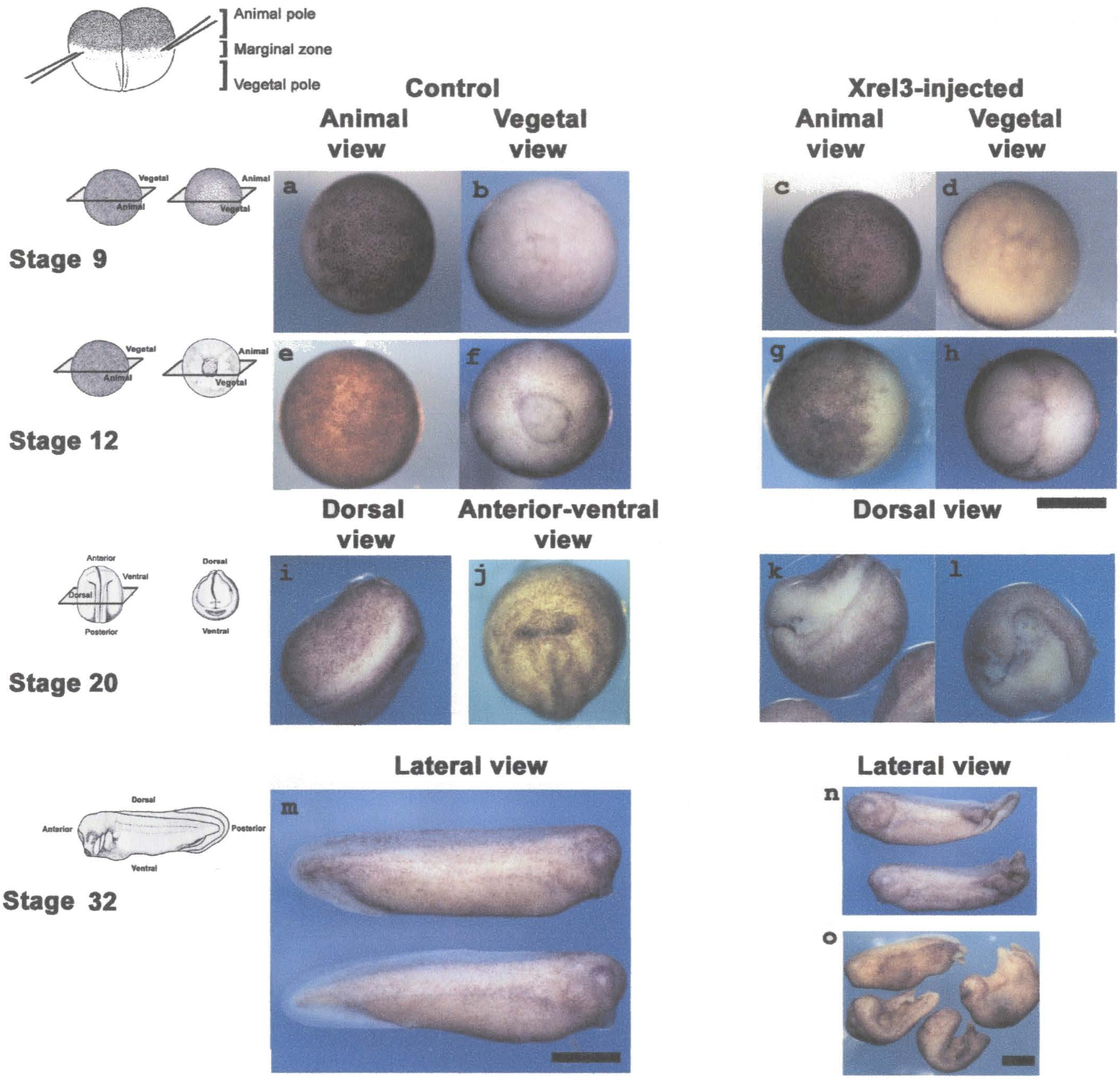

Figure 3.7. Gastrulation defects in *Xenopus laevis* when *Xrel3* is overexpressed in the marginal zone of early embryos.
Embryos were injected in the marginal zone of both cells at the 2-cell stage with either 0.5 ng *Xrel3* mRNA (**c-d, g-h, k-l, n-o**) or DEPC-treated water as control (**a-b, e-f, i-j, m**). Embryos were fixed and photographed at stage 9 (**a-c**), 12 (**e-h**), 20 (**i-j**) and 32 (**m-o**). *Xrel3*-injected embryos fail to close the blastopore and complete gastrulation (**h, k-l**) and display posterior axial deficiencies (**n-o**). While a comparatively normal head is formed (**n**), indicating the involution of the dorsal mesoderm has occurred, trunk structures are absent or severely diminished (**n-o**). Scale bar, 1 mm.

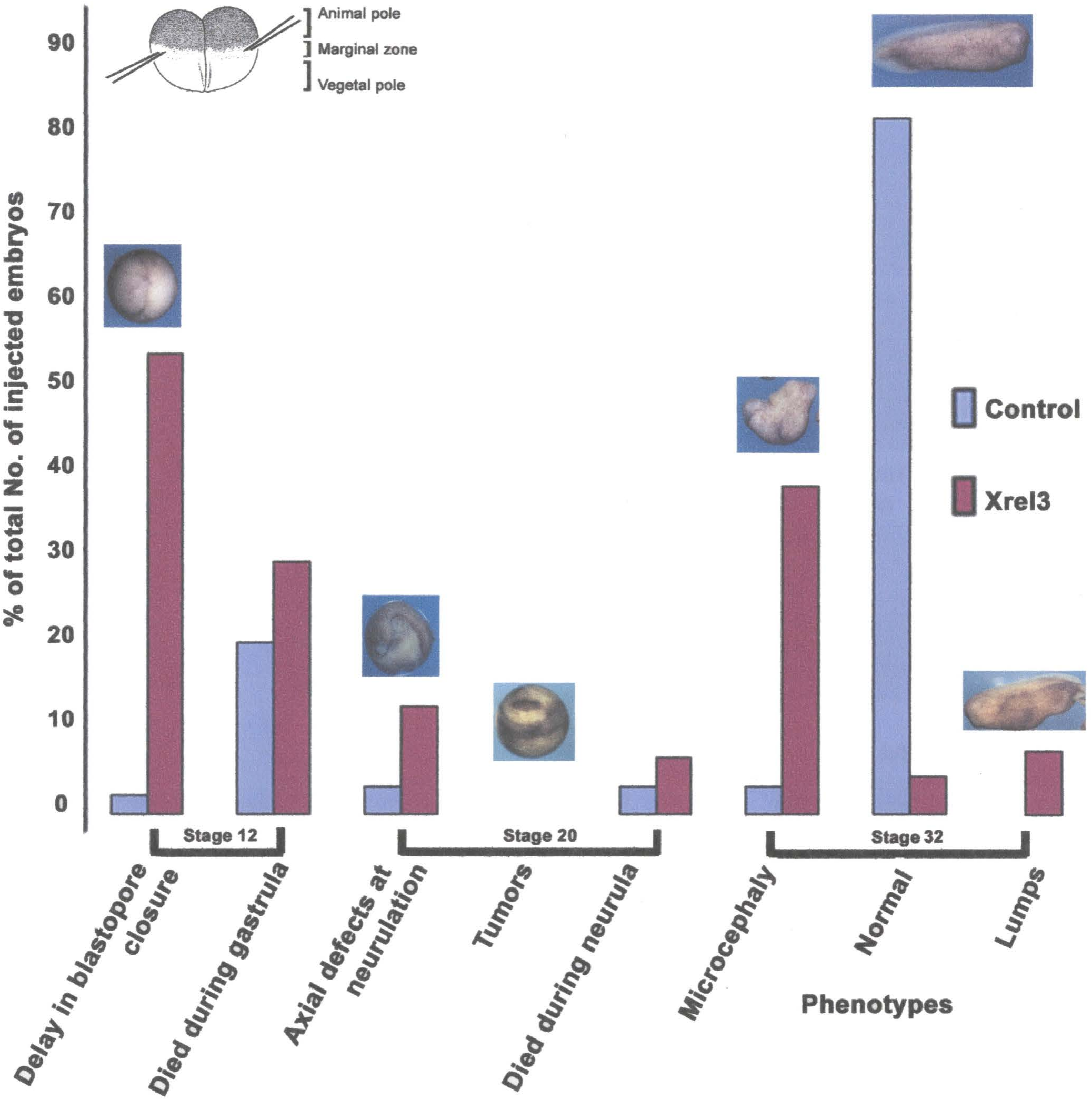

Figure 3.8. Phenotypes observed upon overexpression of *Xrel3* mRNA at the marginal zone of two-cell stage embryos.
Embryos were injected at the 2-cell stage in the marginal zone with either 0.5 ng *Xrel3* mRNA or DEPC-treated water as control. Embryos were fixed and assessed at stages 12, 20 and 32. Horizontal axis represents the phenotypes obtained. Pictures of representative phenotypes are shown on top of histograms.
Vertical axis represents the percentage of embryos relative to a total number of embryos injected and scored in three separate experiments (for values see Appendix Table 2).

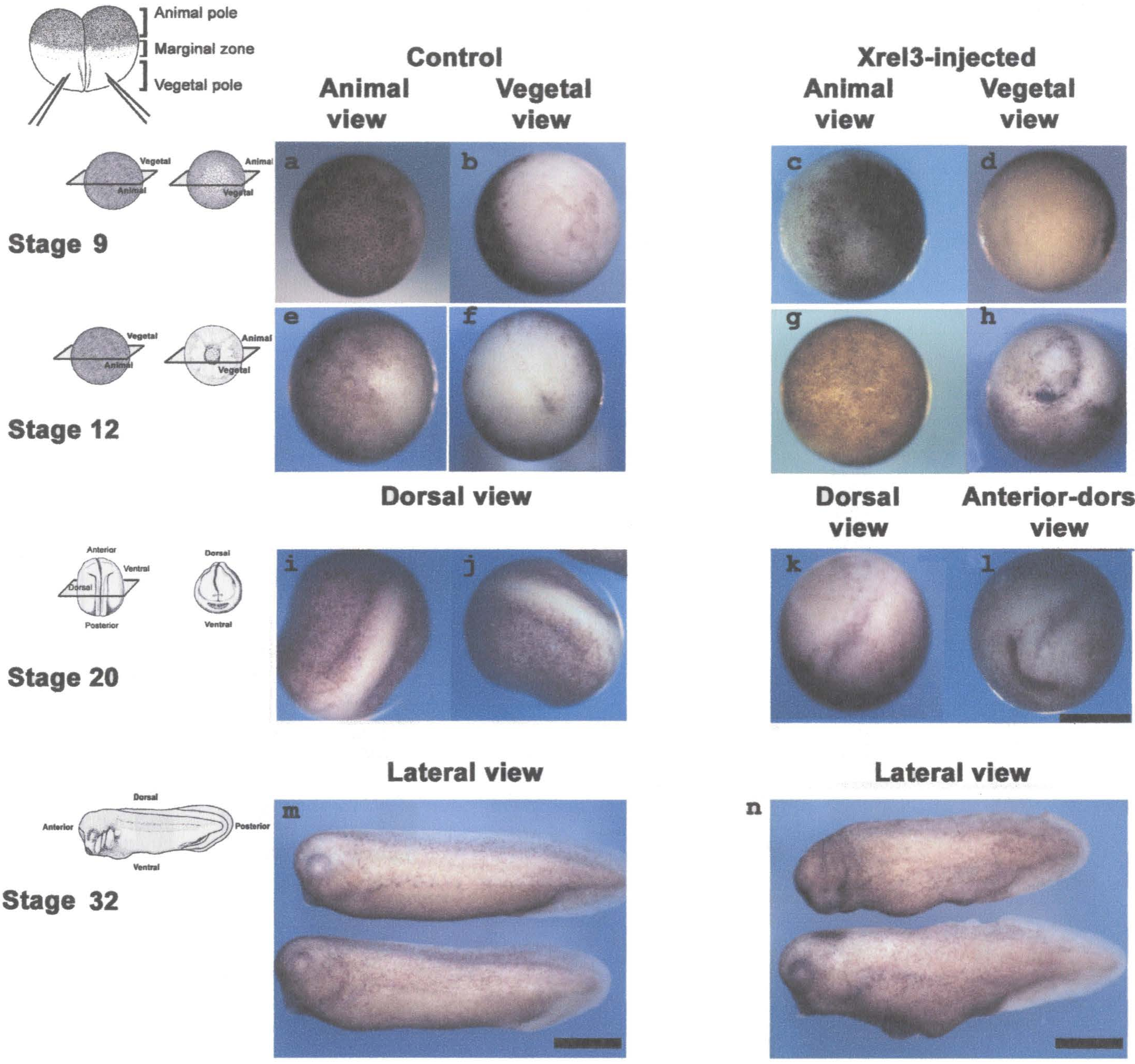

Figure 3.9. Formation of internal tumours and gastrulation defects in *Xenopus laevis* when *Xrel3* is overexpressed in the vegetal region of early embryos.
Embryos were injected in the vegetal pole at the 2-cell stage with either 0.5 ng *Xrel3* mRNA (**c-d, g-h, k-l, n**) or DEPC-treated water as control (**a-b, e-f, i-j, m**). Embryos were fixed and photographed at stage 9 (**a-c**), 12 (**e-h**), 20 (**i-j**) and 32 (**m-n**). *Xrel3*-injected embryos delay the closure of the blastopore (**k-l**) and display abnormal tumour-like lumps in later stages (**n**), while a comparatively normal head is formed. Scale bar, 1 mm.

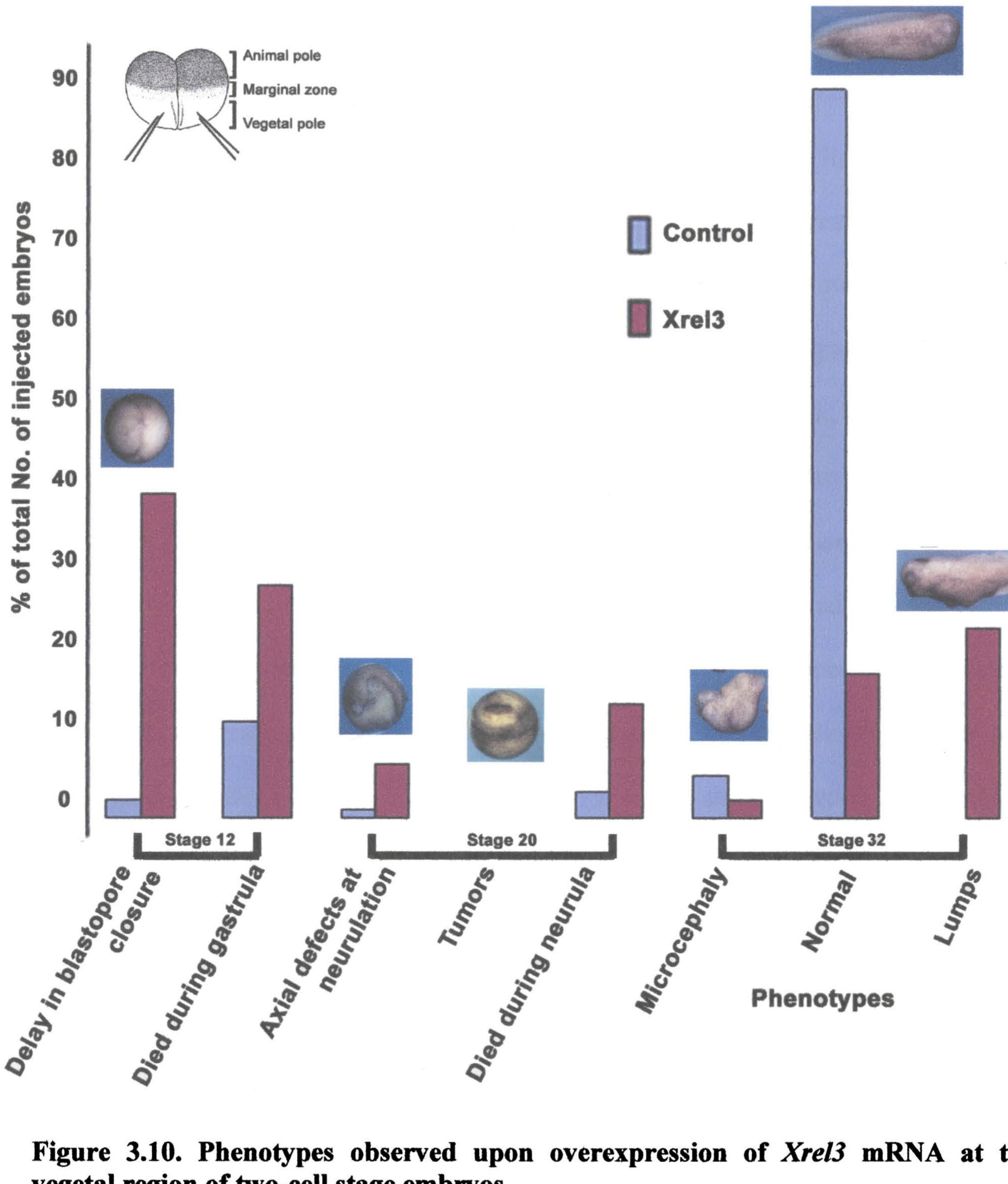

Figure 3.10. Phenotypes observed upon overexpression of *Xrel3* mRNA at the vegetal region of two-cell stage embryos.

Embryos were injected at the 2-cell stage in the vegetal pole region with either 0.5 ng *Xrel3* mRNA or DEPC-treated water as control. Embryos were fixed and assessed at stages 12, 20 and 32. Horizontal axis represents the phenotypes obtained. Pictures of representative phenotypes are shown on top of histograms.

Vertical axis represents the percentage of embryos relative to a total number of embryos injected and scored in three separate experiments (for values see Appendix Table 2).

3.3 Effects of *Xrel3* injected into the dorsal marginal zone.

At about eight to ten hours following fertilization, the blastula undergoes the movements of gastrulation with the formation of the dorsal blastopore lip in the subsequatorial region of the embryo. Concomitant with epiboly, or spreading of the animal pole cells, the marginal zone undergoes involution and then migrates towards the animal pole, to underlie the future neural plate. The extent of mesodermal migrations is an important determinant for the degree of anterior development (Kao and Danilchik, 1991).

Since marginal zone injections described above appeared to cause gastrulation defects in embryos, I decided to correlate the injection site of *Xrel3* with the disruption in gastrulation. I wanted to test the effects that overexpression of *Xrel3* had if injected into either the dorsal or lateral marginal zone. To fix the position of the dorsal side, fertilized eggs were immersed in agarose wells in 4% Ficoll solution and tilted with the sperm entry point facing gravity as described previously (Gimlich, 1986; Kao and Lockwood, 1996). RNA was injected at the animal-vegetal pigment border at the two-cell stage on either side of the cleavage furrow for dorsal injections. For lateral injections, embryos were allowed to enter the second cell division and were injected on either side of the forming cleavage furrow, when it reached the marginal zone.

Injections of 0.5 ng *Xrel3* RNA into the dorsal side caused severe phenotypes. Of the embryos injected dorsally with *Xrel3*, 90% developed axial abnormalities, which include the reduction in dorsoanterior structures. About 79% of embryos had kinked backs and shortened tail, and 31% were observed to have small heads (Figure 3.11j and 3.12). Most of them failed to form the blastopore lip and initiate gastrulation movements (Figure 3.11b). Also the

failures in closure of the blastopore lead to defects during neurulation (Figure 3.11f). Injection of controls in the dorsal side had no effect on development (Figure 3.11a, e, i and 3.12).

When injected into the lateral side, 0.5 ng of *Xrel3* RNA had a lesser but also significant effect on development. A large number of embryos developed gastrulation (51%) or neurulation (36%) abnormalities (Figure 3.11d, h, l and 3.12). In lateral injections there was a reduction in numbers of dorsoanterior defects as compared to dorsal injection phenotypes, but still about 48% the embryos injected laterally had kinked backs and shortened tails, and 12% were observed to have small heads (Figure 3.11d, h, l and 3.12). Tumours were formed in 23% of the embryos injected dorsally and 10% injected laterally (Figure 3.12-3.13). The large numbers of dorsoanterior defects in lateral injections could be due to diffusion of *Xrel3* RNA to the dorsal side.

The results presented here indicate that *Xrel3* overexpression affects the dorsoventral patterning by negatively regulating dorsal development. Dorsal and ventral type mesoderm is qualitatively different and different factors induce the differentiation of specific mesodermal tissues. The injection site is of importance in the extent of the disruption in gastrulation. More damage and disruption in gastulation and subsequently neurulation was observed when embryos were injected into the dorsal marginal site, as compared to the lateral marginal site. Embryos injected with *Xrel3* RNA into the dorsal side were more sensitive to gastrulation defects than injected into the lateral side.

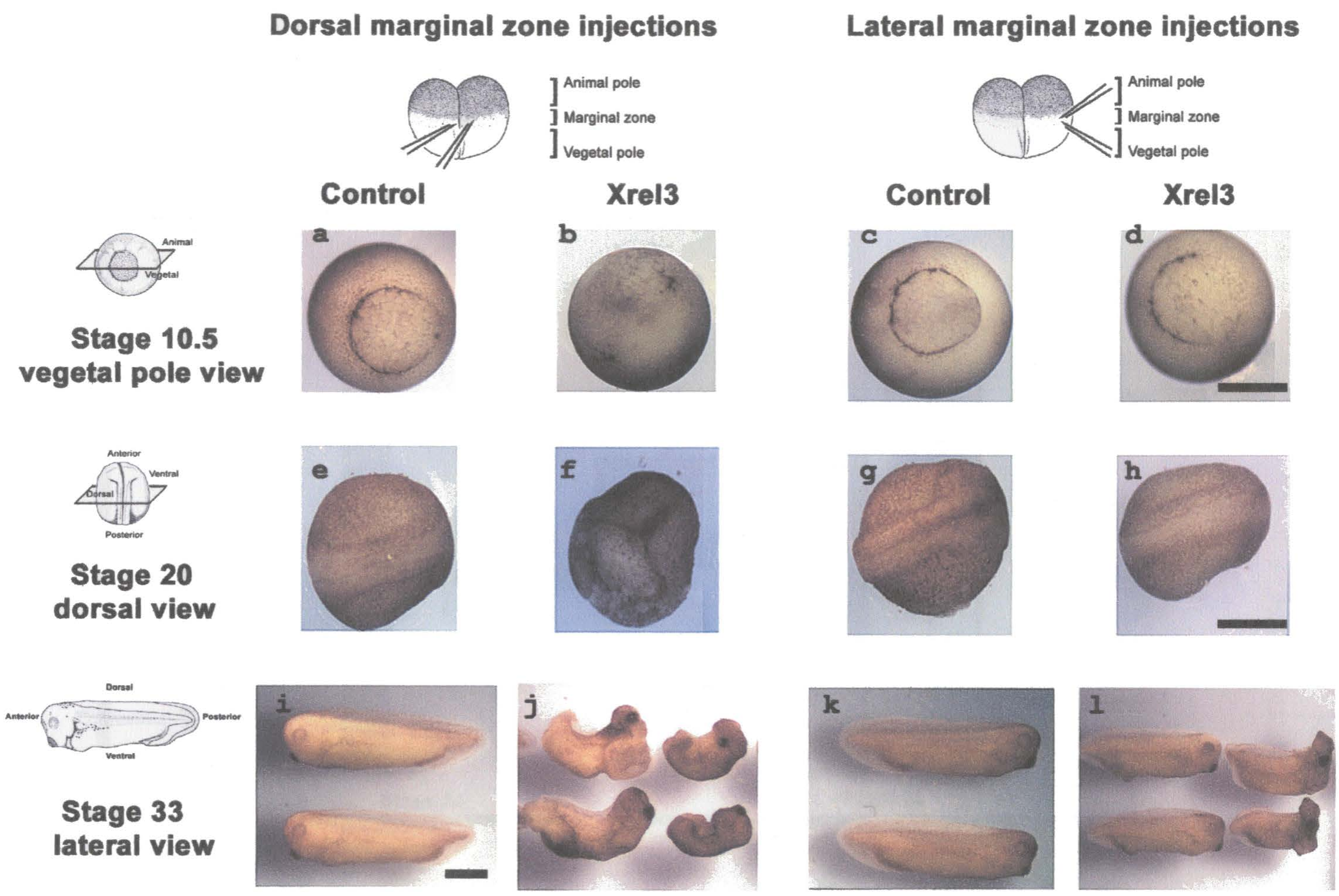

Figure 3.11. Overexpression of *Xrel3* into the dorsal marginal zone causes a reduction in dorsal structures in embryos.
Wild-type embryos were injected at the two-cell stage with 0.5ng *Xrel3* mRNA (**b, d, f, h, j, l**) or control (**a, c, e, g, i, k**) in the dorsal (**a-b, e-f, i-j**) or lateral (**b-c, g-h, k-l**) region of marginal zone (MZ). Embryos were fixed and photographed at stage 10.5 (**a-d**), 20 (**e-h**) and 33 (**i-l**). Most of embryos injected dorsally with *Xrel3* failed to form a dorsal lip and the formation of a circular blastopore lip was at a delayed time (**b**), when compared to control embryos (**a**). Formation of a dorsal lip was observed in laterally injected embryos (**d**). Formation of tumours as dark pigmented spots are visible in the *Xrel3*-injected embryos (**j, l**). No dark spots are seen in the control embryos (**i, k**).

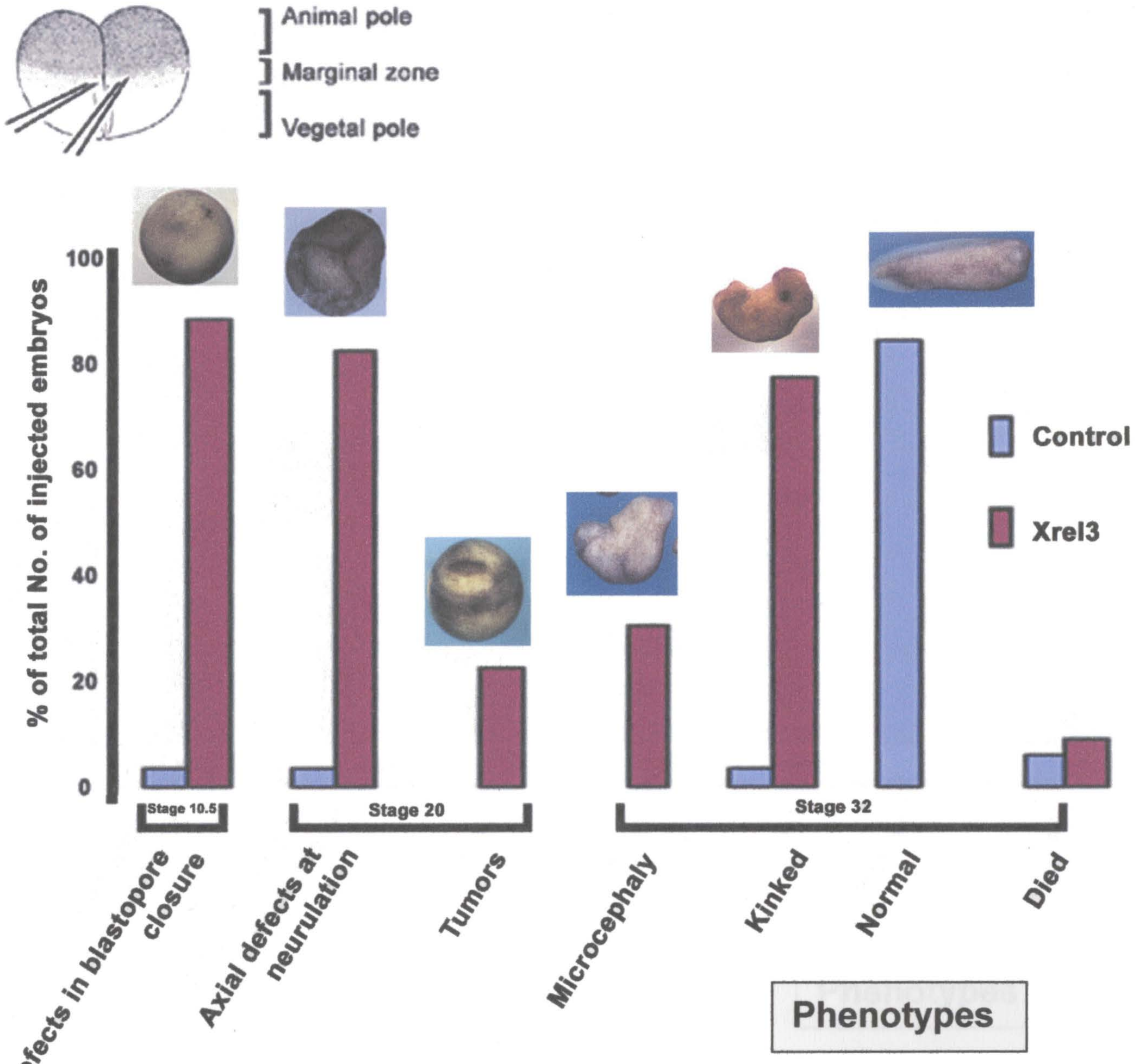

Figure 3.12. Distribution of phenotypes caused by overexpression of *Xrel3* into the dorsal marginal zone.
Horizontal axis represents the phenotypes obtained. Vertical axis represents the percentage of embryos relative to a total number of embryos injected and scored in three separate experiments (for values see Appendix Table 3).

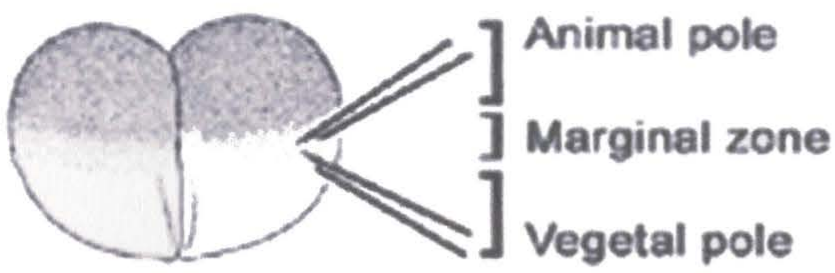

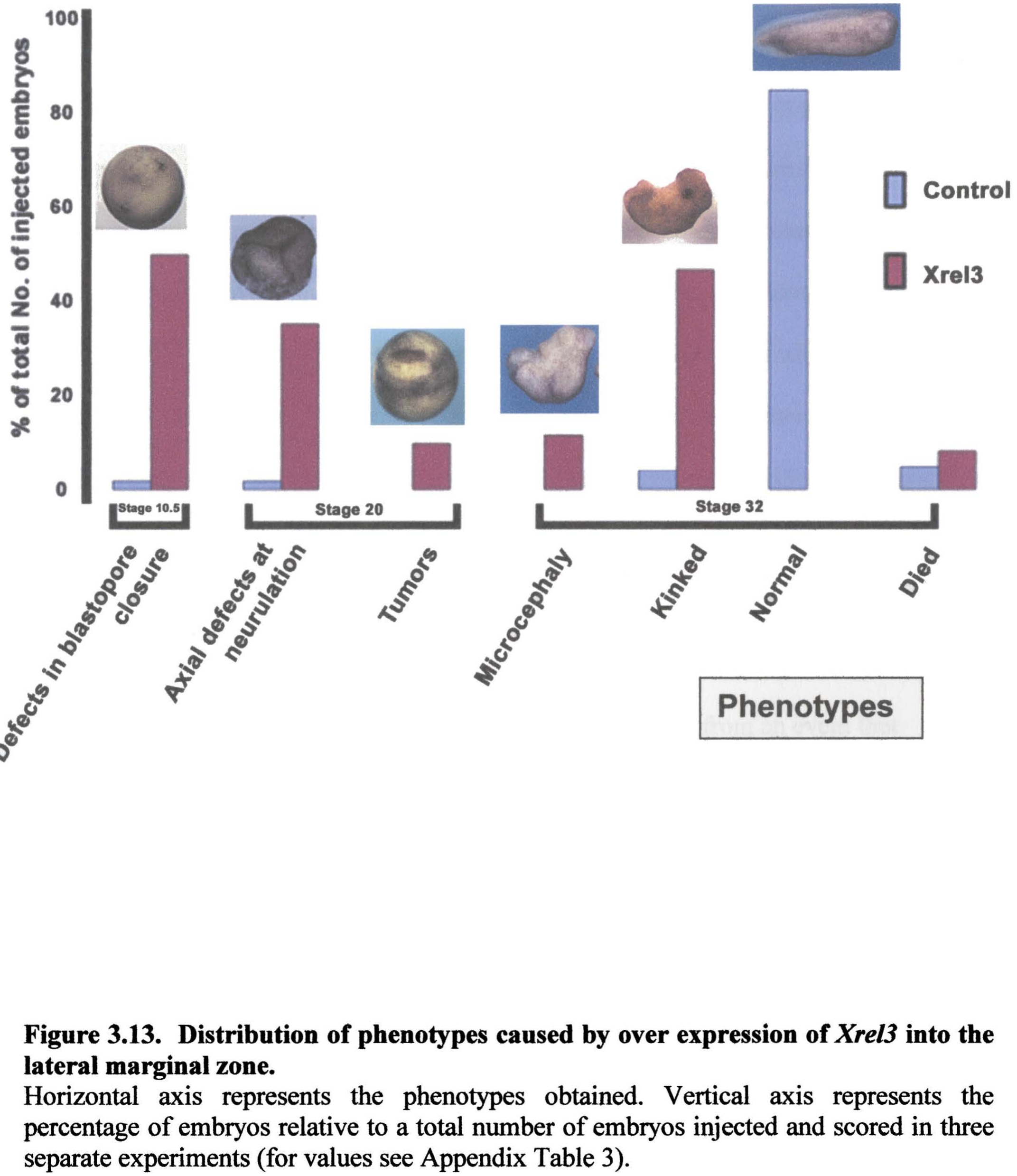

Figure 3.13. Distribution of phenotypes caused by over expression of *Xrel3* into the lateral marginal zone.
Horizontal axis represents the phenotypes obtained. Vertical axis represents the percentage of embryos relative to a total number of embryos injected and scored in three separate experiments (for values see Appendix Table 3).

3.4 Possible involvement of *Xrel3* in regulation of MBT.

Previous results from our lab (Kao *et al.*, unpublished data) indicated that in embryos injected with *Xrel3* RNA, the blastocoel roof, or prospective ectoderm of late blastula and gastrula stage embryos were composed of more cells than in corresponding controls with an average blastocoel roof thickness of about 10 μm as opposed to 6.5 μm in controls. In spite of the increased number of cells, the embryos gastrulated normally and developed normal axial structures. After gastrulation, tumours present within the epidermal layer showed many more cells than the corresponding epidermis of control embryos, which is arranged in a typical stratified squamous histology with apparent little cell division. The tumour cells showed rounded morphology, and numerous mitotic figures were present within the tumours. Also, when fluorescently labeled injected animal cap cells were transferred to an uninjected host in early blastula stage, the cells do not distribute amongst the epidermis as in controls (Kao, unpublished data). These observations led to the hypothesis on the possible role of *Xrel3* in pre-gastrula embryos, and that the tumours develop in *Xrel3*-overexpressed embryos from an event that occurred before gastrula, possibly at MBT. MBT occurs at stage 8.5 of *Xenopus* development, after the 12^{th} cleavage division (approximately 4096 cells), and is associated with major changes in cell cycle checkpoints, slowing down the rate of DNA synthesis, initiation of zygotic transcription, loss of cell cycle synchrony and increase in cell motility (Newport and Kirschner, 1982a,b). It is possible that *Xrel3* overexpression retains cells in the pre-MBT state by blocking the deceleration of DNA synthesis, delaying the initiation of embryonic transcription with activation of transcripts of MBT,

and/or is interfering with increase in cell motility. This hypothesis might also explain the profound effect on embryo development when Xrel3 is overexpressed at the two-cell stage.

3.4.1 Expression of Ornithine Decarboxylase, Elongation Factor 1-alpha, Brachyury and Chordin in embryos injected with different concentrations of Xrel3 in the animal poles.

Next, I attempted to determine the expression levels of some of the transcripts that appear after MBT in the *Xrel3*-injected embryos, such as *Ornithine Decarboxylase (ODC), Elongation Factor 1-alpha (EF-1α),* the early response gene characterizing mesoderm, *Xbra,* and a marker of dorsal mesoderm, *Chordin*. Pigmented two-cell-stage embryos were injected into the animal pole region with 0 ng; 0.5 ng; 1.0 ng; 2.0 ng; 4.0 ng *Xrel3* mRNA and cultured in 4% Ficoll. Two whole embryos from each stage were collected at stages 7, 9 and 11 for RT-PCR analysis with oligonucleotide primers specific to *Xenopus*: *Histone, ODC, EF-1α, Xbra* and *Chordin* and *Xrel3* to check if overexpression of *Xrel3* had any effect on activation of these genes. *EF-1α* and *ODC* were strongly expressed at the MBT in all embryonic cells. They were also abundant in oocytes and transiently expressed in early embryos (Amaldi *et al.,* 1993). The transcription of *ODC* and *EF-1α* markers is usually initiated with the onset of MBT. ODC levels normally increase at gastrulation while *EF-1α* levels (Krieg *et al.,* 1989) increase immediately at the MBT. *Xbra* transcription starts soon after MBT and reaches its maximum levels at stage 11.5. Its expression is first apparent at stage 9/10 of early gastrula, and this coincides with a slight increase in *EF-1α* levels, marking the MBT (Smith *et al.,* 1991), making it an excellent pan-mesodermal marker during gastrulation.

Brachyury is also required for the morphogenetic movements of gastrulation. *Chordin* is expressed in dorsal mesoderm and its transcription starts soon after MBT. The expression of *chordin* starts in Spemann's Organizer at a stage 9/10 of *Xenopus* development. This molecule is a potent dorsalizing factor that regulates cell-cell interactions in the organizing centres of head, trunk, and tail development (Sasai *et al.,* 1994).

The expression levels of molecular markers such as *ODC, EF-1α, Xbra* and *chordin* at stages 7, 9 and 11 did not seem to be different between controls (0 ng of *Xrel3* injected) and injected with higher concentrations of *Xrel3* embryos (0.5-4.0 ng) despite differences in *Xrel3* levels (Figure 3.14).

There is a definite increase in the histone levels in embryos injected with higher concentration of *Xrel3* as compared to embryos injected with lower concentrations of *Xrel3*. Also, the levels of histone progressively increased as development progressed (Figure 3.14).

ODC levels were abundantly expressed all throughout the development in all embryos. Maternal levels of *ODC* at stage 7 were higher in control embryos and lower in embryos injected with higher concentrations of *Xrel3*, but at stage 9, it was reversed, the levels of *ODC* were higher in *Xrel3* injected with higher concentrations of *Xrel3* and lower in controls. The levels of *ODC* did not seem to increase dramatically at stage 9 soon after the MBT. Higher and equal levels of *ODC* were observed at stage 11 (Figure 3.14).

EF-1α levels increased soon after MBT reaching high levels at stage 11 in all embryos. The same can be said about the levels of *Xbra* and *chordin* transcripts, which

accumulated during stage 11. At stage 11 *chordin* levels were higher in control embryos and lower in embryos injected with higher concentrations of *Xrel3*. As expected, endogenous *Xrel3* levels in controls (0 ng of *Xrel3* injected) were highest during early stages but decline during stages 9 to 11. *Xrel3* levels in injected embryos stayed high (Figure 3.14).

Looking at the levels of *Xrel3* at stage 7, the limitations of the RT-PCR assay can be demonstrated. Injection of Xrel3 mRNA at a saturating level cannot be quantified reliably by simple RT-PCR, which is what I used. The gel did not show different concentrations of *Xrel3* that were injected into embryos, and by examination of the gel I concluded that the concentrations of *Xrel3* were the same in all embryos, except for controls (Figure 3.14), which, given the extensive range of injected RNA, is not likely reflective of the levels of this message in the embryos. RT-PCR analysis is not sensitive enough to show us the differences in levels of injected *Xrel3* between 0.5 ng or 4.0 ng. RT-PCR assay is not a good way to quantitatively show the expression of each marker, but it is sensitive enough to show the presence of transcripts, such as *Xbra* at stage 11 in injected with higher concentrations of *Xrel3* embryos, which is contradictory to the gastrulation defects in phenotypes of embryos injected with high doses of *Xrel3* 1.0-4.0 ng (results above, Figure 3.1). It could be due to the fact, that since we used two whole injected embryos in this assay, the injected *Xrel3* mRNA tends to localize at the site of injection and did not reach or influence the cells of the mesodermal region where the expression of *Xbra* is initiated.

In conclusion, I did not observe differences in activation patterns of MBT markers including *EF-1α*, *ODC,* and *Xbra,* between control and *Xrel3*-injected embryos.

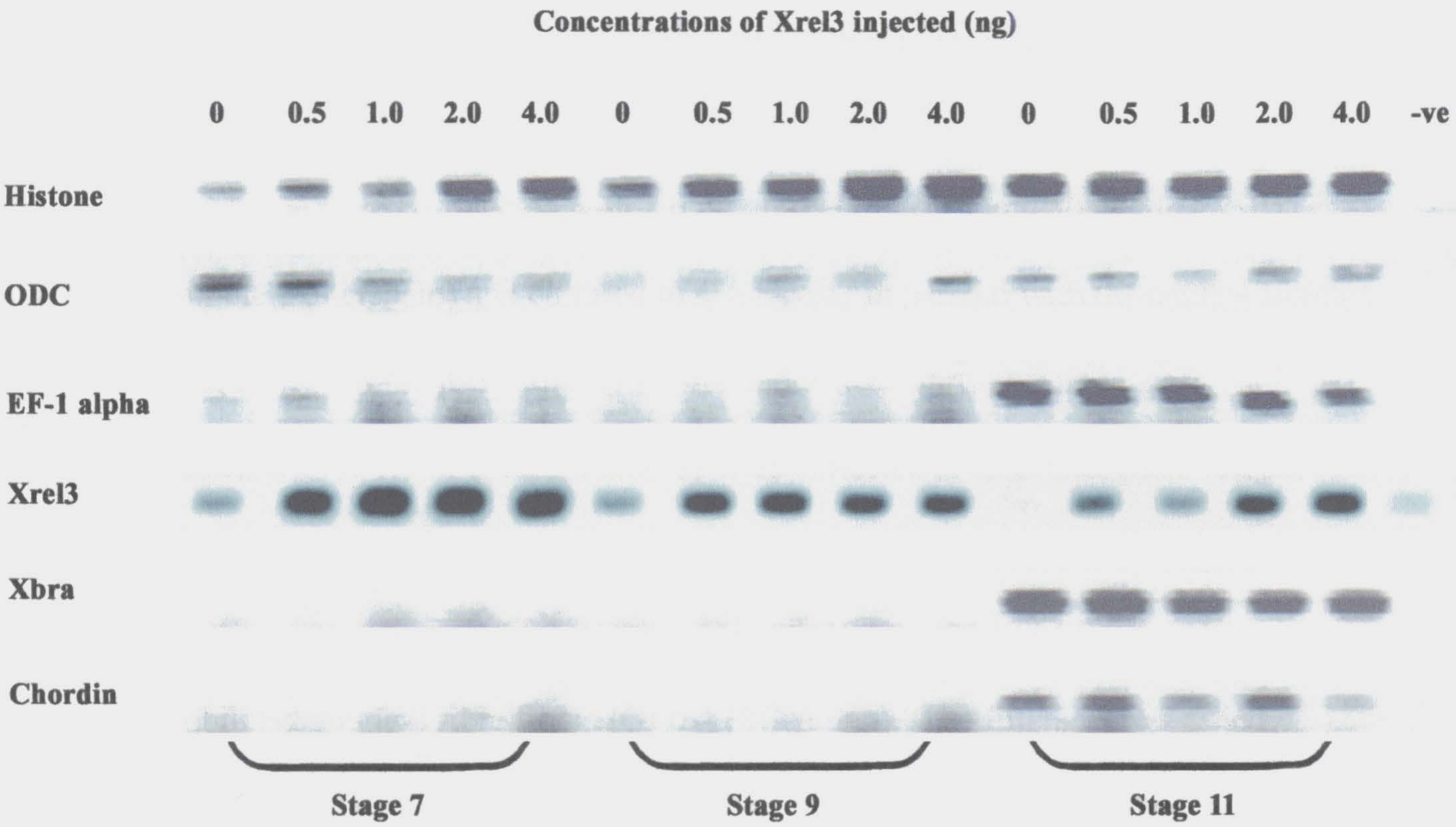

Figure 3.14. Overexpression of different concentrations of *Xrel3* at the animal region of embryos does not influence the expression of such marker as *ODC, EF-1α, Xbra* and *Chordin.*

RT-PCR analysis of Xrel3 and control injected embryos (two whole embryos per time point) extracted at 7, 9 and 11 stages for the transcripts of ***Ornithine decarboxylase (ODC), Elongation Factor 1-alpha (EF-1α)***, markers that are strongly expressed at the MBT in all embryonic cells, and also markers of mesoderm ***brachyury (Xbra)*** and ***chordin.*** *Xrel3, ODC* and *EF-1α* transcripts visible at stage 7-9 are maternal. Zygotic expression of *Xbra, chordin, ODC* and *EF-1α* transcripts are visible at stage 11.
Levels of these markers were normalized by *histone* levels.

3.4.2 Whole embryo run-on experiment of [α-^{35}S]-labeled UTP incorporation between Xrel3 overexpressed and control embryos.

Zygotic transcription usually initiates at stage 8.5 (at about the same time of the MBT) of development. As a test for *de novo* transcriptional activation, I measured the incorporation of radioactively labeled Uridine Triphosphate ([α-^{35}S]-labeled UTP) into total RNA when it was coinjected into control and *Xrel3* mRNA-injected blastulae and gastrulae. Pigmented two-cell-stage embryos were co-injected with 1.0 ng of *Xrel3* mRNA and 50 nCi [α-^{35}S]UTP (400 Ci/ mmole, Amersham) and cultured in 4% Ficoll, in parallel with the control siblings injected with 50 nCi [α-^{35}S]UTP and DEPC-treated water. Starting from stage 7, samples of fifteen injected with *Xrel3* or control embryos were collected at each time point (stages 7, 8, 9, 10, 11) and frozen at -20°C prior to being processed. Total RNA was purified by the use of NETs/LiCl RNA extraction method (Hopwood *et al.*, 1989), and 10 µl from each sample were immobilized on glass fibre filters (GF/A) (Whatman). The filters were washed subsequently with ice-cold 20%, 10%, and 5% trichloracetic acid. Incorporated label was detected by a Liquid Scintillation Analyzer (Beckman LS-3801, USA) (Stancheva and Meehan, 2000). The control embryos did not incorporate label above background levels until stage 8 of development (see Appendix Table 5; Figure 3.15). In contrast I detected up to a two-fold decrease in incorporation of [α-^{35}S] UTP much later in the *Xrel3*-injected embryos at stage 9, less than 50% of that seen at stage 9 in control embryos. The level of incorporation in injected embryos never reached the level of controls. This decline is either due to a decrease in transcriptional rate, or more likely due to the depleting injected free label.

In conclusion, using the incorporation of radioactively labeled Uridine Triphosphate ([α-^{35}S]-labeled UTP) in control and *Xrel3* mRNA-injected blastulae and gastrulae, as a measure of transcriptional activation, I concluded that *Xrel3*-injected embryos initiate zygotic transcription approximately one or two cell cycles after the MBT.

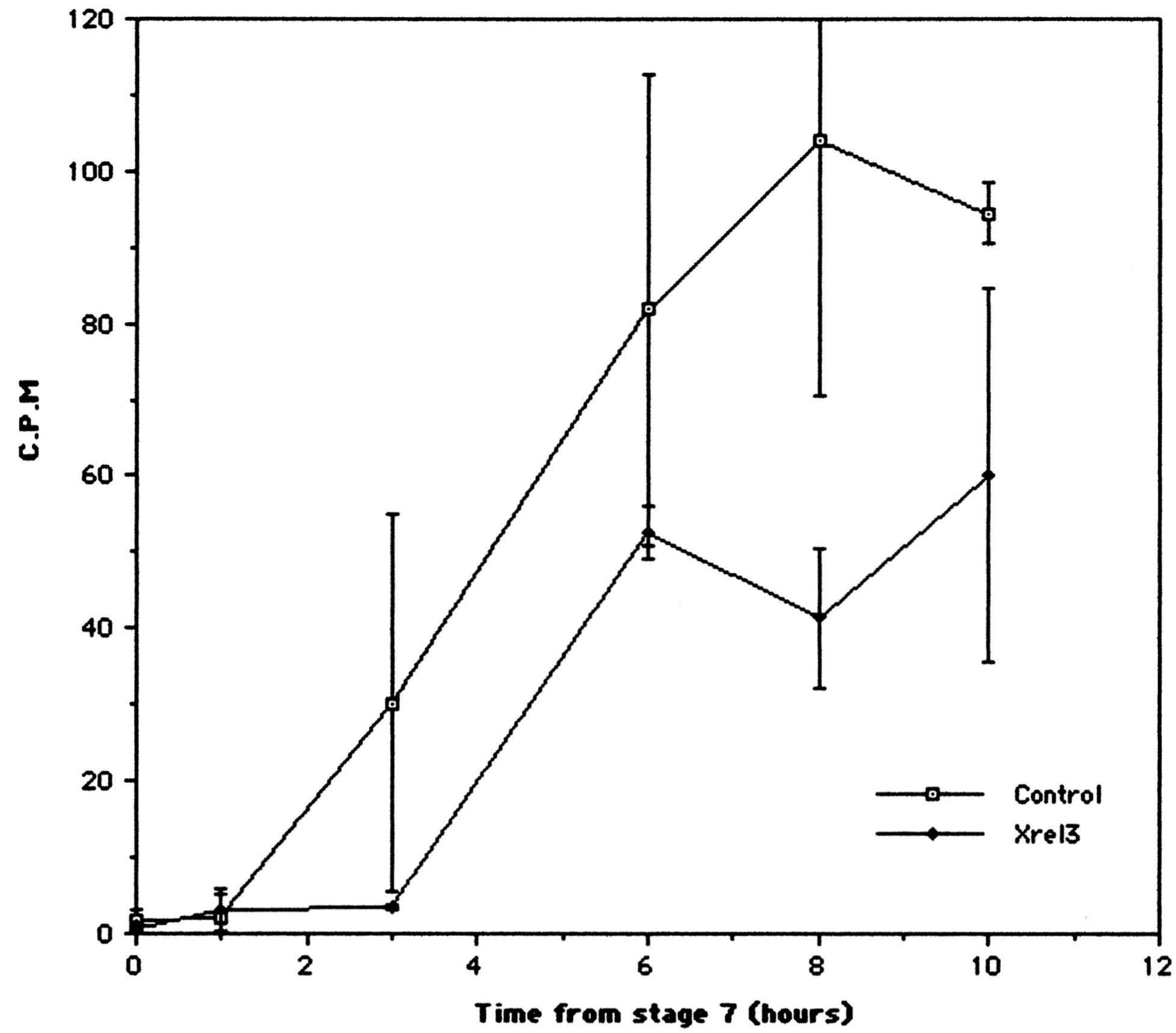

Figure 3.15. *Xrel3* injected embryos delay the onset of transcription at midblastula transition (MBT).

The incorporation of microinjected (50 nCi) [α-^{35}S]- labeled Uridine Triphosphate (UTP) was used to detect the activation of gene expression in *Xrel3* and control injected embryos. Embryos were injected with [α-^{35}S]-UTP along with 1.0 ng *Xrel3* RNA or control DEPC-treated water. Total RNA from fifteen embryos was extracted at hourly intervals following stage 7 (four hours after fertilization at room temperature) and 10 μL of extracted RNA were counted to determine the incorporation of label. Vertical axis represents counts per minute of incorporation of a label of 1 μg of total RNA. Horizontal axis represents time after stage seven. These data indicate the mean and standard deviation (error bars) for three separate experiments (for values for each experiment see Appendix Table 5).

3.4.3 Analysis of gene expression in Xrel3-overexpressed animal caps.

To confirm that *Xrel3* overexpression inhibited transcription, the expression of *EF-1α* and *ODC* was determined in animal caps dissected from embryos injected with 1.0 ng of *Xrel3*. Animal caps are relatively homogeneous populations of cells, which lack the heavy yolk found in vegetal cells, that can interfere with RNA extraction causing undue experimental variability. I asked, if *Xrel3*-expressing animal caps delay increase in *EF-1α* and/or *ODC* expression.

Embryos were injected into the animal pole at the two-cell stage with 1.0 ng *Xrel3* RNA or injected with control RNA and were allowed to develop until stage 7 at room temperature. Animal caps (five caps at each time point) were isolated from control and *Xrel3*-injected embryos starting at stage 7. Samples were collected every thirty minutes initially until stage 9, and then collected at such stages as 10 and 11. Total RNA was extracted from dissected animal caps according to NETs/LiCl protocol (Hopwood *et al.*, 1989). Reverse transcription was performed with random primers. PCR was performed with ^{32}P-ATP trace labeling and gene-specific primers for *EF-1α, ODC* and histone. The expression of these transcripts was analyzed on 6% polyacrylamide sequencing gel. Levels of *EF-1α* and *ODC* were normalized by *histone*. Levels of each markers on the gel were assessed by spot densitometry analysis and the Integrated Density Values (IDV) obtained for each marker are presented in Tables 5-7 (see Appendix).

RT-PCR analysis demonstrated very inconclusive results. The experiment was performed four times (Figure 3. 16a, b) and two of the experiments showed that *Xrel3* delayed the induction of activation of both of these markers. The other two gels (Figure

3.13c-d) only demonstrated a slight to no difference in the delay of expression of *EF-1α* and *ODC* in control or *Xrel3*-injected animal caps. RT-PCR analysis has its limitations in measuring the levels of markers. A different method should have been used, not RT-PCR but ribonuclease (RNase) protection assay or Northern blot to better quantify the levels of *EF-1α* and *ODC*. Histone is not a good marker used for normalization the levels of *EF-1α* and *ODC*, since the levels of histone also increase after MBT (Figure 3.16.)

In conclusion, it can be concluded that analysis of gene expression using RT-PCR of *EF-1α* and *ODC* in animal caps dissected from embryos injected with 1.0 ng of *Xrel3*, could not confirm that the activation of these markers of MBT was delayed. RT-PCR analysis had limitations in demonstrating conclusive results, so we cannot say for sure that *Xrel3* delays the induction of activation of both of these markers.

a

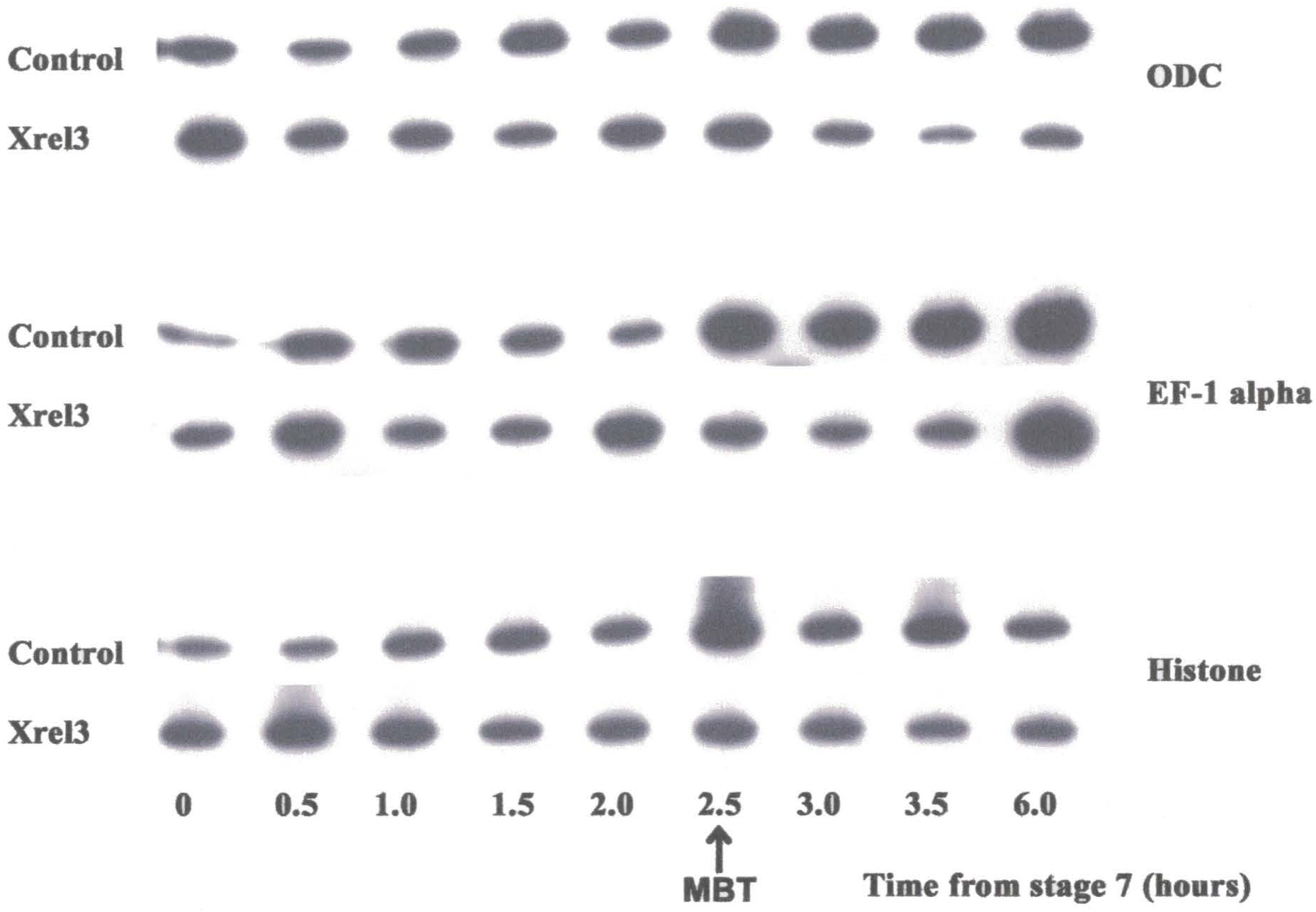
Control
Xrel3
ODC
Control
Xrel3
EF-1 alpha
Control
Xrel3
Histone
0
0.5
1.0
1.5
2.0
2.5
3.0
3.5
6.0
MBT
Time from stage 7 (hours)

b

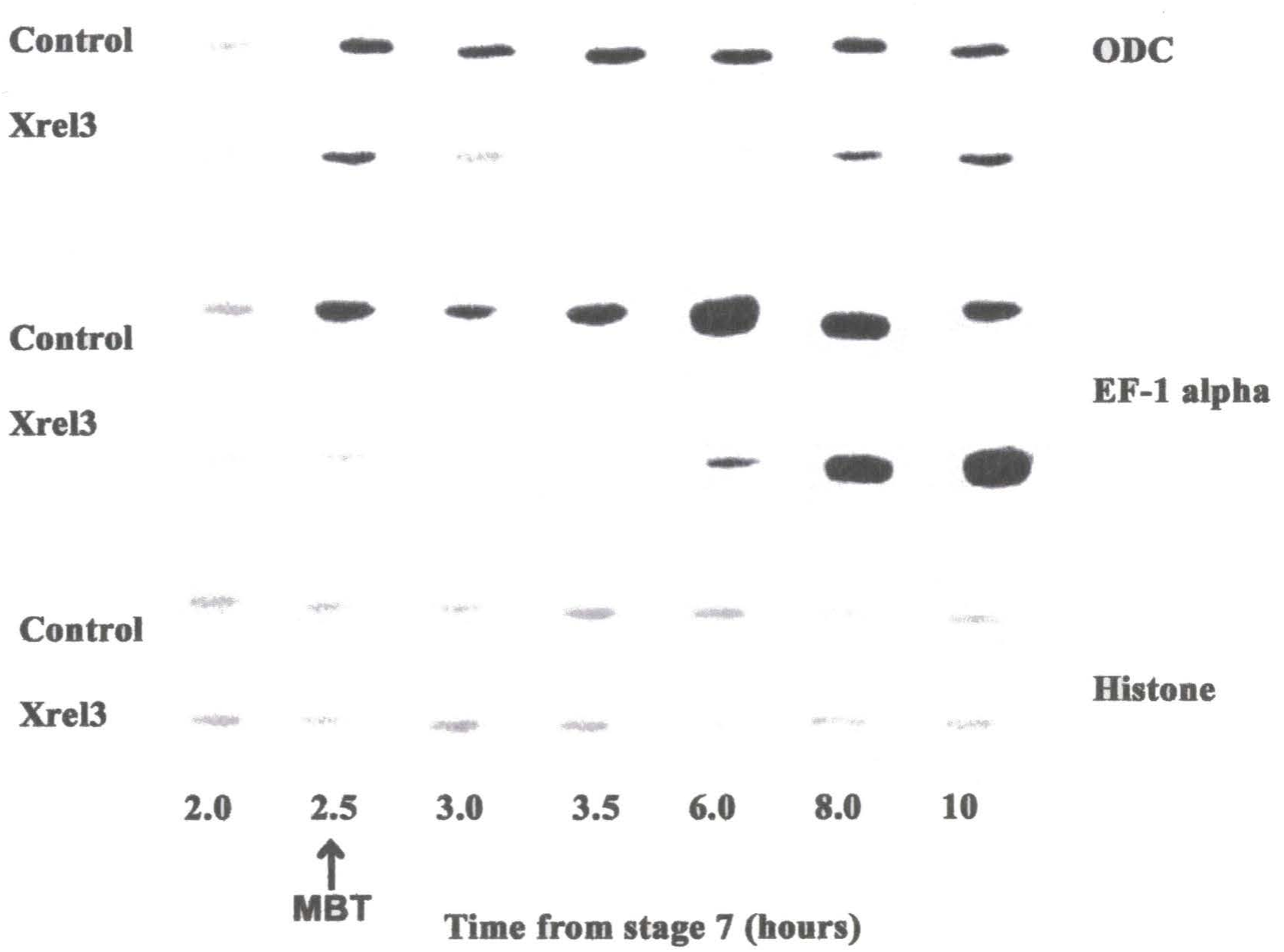
Control
Xrel3
ODC
Control
Xrel3
EF-1 alpha
Control
Xrel3
Histone
2.0
2.5
3.0
3.5
6.0
8.0
10
MBT
Time from stage 7 (hours)

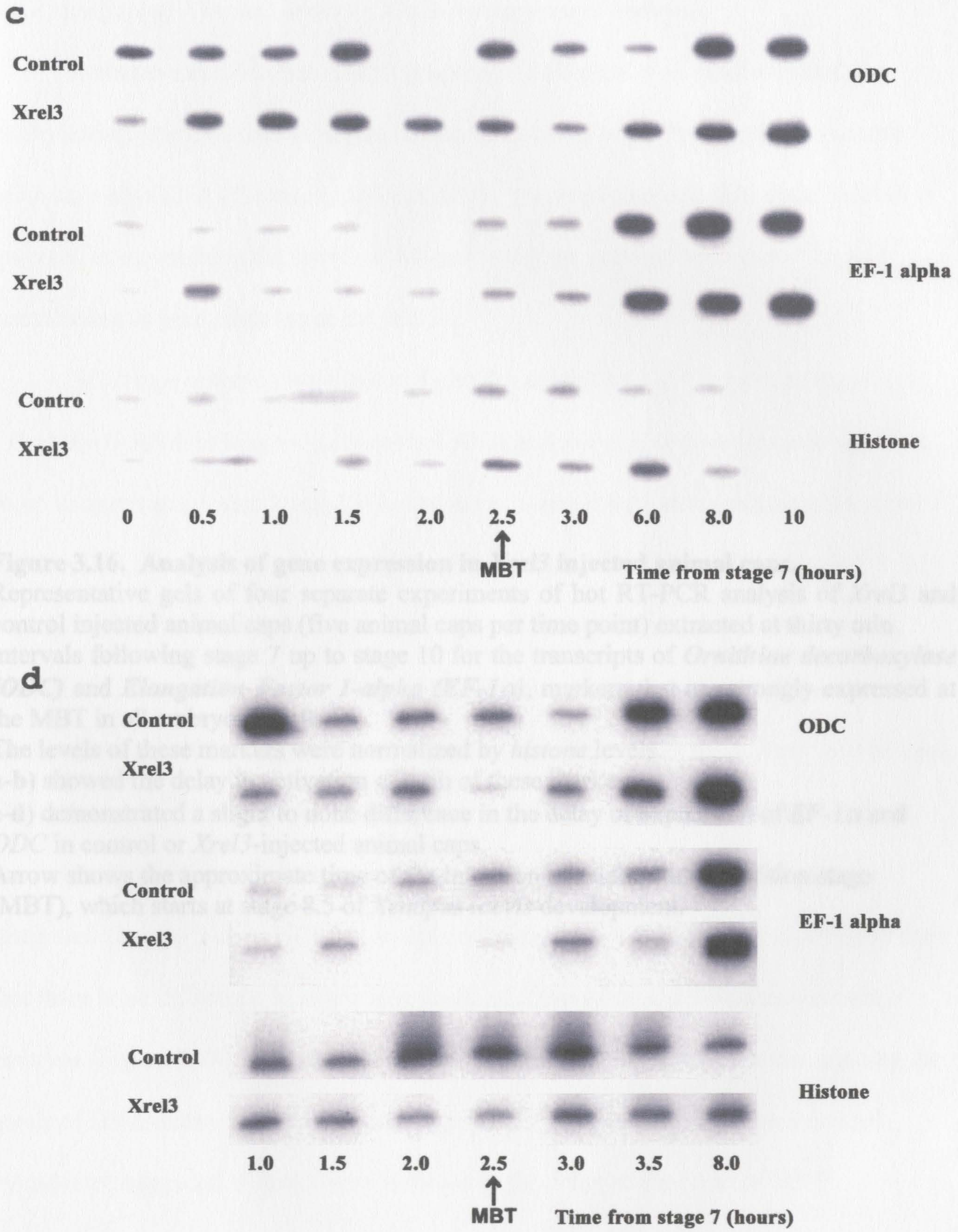
c
Control
Xrel3
ODC
Control
Xrel3
EF-1 alpha
Contro
Xrel3
Histone
0
0.5
1.0
1.5
2.0
2.5
3.0
6.0
8.0
10
MBT
Time from stage 7 (hours)
d
Control
Xrel3
ODC
Control
Xrel3
EF-1 alpha
Control
Xrel3
Histone
1.0
1.5
2.0
2.5
3.0
3.5
8.0
MBT
Time from stage 7 (hours)

Figure 3.16. Analysis of gene expression in *Xrel3* injected animal caps.
Representative gels of four separate experiments of hot RT-PCR analysis of *Xrel3* and control injected animal caps (five animal caps per time point) extracted at thirty min intervals following stage 7 up to stage 10 for the transcripts of ***Ornithine decarboxylase (ODC)*** and ***Elongation Factor 1-alpha (EF-1α)***, markers that are strongly expressed at the MBT in all embryonic cells.
The levels of these markers were normalized by *histone* levels.
a-b) showed the delay in activation of both of these markers.
c-d) demonstrated a slight to none difference in the delay of expression of *EF-1α* and *ODC* in control or *Xrel3*-injected animal caps.
Arrow shows the approximate time of the initiation of midblastula transition stage (MBT), which starts at stage 8.5 of *Xenopus laevis* development.

3.4.4 Analysis of XDnmt1 levels in Xrel3-overexpressed embryos.

Stancheva and Meehan (2000) proposed that depletion of the *Xenopus* DNA methyltransferase (XDnmt1) enzyme, which is involved in DNA methylation, caused premature activation of transcription and MBT. I wanted to check, therefore, if *Xrel3* is involved in maintaining the levels of XDnmt1 enzyme, preventing its depletion and contributing to gene silencing at the MBT.

Wild-type embryos were injected into the animal pole at the two-cell stage with 1.0 ng *Xrel3* RNA or injected with control RNA and allowed to develop until stage 7 at room temperature. Animal caps (five caps at each time point) were isolated from control and *Xrel3*-injected embryos starting at stage 7. Samples were harvested at stage 7, 8, 9, 11, 13, 16 and 20. Total RNA was extracted from collected animal caps according to NETs/LiCl protocol (Hopwood *et al.*, 1989). Reverse transcription was performed with random primers. PCR was performed with gene-specific primers for *XDnmt1* and *histone*. The expression of these transcripts was analyzed on 2% agarose gel. Levels of *XDnmt1* normalized by *histone* levels, were assessed by spot densitometry analysis, and the Integrated Density Values (IDV) obtained and compared. RT-PCR analysis demonstrated that there is no difference in expression levels of *XDnmt1* in *Xrel3*-injected or control embryos (Figure 3.17). Therefore, *Xrel3* does not seem to be involved in maintaining the levels of DNA methyltransferase enzyme or preventing its depletion, which is what would have happened if *Xrel3* were involved in the delay of the onset of MBT.

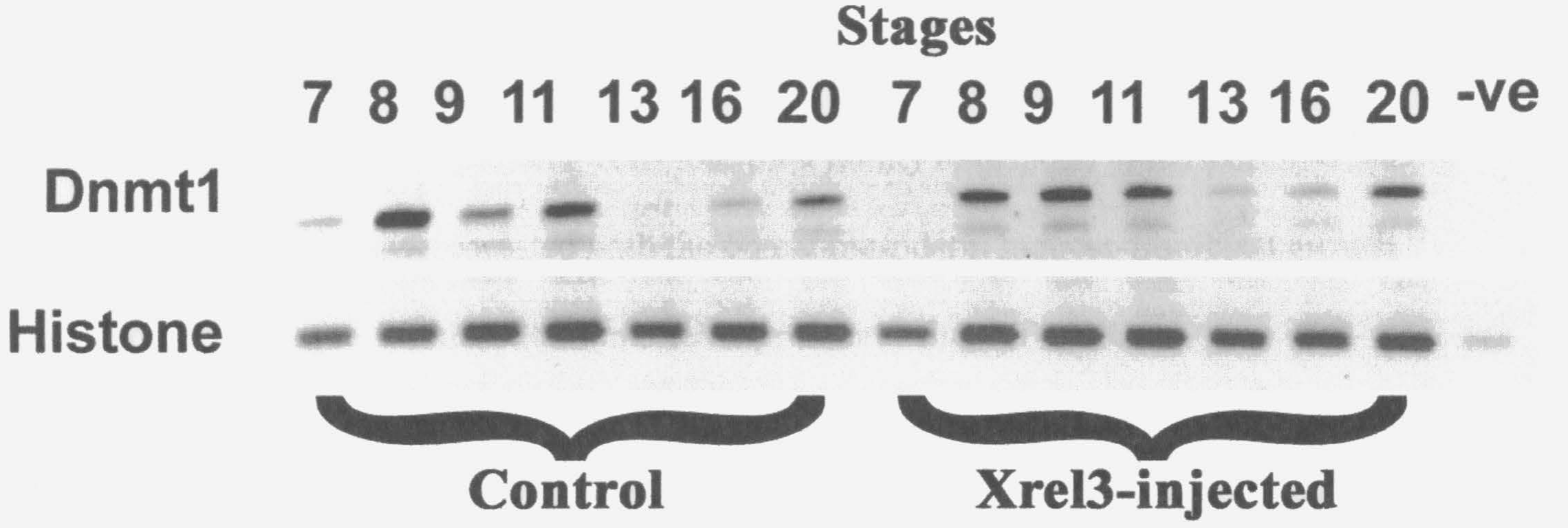

Figure 3.17. *Xrel3* does not prevent the depletion of *DNA methyltransferase*, which is necessary for the onset of MBT.
Representative gel of RT-PCR analysis of *Xrel3* and control injected animal caps (five animal caps per time point) extracted at stages 7, 8, 9, 11, 13, 16 and 20 for the transcripts of ***DNA methyltransferase (XDnmt1)***, another markers of MBT. The levels of *XDnmt1* drop prior the onset of MBT. There is not difference in levels of *XDnmt1* in control and *Xrel3*-injected animal caps. Levels of this marker were normalized by *histone.*

3.5 *Xrel3* does not prevent fibroblast growth-factor mediated mesoderm induction and expression of *Xbra* in animal caps.

When *Xrel3* is injected in the marginal zone of two-cell stage embryos, they develop defects in gastrulation. When these embryos are let to develop further, they seem to have defects in notochord development, when examined at stage 28 (Figure 3.3). This observation suggests that *Xrel3*-injected embryos have defects in mesoderm specification. To test whether *Xrel3*-expressing cells lose their ability to respond to mesoderm-inducing factors, animal caps were treated with the potent mesoderm inducer-fibroblast growth factor, and assayed for mesoderm marker expression using RT-PCR.

Animal caps were dissected from embryos injected with 0.5 ng *Xrel3* mRNA or control RNA at stage 8, treated with varying concentrations of basic FGF and assayed for the expression of the early mesoderm marker *Xbra*. Control and *Xrel3*-injected animal caps treated with bFGF show elongation corresponding to mesoderm induction at stage 13 (Figure 3.18A) and at stage 28 they form into "embryoid bodies," because they resemble miniature embryos (Figure 3.18C). Molecular analysis with the mesodermal marker *Xbra* confirmed the expression at stage 10.5 of *Xbra* in control animal caps and animal caps from embryos injected with *Xrel3* at concentrations as low as 50 ng/mL (Figure 3.18D). No induction or expression of *Xbra* was observed in control or *Xrel3*-injected animals caps untreated with FGF (Figure 3.18D). These results suggest that *Xrel3* does not reduce FGF-mediated induction of animal caps or the expression of Xbra in FGF-treated embryos (Figure 3.19).

Animal caps from embryos injected with different concentrations of *Xrel3* (0 ng; 0.25 ng; 0.5 ng; 1.0 ng) and treated with 125 ng/mL of bFGF undergo dramatic elongation when control embryos are gastrulating at stage 11 and form "embryoid bodies" at stage 28 (Figure 3.20), although they exhibit reduction of elongation relative to the injection dosage. High dosages, such as 1.0 ng *Xrel3* RNA caused a reduction of about 25% in the average length of FGF-treated animal caps (Figure 3.19, Figure 3.20). No elongations were observed in untreated animal caps from embryos injected with *Xrel3* (Figure 3.20). These findings indicate that *Xrel3* does not prevent FGF-induced elongation of animal caps.

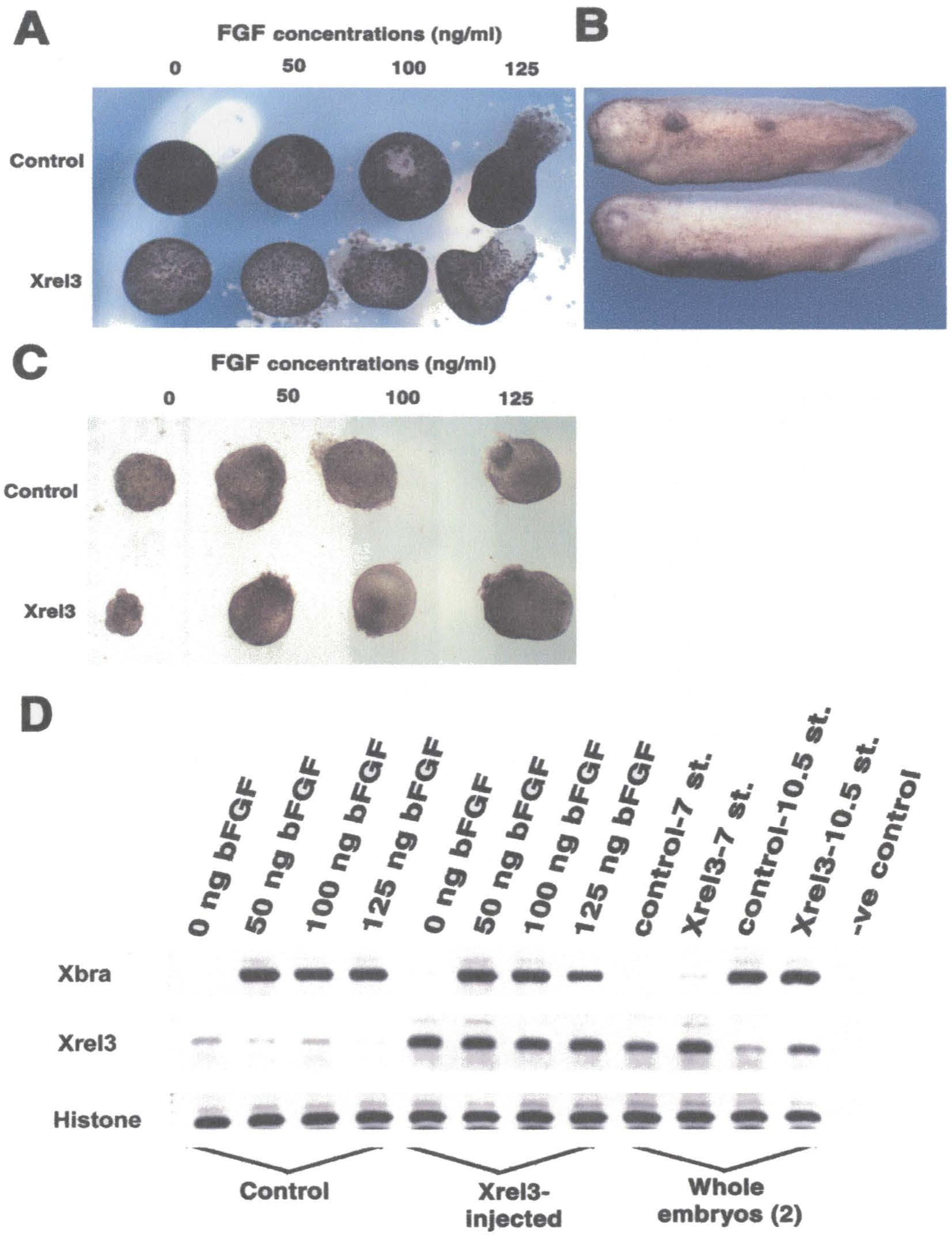

Figure 3.18. *Xrel3* does not prevent mesoderm induction by bFGF.
Animal caps were dissected at stage 8 from embryos injected with 0.5 ng either *Xrel3* or control, treated with varying concentration of recombinant *Xenopus basic FGF*: 0 ng/mL; 50 ng/mL; 100 ng/mL; 125 ng/mL; and (**A**) photographed for elongation characteristics of mesoderm induction at stage 13, or (**C**) at stage 28; (**D**) harvested at stage 10.5 for RT-PCR analysis using primers for ***brachyury (Xbra), Xrel3*** and ***histone.*** Levels of these markers were normalized by *histone* levels. Negative control is a control PCR reaction of RNA sample without reverse transcription. Injected embryos were left to develop and assayed for the formation of tumours (**B**). Scale bar, 1 mm.

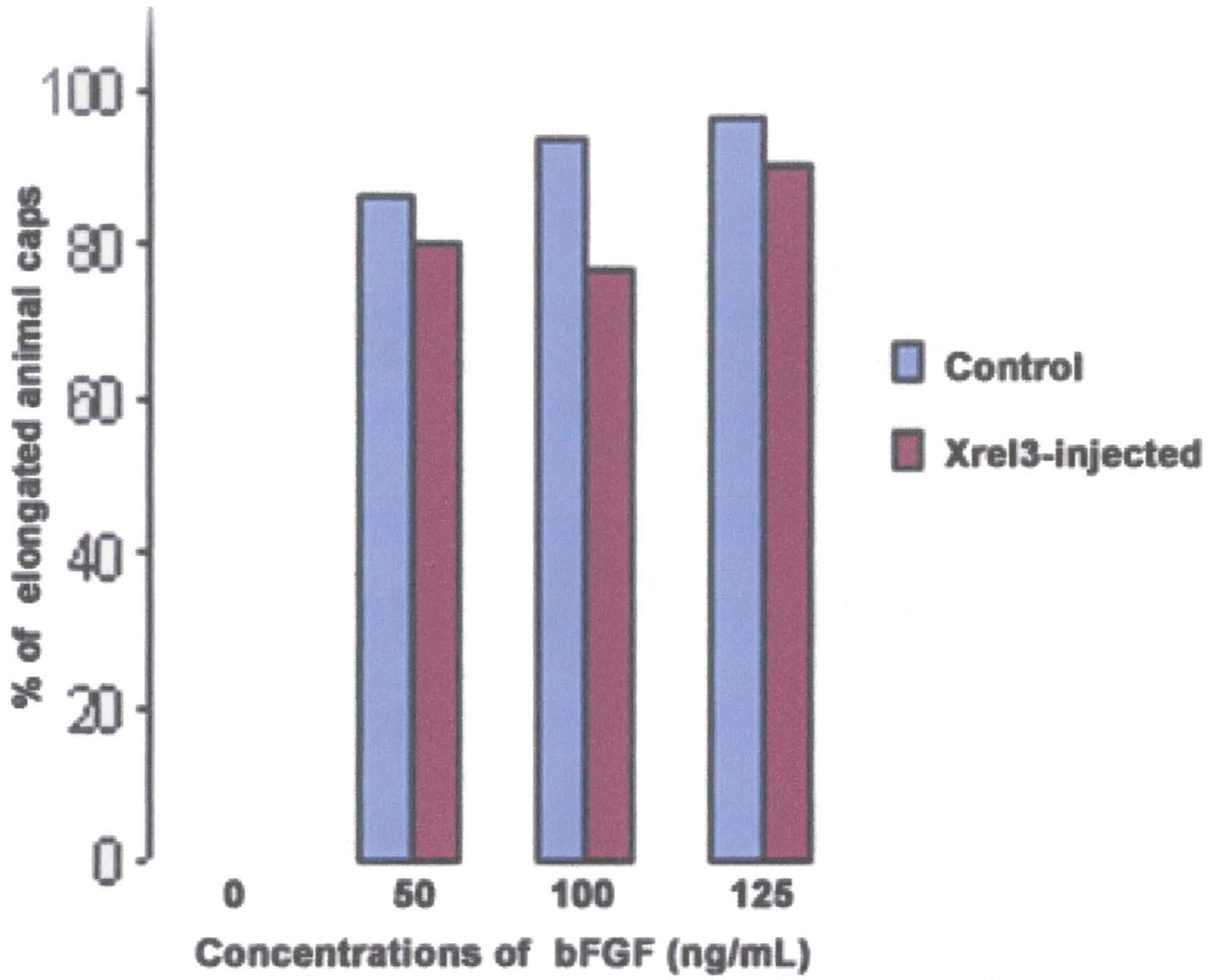

Figure 3.19. Percentages of FGF-induced animal caps obtained from embryos injected with *Xrel3* or control into the animal region.

Horizontal axis represents varying concentration of recombinant *Xenopus basic* FGF: 0 ng/mL; 50 ng/mL; 100 ng/mL; 125 ng/mL. Vertical axis represents the percentage of embryos relative to a total number of embryos injected and scored in three separate experiments (for values see Appendix Table 8).

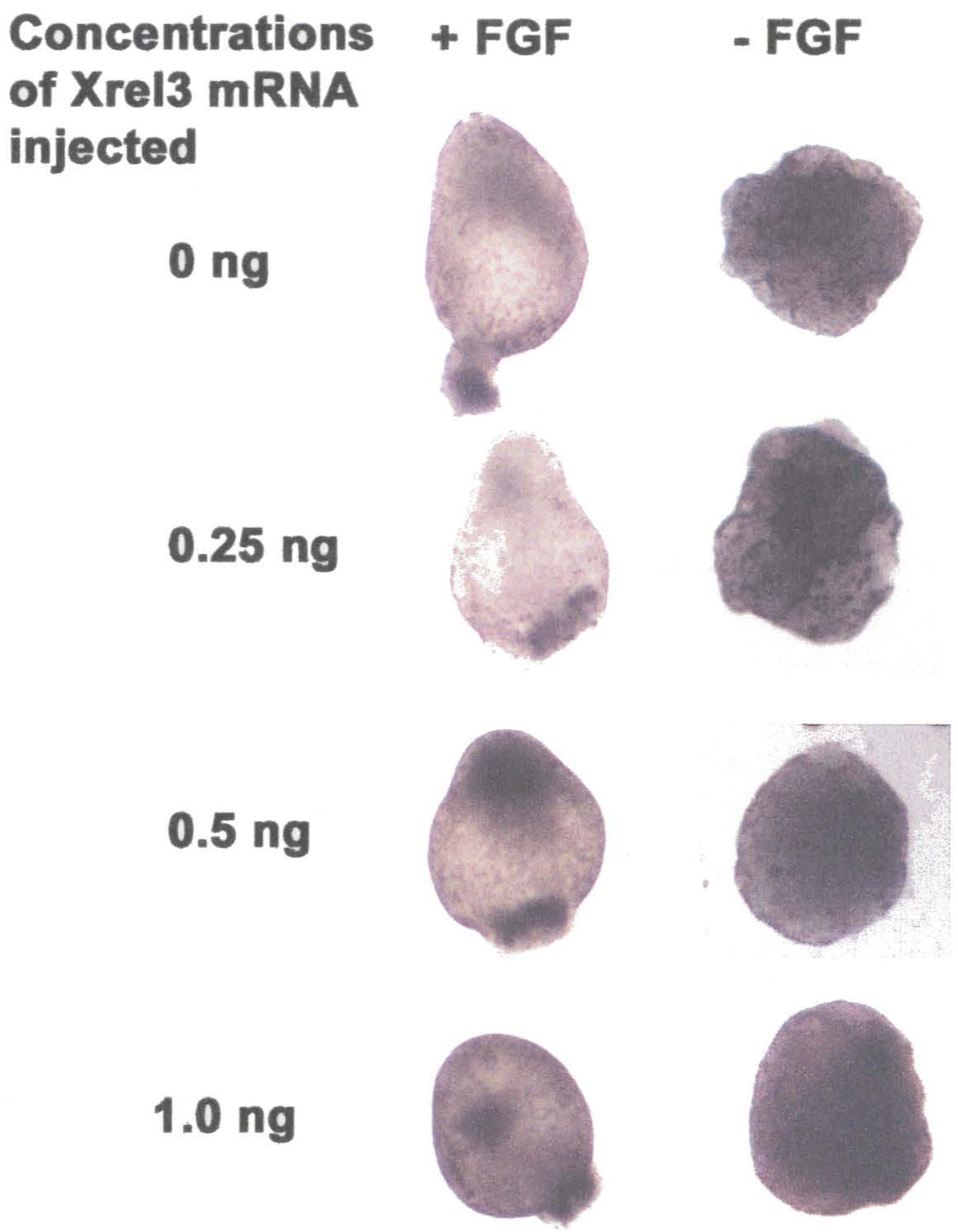

Figure 3.20 Injections of *Xrel3* in different concentrations does not prevent FGF-induced elongation of animal caps.

Animal caps (stage 28) collected from embryos injected with different concentrations of *Xrel3* at the two-cell stage in the animal region and treated with **125 ng/mL** of recombinant ***Xenopus* basic FGF**: Animal caps from embryos injected with *Xrel3* and treated with *bFGF* undergo reduction of elongation relative to the injection dosage. No induction is observed in untreated animal caps.

3.9 Effects of *Xrel3* on activin-induced elongation of animal caps.

The origin of phenotypes we have observed by *Xrel3* over expression might be explained by alterations in gastrulation movements. It is possible to mimic the elongation movements associated with dorsal development *in vitro* by treating animal cells at the early blastula stage with factors known to cause differentiation of dorsal tissues. We have taken advantage of this technique to examine what effect *Xrel3* RNA injections have on convergent extension, a central process to dorsal differentiation (Kao and Lockwood, 1996).

Animal caps were treated with media conditioned from XTC cells, which contains activin, a strong dorsoanteriorizing growth factor, and is able to induce convergent extension *in vitro* (Smith *et al.,* 1990; Kao and Lockwood, 1996). As expected, animal caps isolated from *Xrel3*-injected and control embryos that are exposed to XTC-conditioned medium (XTC-CM) undergo dramatic elongation when control embryos are gastrulating at stage 11 (Figure 3.21). Animal caps from embryos injected with *Xrel3* and treated with XTC-CM undergo reduction of elongation relative to the injection dosage (Figure 3.21). Low dosages, such as 0-0.25 ng *Xrel3* RNA caused a reduction of about 50-75% in the average length of XTC-CM treated animal caps (Figure 3.21), while higher concentrations of *Xrel3* (from 0.5-1.0 ng) caused a complete reduction of elongation, and the animal caps appeared indistinguishable from the untreated cases. These findings indicate that *Xrel3* reduces activin-induced elongation of animal caps.

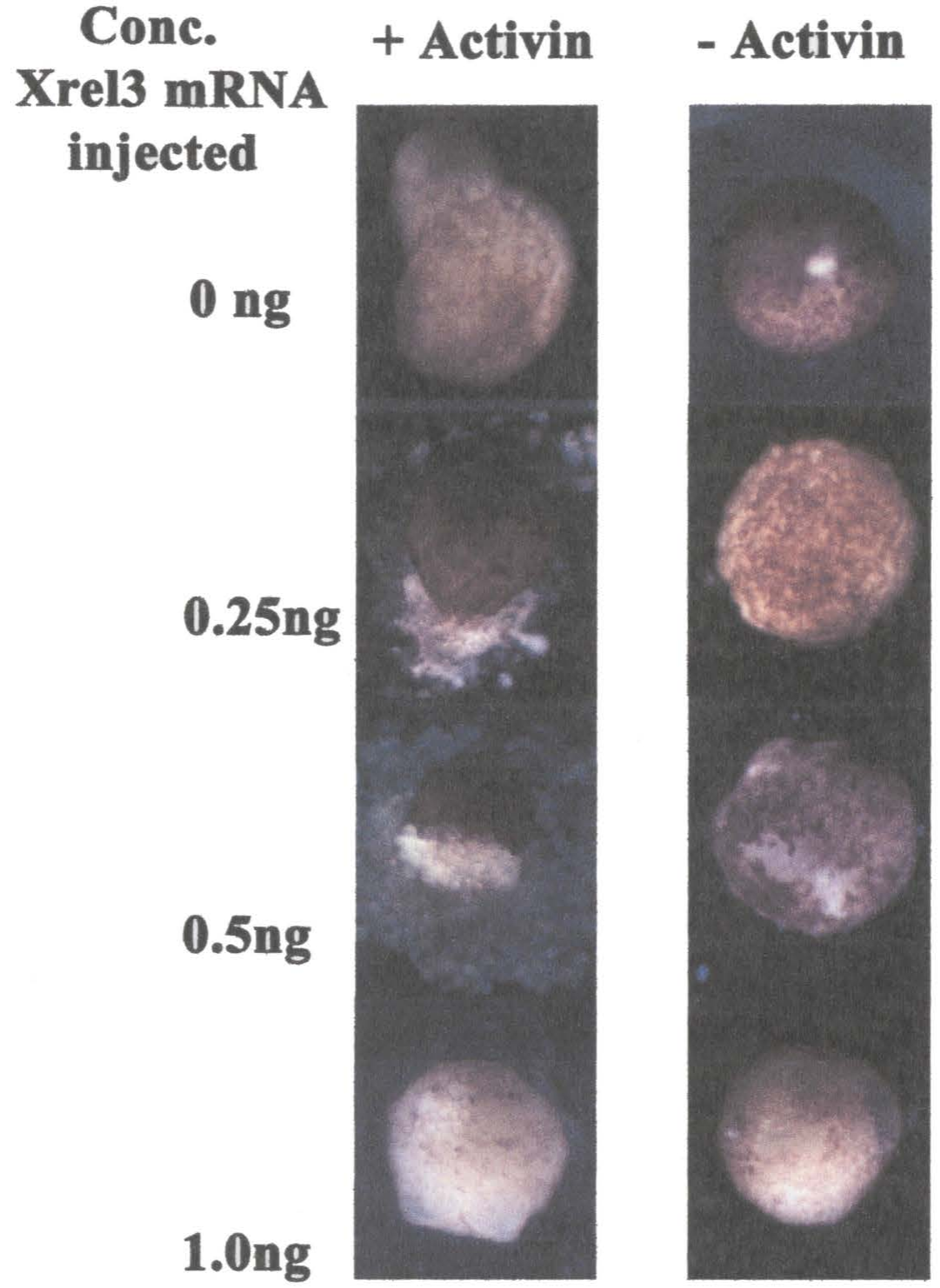

Figure 3.21 *Xrel3* reduces activin-induced elongation of animal caps.
Animal caps (stage 11) collected from embryos injected with different concentrations of *Xrel3* at the two-cell stage in the animal region and treated for one hour with 18 ng/mL *activin*. Animal caps from embryos injected with *Xrel3* and treated with XTC-CM undergo reduction of elongation relative to the injection dosage. No induction is observed in untreated animal caps.

CHAPTER 4.

DISCUSSION.

4.1 Possible mechanisms of tumour formation in *Xrel3*-injected embryos.

In this project I attempted to determine why *Xrel3* overexpression causes tumours in embryos. My findings suggested that *Xrel3* overexpression causes the formation of tumours by limiting cell migration and differentiation before gastrulation. However, my experiments to determine if the tumours are formed by increased cell proliferation were inconclusive.

The use of the *Xenopus laevis* embryo as a model system for tumourigenesis is still in its infancy, but it has become an effective approach to the study of formation and development of neoplasia (Wallingford, 1999). The key question that must be answered is whether or not these masses of cells that are formed as a result of *Xrel3* overexpression are actually tumours.

Another possibility to explain tumour formation as a result of *Xrel3*-overexpression is that Xrel3, like other Rel/NF-κB proteins (see review by Li and Stark, 2002) is able to prevent apoptosis (programmend cell death) in cells of the developing embryo. Programmed cell death refers to the naturally occurring cell death that is part of the developmental program of an organism (Jacobson *et al.,* 1997). Previous studies have shown that in *Xenopus* development the maternal cell death program is set up at fertilization and abruptly activated at the onset of gastrulation at stages 10.5 to 11.5, when any damaged cells that have accumulated since fertilization are removed. Also,

large numbers of apoptotic cells were detected in the developing *Xenopus* neurula (Hensey and Gautier, 1997; 1998).

During MBT a dramatic change occurs in response of the embryo to DNA damage. Before MBT, the *Xenopus* embryo is able to initiate apoptosis in response to ionizing radiation, but loses its ability to do this after MBT, becoming resistant to apoptosis (Finkielstein *et al.*, 2001). It is possible that *Xrel3* prevents the activation of apoptotic pathways before MBT, which leads to cell accumulation and tumour formation.

In my study, the analysis of molecular markers demonstrated that *Xrel3*-induced ectodermal tumours aberrantly express *Shh* and *Gli* genes (Lake *et al.,* 2001), which are involved in tumourigenesis (Dahmane *et al.,* 1997). Similar tumours are caused by overexpression of *Gli1* (Dahmane *et al.,* 1997) and a dominant negative form of the p53 tumour suppressor and its wild-type antagonist *Mdm2*, when injected into the early embryo (Wallingford *et al.,* 1997). What is confusing is that activation of these genes, due to overexpression of *Xrel3* occurs in later stages, long after the MBT, when the *Xrel3* message has disintegrated (Lake *et al.,* 2001). Thus, the origin of tumours must not depend entirely on *Shh* expression.

It is more likely that *Xrel3*-induced tumours arise from cells not participating in a normal process of cell movements and rearrangements that result from growth factor dependent processes occurring during gastrulation. In my experiments presented in this thesis, animal cells from embryos injected with *Xrel3* RNA and then treated with the inducing factor activin A did not differentiate into mesoderm, nor did they undergo morphological changes characteristic of induction. Xrel3 however, did not prevent animal

caps to form mesoderm and express mesoderm specific markers in response to bFGF. It is possible, therefore, to propose that *Xrel3* interferes with specific cellular properties, such as adhesion and cell motility, which are necessary for gastrulation movements. Not enough or too much adhesion between cells, for instance has detrimental effects on gastrulation movements in *Xenopus* development (Popsueva *et al.*, 2001), and *Xrel3* overexpression, or the subsequent effects of this overexpression may be involved in this process.

4.2. Effects of *Xrel3* overexpression on embryo phenotype.

The results presented in this work confirm and extend the results obtained previously by Yang *et al.* (1998), who also reported the effect of *Xrel3* overexpression; in particular I asked what factors might contribute to the formation of tumours in the earlier stages of development, before the onset of embryonic transcription and gastrulation. Ectopic expression of *Xrel3* seems to have a major effect on pre-gastrula development, because there are definite morphological, molecular and cellular differences between control and *Xrel3*-injected embryos before and during gastrulation.

The site of injection of *Xrel3* mRNA seemed to play a major role in the generation of embryonic phenotypes. In particular, overexpression of *Xrel3* into the dorsal marginal zone caused a reduction in dorsoanterior structures in embryos, with the majority of embryos having small heads, kinked backs and shortened tail. Most of them failed to form the blastopore lip and initiate gastrulation movements, as compared to controls. This indicates that the target of *Xrel3* overexpression resides in the dorsal region of the embryo. Embryos injected in prospective lateral regions had fewer dorsoanterior defects as compared to dorsal injection

phenotypes. The large numbers of dorsoanterior defects in lateral injections could be due to diffusion of *Xrel3* RNA to the dorsal side. It is possible that *Xrel3* overexpression in the dorsal marginal zone mimics the effect of ventralizing agents such as *BMP-4, X-vent*. More investigation is necessary to determine the various interactions of *Xrel3* with factors such as these in ventral development.

4.3 Role of *Xrel3* in regulation of MBT.

MBT occurs at stage 8.5 of *Xenopus* development, after the 12th cleavage division (approximately 4096 cells), and is associated with major changes in cell cycle checkpoints, slowing down the rate of DNA synthesis, initiation of zygotic transcription, loss of cell cycle synchrony and increase in cell motility (Newport and Kirschner, 1982a,b). How MBT is controlled is not completely understood.

My results show that *Xrel3* overexpression does not contribute to the maintainance of the dividing cells in the pre-MBT state by blocking the slowing down of DNA synthesis, delaying the initiation of embryonic transcription or premature activation of transcripts of MBT.

It is possible, however, that *Xrel3* might interfere with the increase in cell motility, which usually occurs at MBT (Newport and Kirschner, 1982a,b). This hypothesis would explain the delays in gastulation movements that I observed in *Xrel3*-overexpressed embryos. The mechanism of action is not clear how *Xrel3* overexpression might affect those molecules that are involved in cell movements. The accumulation of non-moving cells due to both inhibition of migration and increased proliferation might be factors that contribute to tumour formation in developing embryos.

4.4 Effects of *Xrel3* overexpression on mesoderm induction in animal caps.

I have described the effects of *Xrel3* overexpression in the marginal zone of two-cell stage embryos on mesoderm differentiation, an event, which also coincides with MBT. The period of competence for mesoderm induction is thought to begin before the MBT at about stage 6.5 and extend until gastrulation (Domingo and Keller, 2000). The transcription of mesoderm specific genes is activated at MBT, so the embryos overexpressing *Xrel3* develop defects in gastrulation and later in development they show defects in notochord development, when examined at stage 28, which corresponds to reduction in *Xbra* expression in developing embryos (Figure 3.3).

When *Xrel3*-overexpressed animal caps were assayed for mesoderm induction using bFGF and assayed for *Xbra*, an immediate early gene expressed in response to mesoderm induction (Smith *et al.*, 1991), *Xrel3*-expressing cells do not seem to lose their ability to respond to mesoderm-inducing factors. The animal caps continue to respond to *bFGF*, showing elongation movements and the expression of *Xbra*. This suggests that the effects of Xrel3 do not interfere with FGF-induced mesoderm induction. It is possible, therefore that Xrel3 acts upstream of FGF-mediated induction.

The above observations suggest that *Xrel3* inhibits mesoderm induction, not by interfering with bFGF pathway, but by regulating activin A signaling. The results presented here show that when animal caps from embryos injected with *Xrel3* were treated with activin, Xrel3 reduced their ability to elongate. This suggests a link between *Xrel3* and activin signalling, which must be investigated further. One possibility is that

Xrel3 is not able to inhibit zygotic FGF, but is able to inhibit the specification of competence to respond to activin-like signals, which depends on maternal FGF expression. If this were the case, then the immediate early response to activin would be affected. In this work, I did not assay for *Xbra* expression in activin-treated animal caps, but the reduction in elongation movements is good evidence that *activin* was not able to cause the mesoderm induction in *Xrel3*-treated animal caps. The induction of mesoderm in animal caps by bFGF suggests that *Xrel3* might repress genes that are required for the synthesis or release of eFGF, or that *Xrel3* might act as a brake on eFGF-Xbra autocatalytic loop that is required for the stability of mesodermal phenotype in marginal zone during gastrulation (Issacs *et al.*, 1994).

XrelA has also shown to be involved in mesoderm induction. The deletion mutant of *XrelA* was able to inhibit FGF-induced and activin-induced mesoderm induction (Beck *et al.*, 1998; Kao and Lockwood, 1996). In this work we observe the opposite, that mesoderm can be rescued by bFGF in *Xrel3*-injected animal caps. It indicates that *XrelA* and *Xrel3* might have different functions in *Xenopus* development, although, overexpression of both genes leads to the formation of tumour-like epidermal protrusions, so some similarity must still exist (Kao and Hopwood, 1991; Yang *et al.*, 1998).

On the basis of the results presented here, I propose that *Xrel3* overexpression does not permit dorsal cell differentiation in animal caps treated with activin. In this regard, it is also possible that there might be a link between activin signaling and *Xrel3* expression. This link was demonstrated by other workers between TGF-β signalling and NF-κB proteins. In particular, NF-κB was found to inhibit activities of TGF-β in matrix

synthesis, inflammation, apoptosis, and hematopoiesis (Oberhammer *et al.,* 1992; Snoeck *et al.,* 1996; Bitzer *et al.,* 2000). The activation of NF-κB/RelA by a variety of pathogenic and proinflammatory stimuli inhibits TGF-β signaling at the level of TGF-β type I receptor function through increase of transcription of the Smad7 gene and elevation of intracellular levels of Smad7 protein (Bitzer *et al.,* 2000). It is possible that *Xrel3* might be able to activate Smad7 regulatory protein, which is able to inhibit activin signalling. Futher investigation is necessary to confirm that this interaction exists between these two signalling pathways in *Xenopus* development.

In conclusion, work presented in this thesis is directed towards supporting the hypothesis that *Xrel3* is involved in *Xenopus* development and cell differentiation. This work will be important for future studies and technological advances in development and human cancer research. Further studies are needed to continue analysis and discoveries of the novel genes of both development and human cancer using the *Xenopus* system to generate novel information and determine the function of novel genes.

APPENDIX A.

TABLE 1A. Components of NAM (10x)

	g/L (in 10xNAM)	Final Concentrations (mM		
		1x NAM	NAM/2	NAM/20
NaCl	65	110	55	5.5
KCl	1.5	2	1	0.1
$Ca(NO_3)_2 \cdot 4H_2O$	2.4	1	0.5	0.05
$MgSO_4 \cdot 7H_2O$	2.4	1	0.5	0.05
EDTA (0.5 M, pH 8.0)	2	0.1	0.05	0.005
HEPES (1M, pH 7.5)	100	10	5	0.5

TABLE 1B. Components of NAM Solutions

For 100 mL of 1x solution, add:

	NAM (mL)	NAM/2 (mL)	NAM/20 (mL)
10xNAM (see Table 1A)	10	5	0.5
Gentamycin (10 mg/mL)	0.25	0.25	0.25
Sodium Bicarbonate (0.1 M)	1.0	1.0	----
Sterile H_2O	88.27	93.75	99.25

TABLE 2. RNA production using Sp6 RiboMAX kit (Promega)

Reagent added	Volume added (μL)	Final concentrations (mM)
Sp6 5x transcription buffer 400 mM HEPES-KOH, pH 7.5 160 mM gCl_2 10 mM spermidine 200 mM DTT	10	**Sp6 1x buffer** 80 32 2 40
rATP (100 mM)	2.5	5
rCTP (100 mM)	2.5	5
rUTP (100 mM)	2.5	5
rGTP (100 mM)	0.3	0.6
40 mM Ribo m^7G Cap Analog ($m^7G(5')ppp(5')G$) (Promega).	15	12
linear (*pCS2+/-Xrel3*) template (5 μg)	9	0.9 μg
SP6 RNA polymerase enzyme mix	5	---
nuclease-free H_2O	3.5	---
Total	50	

TABLE 3. Reverse transcription reaction mixture volumes per each sample in a 22 μL total volume.

Reagents	Volumes (μL)	Final concentrations (mM
5X First Strand Buffer	4	45.5 mM Tris-HCl 68.2 mM KCl 2.7 mM $MgCl_2$
DTT (0.1 M)	2	9.1 mM
dNTPs (10 mM)	2	0.9 mM (0.23 mM of each of dATP, dCTP, dGTP, dTTP)
random primers (0.1 μg/μL)	2	9.1 ng/μL
RNA guard (100 U/mL)	1	4.5 U/ mL
Reverse Transcriptase enzyme (M- MLV) (200 U/μL)	1	9.1 U/μL
RNA sample (~1 μg) in 10 μL DEPC· H_2O	10	----
Total	22	

TABLE 4. Primers used for RT-PCR analysis.

Primer Name	Primer sequence	Tm	Size of product (bp)	Cycles	References
Xrel3 (crp 18) (crp 20)	Forward 5'-TCCTTGGAGATATTTGTGGGG-3 Reverse 5'-TTTAAACCGGCCATGTTGATG-3'	65.0°C 70.0°C	153	25	Yang *et al.*, 1998
Histone (H4-1) (H4-2)	Forward 5'- CGGGATAACATTCAGGGTATCACT-**3'** Reverse 5'-ATCCATGGCGGTAACTGTCTTCCT-3'	72.2°C 74.0°C	188	23	Niehrs *et al.*, 1994
Dnmt1 (XDnmt1) (XDnmt2)	Forward 5'-TCTTGTGGATGAATGCGAGG-3' Reverse 5'-CCACATCATCCTTCCTCT-3'	68.0°C 65.0°C			Stancheva and Meehan, 2000
EF-1α (XR-1) (XR-2)	Forward 5'-CAGATTGGTGCTGGATATGC-3' Reverse 5'-ACTGCCTTGATGACTCCTAG-3'	68.3°C 68.3°C	221	20	Agius *et al.*, 2000
ODC (ODC-D) (ODC-U)	Forward 5'-TCCATTCCGCTCTCCTGAGCAC-3' Reverse 5'- GTCAATGATGGATGTATGGATC-3'	75.0°C 70.0°C	228	25	Agius *et al.*, 2000
Xbra (LO-1) (LO-2)	Forward 5'-GGGCCCAACCAGGTGTGGGTG-3' Reverse 5'-GTAGTCRGTAGCAGCAGTCCC-3'	64.5°C 64.5°C	390	25	Agius *et al.*, 2000
Chordin (VG-1) (VG-2)	Forward 5'-AACTGCCAGGACTGGATGGT-3' Reverse 5'-GGCAGGATTTAGAGTTGCTTC-3'	70.3°C 68.9°C	267	25	Sasai *et al.*, 1994

TABLE 5. Volumes used and final concentrations of each PCR component constituting a 50 μL of total reaction.

PCR components	Volumes used (μL)	Final concentrations (mM)
10xPCR buffer	5	50 mM KCl 10 mM Tris-HCl (pH 9.0) 0.1% Triton X-100
50 mM $MgCl_2$	1.5	1.5 mM
10 mM dNTP	4	0.8 mM (0.2 mM of each of dATP, dCTP, dGTP, dTTP)
100 μg/mL Primer #1	2	4 μg/mL
100 μg/mL Primer #2	2	4 µg/mL
Platinum Taq DNA polymerase (5 U/μL)	0.2	0.02 U/μL
cDNA	2	---
Distilled water	33.3	---
Total volume	50	

APPENDIX B

TABLE 1 **Assessment of phenotypes observed upon overexpression of different concentrations of *Xrel3* mRNA in the animal regions of two-cell stage embryos (average of three experiments).**

[C] of Xrel3 injected (ng)	Numbers of embryos with phenotypes							
	Total n	Delays in blastopore closure at gastrulation (stage 11) n (%)	Died during gastrula (stage 11) n (%)	Axial defect at neurulation (stage 20) n (%)	Tumour forming (stage 20) n (%)	Died during neurula (stage 20) n (%)	Microcephaly shortened trunk (stage 25) n (%)	Normal looking (stage 25) n (%)
0 ng	30	2 (6)	2 (6)	1 (3)	--	1 (3)	0	27 (90)
0.5 ng	30	4 (13)	2 (6)	2 (6)	23 (76)	0	10 (33)	3 (10)
1.0 ng	30	9 (30)	4 (13)	5 (16)	26 (86)	1 (3)	13 (43)	0
2.0 ng	30	22 (73)	21 (70)	29 (96)	27 (90)	8 (26)	0	0
4.0 ng	30	26 (86)	23 (76)	30(100)	27 (90)	7 (23)	0	0

TABLE 2. **Assessment of phenotypes observed upon overexpression of *Xrel3* mRNA in the animal, marginal and vegetal regions of two-cell stage embryos (average of three experiments).**

Site of injection	Numbers of embryos with phenotypes									
	Sample	Total n	Delays in blastopore closure at gastrulation (stage 11) n (%)	Died during gastrula (stage 11) n (%)	Axial defect at neurulation (stage 20) n (%)	Dark spots at neurula forming on the surface (stage 20) n (%)	Died during neurula (stage 20) n (%)	Microcephaly shortened trunk (stage 32) n (%)	Normal looking (stage 32) n (%)	Tumour -like lumps (stage 32) n (%)
Animal pole	Control	100	4 (4)	7 (7)	3 (3)	0	5 (5)	4 (4)	81 (81)	0
	Xrel3	100	26 (26)	20 (20)	11 (11)	57 (57)	6 (6)	26 (26)	12 (12)	24 (24)
Marginal zone	Control	100	2 (2)	19 (19)	3 (3)	0	3 (3)	3 (3)	77 (77)	0
	Xrel3	100	51 (51)	28 (28)	12 (12)	0	6 (6)	36 (36)	4 (4)	7 (7)
Vegetal pole	Control	100	2 (2)	11 (11)	1 (1)	0	3 (3)	5 (5)	85 (85)	0
	Xrel3	100	38 (38)	27 (27)	6 (6)	0	13(13)	2 (12)	17 (17)	22 (22)

TABLE 3. **Distribution of phenotypes caused by dorsal or lateral marginal zone injections of *Xrel3*.**

Injection site	Numbers of embryos with phenotypes								
	Sample	Total n	Defects at gastrulation (Stage 10.5) n (%)	Axial defects at neurulation (Stage 20) n (%)	Tumour forming (Stage 20) n (%)	Microcephaly (Stage 32) n (%)	Kinked, shortened trunk (Stage 32) n (%)	Normal (Stage 32) n (%)	Died n (%)
dorsal	Control	126	4 (3)	4 (3)	0	0	4 (3)	106(86)	8 (6)
	Xrel3	115	104 (90)	97 (84)	27(23)	36 (31)	91 (79)	0	11(9)
ventral	Control	119	3 (2)	2 (2)	0	0	4 (4)	104(87)	6 (5)
	Xrel3	105	54 (51)	38 (36)	11(10)	13 (12)	51 (48)	0	9 (8)

TABLE 4. **Measurement of the incorporation of radioactively labeled Uridine Triphosphate ([α-^{35}S]-labeled UTP) in control and *Xrel3* mRNA-injected blastulae and gastrulae.**

Sample		Stages (hours from stage 7)					
		St. 7 (0)	St. 8 (1.0)	St. 9 (3.0)	St.10 (6.0)	St.11 (8.0)	St.13 (15)
		Counts per minute (cpm) of 1 μg of total RNA					
Ex#1	Control	0	0.26	12.6	55.3	67.4	--
	Xrel3	0	0	3.6	52.0	30.9	--
Ex#2	Control	2.29	5.55	--	115.9	133.0	97.3
	Xrel3	0.83	4.94	--	56.1	46.0	42.9
Ex#3	Control	2.59	0.41	47.7	74.4	111.9	91.7
	Xrel3	1.12	4.51	3.07	49.6	47.3	77.5
Ave	Control	1.62	2.07	30.2	81.8	104.1	94.5
	Xrel3	0.65	3.15	3.33	52.5	41.4	60.2
Stdev	Control	1.41	3.01	24.8	30.9	33.4	3.91
	Xrel3	0.58	2.73	0.37	3.29	9.14	24.4

TABLE 5. **Levels of *ODC* marker on the gel assessed by Spot Densitometry Analysis.**

Sample		Stages (hours after stage 7)									
		St.7 (0)	St.7.5 (0.5)	St.8 (1.0)	St.8.2 (1.5)	St.8.5 (2.0)	St.8.7 (2.5)	St.9 (3.0)	9.2 (3.5)	10 (6)	11 (8)
		Integrated Density Values for *ODC*									
Ex#1	Control	1368	7524	--	12996	20520	17784	684	684	--	--
	Xrel3	4218	9842	--	19684	21793	21090	14763	12654	--	--
Ex#2	Control	26714	18981	28823	54131	33041	59052	52022	48507	45695	--
	Xrel3	5600	32900	37800	31500	53200	56700	23100	7700	11200	--
Ex#3	Control	42180	46398	48507	67488	39368	61161	44992	--	35150	67488
	Xrel3	42180	62567	69597	72409	64676	63270	49210	--	58349	60458
Ex#4	Control	--	--	79040	31008	38912	37088	27360	68704	--	80256
	Xrel3	--	--	32224	27968	31616	10336	22496	45600	--	71744
Ave	Control	**23420**	**24301**	**52123**	**41405**	**32960**	**43771**	**31264**	**39298**	**40422**	**73872**
	Xrel3	**17332**	**35103**	**46540**	**37890**	**42821**	**37849**	**27392**	**21986**	**34774**	**66101**
Stdev	Control	20604	19975	25303	24203	8779	20460	22874	34932	7456	9028
	Xrel3	21529	26431	20161	19605	26073	15032	15032	20600	33339	7980

TABLE 6. **Levels of *EF-1α* marker on the gel assessed by Spot Densitometry Analysis.**

Sample		Stages (hours after stage 7)									
		St.7 (0)	St.7.5 (0.5)	St.8 (1.0)	St.8.2 (1.5)	St.8.5 (2.0)	St.8.7 (2.5)	St.9 (3.0)	9.2 (3.5)	10 (6)	11 (8)
		Integrated Density Values for *EF-1α*									
Ex#1	Control	0	684	--	2052	6156	17100	2052	4788	--	--
	Xrel3	0	703	--	3515	9139	10545	47158	7106	--	--
Ex#2	Control	12876	19684	27417	26011	21793	74618	59052	70300	104044	--
	Xrel3	11900	43400	23100	26600	55300	36400	23800	21700	85400	--
Ex#3	Control	14763	23199	29526	33744	30932	38665	40071	--	71003	85766
	Xrel3	26011	43586	40071	43586	43586	45695	45695	--	78736	73815
Ex#4	Control	--	--	5472	7296	15200	23712	26144	29184	--	72352
	Xrel3	--	--	14596	17632	5472	5472	17024	7904	--	63232
Ave	Control	**9213**	**14522**	**20805**	**17275**	**18520**	**38523**	**31829**	**34757**	**87523**	**79059**
	Xrel3	**12637**	**29229**	**25922**	**22833**	**28374**	**24528**	**33419**	**12236**	**82068**	**68523**
Stdev	Control	8034	12112	13320	15042	25698	24000	24000	29073	23363	9485
	Xrel3	13021	24704	12969	16784	24838	19558	15283	8205	4712	7483

TABLE 7. **Levels of *Histone* marker on the gel assessed by Spot Densitometry Analysis.**

Sample		Stages (hours after stage 7)									
		St. 7 (0)	St.7.5 (0.5)	St. 8 (1.0)	St.8.2 (1.5)	St.8.5 (2.0)	St.8.7 (2.5)	St. 9 (3.0)	St.9.2 (3.5)	St.10 (6)	St.11 (8)
		Integrated Density Values for *Histone*									
Ex#1	Control	6840	7524	--	11628	29412	41724	2052	2052	--	--
	Xrel3	1292	5168	--	9690	16796	13566	10982	12274	--	--
Ex#2	Control	6327	14060	28860	33041	30932	64676	27417	37962	9139	--
	Xrel3	26600	44800	41300	32900	33600	37800	32200	17500	12600	--
Ex#3	Control	17575	26714	32338	35150	34447	38665	36556	--	27417	17575
	Xrel3	30229	38665	39368	45695	41477	48507	40774	--	47101	25308
Ex#4	Control	--	--	34048	27360	60192	56544	64448	45600	--	33440
	Xrel3	--	--	35264	29184	20064	16416	30400	29184	--	32832
Ave	Control	**10247**	**16099**	**31748**	**26794**	**38745**	**50402**	**32618**	**28538**	**18278**	**25507**
	Xrel3	**19373**	**29544**	**38644**	**29367**	**27984**	**29072**	**28589**	**19652**	**29850**	**29070**
Stdev	Control	6351	9756	2643	10632	14452	12309	25755	23253	12924	12924
	Xrel3	15764	21332	3082	14903	11569	16877	12580	8658	24396	5320

TABLE 8. **Numbers of *FGF*-induced animal caps from embryos injected with 0.5 ng *Xrel3* mRNA or control (a total of three separate experiments).**

Sample		Concentrations *FGF* (ng)				# embryos that formed tumours out of remaining embryos (stage 25)
		0 ng	50 ng	100 ng	125 ng	
		Number of elongated animal caps out of the number treated with *bFGF*				
Exp. #1	Control	0/10	10/10	8/9	9/9	0/20
	Xrel3	0/10	8/10	5/10	7/9	13/21
Exp. #2	Control	0/10	8/10	10/10	10/10	0/18
	Xrel3	0/10	9/10	9/10	10/10	12/15
Exp. #3	Control	0/10	8/10	10/10	10/10	0/20
	Xrel3	0/10	7/10	9/9	10/10	21/31
Total #	Control	0/30	26/30	28/10	29/30	0/58
	Xrel3	0/30	24/30	23/30	27/30	46/67
% of elongated explants	Control	**0**	**86.6%**	**93.3%**	**96.6%**	**0**
	Xrel3	**0**	**80.0%**	**76.6%**	**90.0%**	**68.7%**

REFERENCES.

Acampora, D., Postiglione, M.P., Avantaggiato, V., Di Bonito, M., and Simeone, A. (2000). The role of *Otx* and *Otp* genes in brain development. *Int. J. Dev. Biol.* **44**:669-77.

Agius, E., Oelgeschlager, M., Wessely, O., Kemp, C., and De Robertis, E.M. (2000). Endodermal *nodal*-related signals and mesoderm induction in *Xenopus*. *Development.* **127**:1173-83.

Agius, P.E., Piccolo, S., and De Robertis, E.M. (1999). The head inducer *cerberus* in a multivalent extracellular inhibitor. *J. Soc. Biol.* **193**:347-54.

Alberts, B., Bray, D., Lewis, J., Raff, M., Roberts, K., and Watson, J.D. (1989). Molecular biology of the cell. 2nd ed., Garland Publishing, New York, pp. 880-89.

Amaldi, F., Loreni, F., and Francesconi, A. (1993). Coordinate translational regulation in the syntheses of elongation factor 1-alpha and ribosomal proteins in *Xenopus laevis*. *Nucleic Acids Res.* **21**:4721-5.

Anderson, J.A. , Lewellyn, A.L., and Maller, J.L. (1997). Ionizing radiation induces apoptosis and elevates cyclin A1-Cdk2 activity before but not after the midblastula transition in *Xenopus*. *Mol. Biol. Cell.* **8**:1195-1206.

Arendt, D., and Nubler-Jung, K. (1999). Rearranging gastrulation in the name of yolk: evolution of gastrulation in yolk-rich amniote eggs. *Mech. Dev.* **81**:3-22.

Armstrong, N.J., Steinbeisser, H., Prothmann, C., DeLotto, R., and Rupp, R.A. (1998). Conserved Spatzle/Toll signaling in dorsoventral patterning of *Xenopus* embryos. *Mech. Dev.* **71**:99-105.

Asashima, M., Nakano,H., Shimada, K., Konoshita, K., Ishii, K., and Shibai H. (1990). Mesodermal induction in early amphibian embryos by activin A (erythroid differentiation factor). *Roux's Arch. Dev. Biol.* **198**:330–335.

Baeuerle, P.A, and Henkel, T. (1994). Function and activation of NF-κB in the immune system. *Ann. Rev. Immunol.* **12**:141-79.

Baichwal, V.R., and Baeuerle, P.A. (1997). Activate NF-κB or die? *Curr. Biol.***7**: R94–6.

Baldwin, A.S. Jr. (1996). The NF-κB and IκB proteins: new discoveries and insights. *Ann. Rev. Immunol.* **14**:649–683.

Bargou, R.C., Leng, C., Krappmann, D., Emmerich, F., Mapara, M.Y., and Bommert, K. (1996). High-level nuclear NF-κB and oct-2 is a common feature of cultured Hodgkin/Reed-Sternberg cells. *Blood.* **87**:4340–7.

Bargou, R.C., Emmerich, F., Krappmann, D., Bommert, K., Mapara, M.Y., Arnold, W., Royer, H.D., Grinstein, E., Greiner, A., Scheidereit, C., and Dorken, B. (1997). Constitutive nuclear factor-kappaB-RelA activation is required for proliferation and survival of Hodgkin's disease tumour cells. *J. Clin. Invest.* **100**:2961-9.

Bearer, E.L. (1994). Distribution of *Xrel* in the early *Xenopus* embryo: a cytoplasmic and nuclear gradient. *Eur. J. Cell Biol.* **63**:255-68.

Beck, C.W., Sutherland, D.J., and Woodland, H.R. (1998). Involvement of NF-kappaB associated proteins in FGF-mediated mesoderm induction. *Int. J. Dev. Biol.* **42**:67-77.

Beg, A.A., Sha, W.C., Bronson, R.T., Ghosh, S., and Baltimore, D. (1995). Embryonic lethality and liver degeneration in mice lacking the RelA component of NF-kappa B. *Nature.* **376**:167-70.

Berger, C., Brousset, P., McQuain, C., and Knecht, H. (1997). Deletion variants within the NF-κB activation domain of the LMP1 oncogene in acquired immunodeficiency syndrome-related large cell lympho-mas, in prelymphomas and atypical lymphoproliferations. *Leuk. Lymphoma.* **26**:239–50.

Bessho, R., Matsubara, K., Kubota, M., Kuwakado, K., Hirota, H., and Wakazono, Y. (1994). Pyrrolidine dithiocarbamate, a potent inhibitor of nuclear factor kappa B (NF-κB) activation, prevents apoptosis in human promyelocytic leukemia HL-60 cells and thymocytes. *Biochem. Pharmacol.* **48**:1883–9.

Bitzer, M., von Gersdorff, G., Liang, D., Dominguez-Rosales, A., Beg, A.A., Rojkind, M., and Bottinger, E.P. (2000). A mechanism of suppression of TGF-beta/SMAD signaling by NF-kappa B/RelA. *Genes Dev.* **14**:187-97.

Boterenbrood, E.C., and Nieuwkoop, P. D. (1973). The formation of the mesoderm in the Urodelian amphibians: V. Its regional induction by the endoderm. *Whilhelm Roux's Arch.* **173**: 319-32.

Bouwmeester, T., Kim, S., Sasai, Y., Lu, B., and De Robertis, E.M. (1996). Cerberus is a head-inducing secreted factor expressed in the anterior endoderm of Spemann's organizer. *Nature.* **382**:595-601.

Brieher, W.M., and Gumbiner, B.M. (1994). Regulation of c-cadherin function during activin induced morphogenesis of *Xenopus* animal caps. *J. Cell. Biol.* **126**:519-527

Britto, J.M., Tannahill, D., and Keynes, R.J. (2000). Life, death and Sonic hedgehog. *Bioessays.* **22**:499-502.

Bushdid, P.B., Brantley, D.M., Yull, F.E., Blaeuer, G.L., Hoffman, L.H., Niswander, L., and Kerr, L.D. (1998). Inhibition of NF-kappaB activity results in disruption of the apical ectodermal ridge and aberrant limb morphogenesis. *Nature.* **392**:615-8.

Carrasco, D., Rizzo, C.A., Derfman, K., and Bravo, R. (1996). The *v- rel* oncogene promotes malignant T-cell leukemia/lymphoma in transgenic mice. *EMBO J.* **15**:3640–50.

Chalmers, A.D., and Slack, J.M. (1998). Development of the gut in *Xenopus laevis*. *Dev. Dyn.* **212**:509-21.

Chen, S., Guttridge, D.C., Tang, E., Shi, S., Guan, K., and Wang, C.Y. (2001). Suppression of tumour necrosis factor-mediated apoptosis by nuclear factor kappaB-independent bone morphogenetic protein/Smad signaling. *J. Biol. Chem.* **276**:39259-63.

Chen, F., Castranova, V., Shi, X., and Demers, L.M. (1999). New insights into the role of Nuclear Factor-kappa B, a ubiquitous transcription factor in the initiation of diseases *Clin. Chem.* **45**:7-17.

Chen, Y., Lebrun, J.J., and Vale, W. (1996). Regulation of transforming growth factor beta- and activin-induced transcription by mammalian Mad proteins. *Proc. Natl. Acad. Sci. USA.* **93**:12992-7.

Chen, X., Weisberg, E., Fridmacher, V., Watanabe, M., Naco, G., and Whitman, M. (1997). Smad4 and FAST-1 in the assembly of activin-responsive factor. *Nature*. **389**:85-9.

Cho, K.W.Y., Blumberg, B., Steinbeisser, H., and De Robertis, E. M. (1991). Molecular nature of Spemann's organizer: the role of the *Xenopus* homeobox gene *goosecoid. Cell.* **67**: 1111–1120.

Christian, J.L., Olson, D. J. and Moon, R. T. (1992). Xwnt8 modifies the character of mesoderm induced by bFGF in isolated *Xenopus* ectoderm. *EMBO J.* **11**: 33–41.

Christian, J.L., and Moon, R.T. (1993). Interactions between Xwnt–8 and Spemann Organizer signaling pathways generate dorsoventral pattern in the embryonic mesoderm of *Xenopus. Genes. Dev.* **7**: 13–28.

Ciau-Uitz, A., Walmsley, M., and Patient, R. (2000). Distinct origins of adult and embryonic blood in *Xenopus. Cell.* **102**:787-796.

Cornell, R.A., and Kimelman, D. (1994). Activin-mediated mesoderm induction requires FGF. *Development.* **120**:453-62.

Cunliffe, V., and Smith, J.C. (1994). Specification of mesodermal pattern in *Xenopus laevis* by interactions between Brachyury, noggin and Xwnt-8. *EMBO J.* **13**:349-59.

Dahmane, N., and Ruiz-i-Altaba, A. (1999). Sonic hedgehog regulates the growth and patterning of the cerebellum. *Development.* **126**:3089-3100.

Dahmane, N., Lee, J., Robins, P., Heller, P., and Ruiz i Altaba, A. (1997). Activation of the transcription factor Gli1 and the Sonic hedgehog signalling pathway in skin tumours. *Nature.* **389**:876-81.

Dale, L., and Jones, C. M. (1999). BMP signaling in early *Xenopus* development. *BioEssays.* **21**:751–760.

Dale, L., and Slack, J. M.W. (1987a). Fate map for the 32-cell stage of *Xenopus laevis. Development.* **99**:527–551.

Dale, L., and Slack, J.M.W. (1987b). Regional specification within the mesoderm of early embryos of *Xenopus laevis. Development.* **100**:279-95.

Dale, L., Smith, J.C., and Slack, J.M. (1985). Mesoderm induction in *Xenopus laevis*: a quantitative study using a cell lineage label and tissue-specific antibodies. *J. Embryol. Exp. Morphol.* **89**:289-312.

Dale, L., Howes, G., Price, B.M.J., and Smith, J.C. (1992). Bone morphogenetic protein- 4: a ventralizing factor in early *Xenopus* development. *Development.* **115**: 573–585.

Danilchik, M.V., and Kao K.R. (1991). Generation of body plan phenotypes in early embryogenesis. *Methods Cell Biol.* **36**:271-84.

David, I.B., and Sargent, T.D. (1988). *Xenopus laevis* in developmental and molecular biology. *Science.* **24**:1443-1447.

De Robertis, E.M., Larrain, J., Oelgeschlager, M., and Wessely, O. (2000). The establishment of Spemann's organizer and patterning of the vertebrate embryo. *Nat. Rev. Genet.* **1**:171-81.

Derynck, R. (1998). SMAD proteins and mammalian anatomy. *Nature*. **393**:737-9.

Derynck, R., and Feng, X.H. (1997). TGF-beta receptor signaling. *Biochim. Biophys. Acta.* **1333**:F105-50.

Derynck, R., Zhang, Y., and Feng, X.H. (1998). Smads: transcriptional activators of TGF-beta responses. *Cell.* **95**:737-40.

Deuchar, E.M. (1975). *Xenopus*: The South African Clawed Frog. Great Britain, John Wiley and Sons, Ltd., London.

Ding, X., Hausen, P., and Steinbeisser, H. (1998). Pre-MBT patterning of early gene regulation in *Xenopus*: the role of the cortical rotation and mesoderm induction. *Mech. Dev.* **70**:15-24.

Domingo, C., and Keller, R. (2000). Cells remain competent to respond to mesoderm-inducing signals present during gastrulation in *Xenopus laevis*. *Dev. Biol.* **225**:226-40.

Drier, E.A., and Steward, R. (1997). The dorsoventral signal transduction pathway and the Rel-like transcription factors in *Drosophila*. *Semin. Cancer Biol.* **8**:83-92.

Drier, E.A., Govind, S., and Steward, R. (2000). Cactus-independent regulation of Dorsal nuclear import by the ventral signal. *Curr. Biol.* **10**:23-6.

Ecochard, V., Cayrol, C., Rey, S., Foulquier, F., Caillol, D., Lemaire, P., and Duprat, A.M. (1998). A novel *Xenopus* Mix-like gene Milk involved in the control of the endo-mesodermal fates. *Development*. **125**:2577-2585.

Fernig, D.G., and Gallagher, J.T. (1994). Fibroblast growth factors and their receptors: an information network controlling tissue growth, morphogenesis and repair. *Prog.Growth Factor Res.* **5**:353-377.

Finco, T.S., Westwick, J.K., Norris, J.L., Beg, A.A., Der, C.J., and Baldwin, A.S. Jr. (1997). Oncogenic Ha-Ras-induced signaling activates NF-kappaB transcriptional activity, which is required for cellular transformation. *J. Biol. Chem.* **272**:24113-6.

Finkielstein, C.V., Lewellyn, A.L., and Maller, J.L. (2001). The midblastula transition in *Xenopus* embryos activates multiple pathways to prevent apoptosis in response to DNA damage. *Proc. Natl. Acad. Sci. USA*. **98**:1006-11.

Furthauer, M., Thisse, C., and Thisse, B. (1997). A role for FGF-8 in the dorsoventral patterning of the zebrafish gastrula. *Development.* **124**:4253-64.

Fukui, A., Nakamura, T., Uchiyama, H., Sugino, K., Sugino, H., and Asashima, M. (1994). Identification of activins A, AB, and B and follistatin proteins in *Xenopus* embryos. *Dev. Biol*. **163**:279-81.

Galsie, Z., Kinsella, A.R., and Smith, J.A. (1997). Fibroblast growth factors and their receptors. *Biochem. Cell Biol*. **75**: 669-685.

Geiser, A.G., Letterio, J.J., Kulkarni,A.B., Karlsson, S., Roberts, A.B., and Sporn, M.B. (1993). Transforming growth factor beta 1 (TGF-beta 1) controls expression of major histocompatibility genes in the postnatal mouse: aberrant histocompatibility antigen expression in the pathogenesis of the TGF-beta 1 null mouse phenotype. *Proc. Natl. Acad. Sci. USA*. **90**:9944-8.

Gerhart J., and Keller, R. (1986). Region-specific cell activities in amphibian gastrulation. *Annu. Rev. Cell Biol*. **2**:201-29.

Gerhart, J., Danilchik, M., Doniach, T., Roberts, S., Rowning, B., and Stewart, R. (1989). Cortical rotation of the *Xenopus* egg: consequences for the anteroposterior pattern of embryonic dorsal development. *Dev. Suppl*. **107**:37-51.

Ghosh, G., and Chen, F.E. (1999). Regulation of DNA binding by Rel/ NF-κB transcription factors: structural views. *Oncogene*. **18**:6928-6932.

Gilmore, T.D. (1999). The Rel/ NF-κB signal transduction pathway: introduction. *Oncogene*. **18**:6925-6927.

Gilmore, T.D., Koedood, M., Piffat, K.A., and White, D.W. (1996). Rel/ NF-κB /IκB proteins and cancer. *Oncogene.* **13**:1367–78.

Gimlich, R.L. (1986). Acquisition of developmental autonomy in the equatorial region of the *Xenopus* embryo. *Dev. Biol*. **115**:340-52.

Godsave, S.F., Isaacs, H.V., and Slack, J.M.W. (1988). Mesoderm inducing factors: a small class of molecules. *Development*. **102**:555–566.

Goodrich, L.V., and Scott, M. P. (1998). Hedgehog and patched in neural development and disease. *Neuron.* **21**:1243-1257.

Goodrich, L.V., Milenkovic, L., Higgins, K.M., and Scott. M. P. (1997). Altered neural cell fates and medulloblastoma in mouse patched mutants. *Science.* **277**:1109-1113.

Govind, S. (1999). Control of development and immunity by rel transcription factors in *Drosophila. Oncogene.* **18**:6875-87.

Green, D., and Reed, J. (1998). Mitochondria and apoptosis. *Science.* **281**:1309-1312.

Green. J.B., and Smith, J.C. (1991). Growth factors as morphogens: do gradients and thresholds establish body plan? *Trends Genet.* **7**:245-50.

Grunz, H. (1983). Change in the differentiation pattern of *Xenopus laevis* ectoderm by variation of the incubation time and concentration of the vegetalizing factor. *Roux's Arch. Dev. Biol.* **192**:130–137.

Hahn, H., Wojnowski, L., Miller, G., and Zimmer, A. (1999). The patched signaling pathway in tumourigenesis and development: lessons from animal models. *J Mol Med.* **77**:459-68.

Harland, R., and Gerhart, J. (1997). Formation and function of Spemann's organizer. *Annu. Rev. Cel.l Dev. Biol.* **13**:611-67.

Hausen, P., and Riebesell, M. (1991). The early development of *Xenopus laevis*: An atlas of the histology. Springer-Verlag, Berlin, Germany.

Heasman, J. (1997). Patterning the *Xenopus* blastula. *Development.* **124**:4179-91.

Heldin, C.H., Miyazono, K., and ten Dijke, P. (1997). TGF-beta signalling from cell membrane to nucleus through SMAD proteins. *Nature.* **390**:465-71.

Hemmati-Brivanlou, A., and Melton, D.A. (1992). A truncated activin receptor inhibits mesoderm induction and formation of axial structures in *Xenopus* embryos. *Nature.* **359**:609-14.

Hemmati-Brivanlou, A., Kelly, O.G., and Melton, D.A. (1994). Follistatin, an antagonist of activin, is expressed in the Spemann organizer and displays direct neuralizing activity. *Cell.* **77**:283-95.

Hemmati-Brivanlou, A., and Melton, D.A. (1994). Inhibition of activin receptor signalling promotes neuralization in *Xenopus*. *Cell.* **77**:273-281.

Hensey, C., and Gautier, J.A. (1997). A developmental timer that regulates apoptosis at the onset of gastrulation. *Mech. Dev.* **69**:183-95.

Hensey, C., and Gautier, J.A. (1998). Programmed cell death during *Xenopus* development: a spatio-temporal analysis. *Dev. Biol.* **203**:36-48.

Herrmann, B.G., and Kispert, A. (1994). The T genes in embryogenesis. *Trends Genet.* **10**:280-6.

Hogan, B.L. (1999). Morphogenesis. *Cell.* **96**:225-33.

Hopwood, N.D., Pluck, A., and Gurdon, J.B. (1989). A *Xenopus* mRNA related to *Drosophila* twist is expressed in response to induction in the mesoderm and the neural crest. *Cell.* **59**:893-903.

Huang, H.C., Murtaugh, L.C., Vize, P.D., and Whitman, M. (1995). Identification of a potential regulator of early transcriptional responses to mesoderm inducers in the frog embryo. *EMBO J.* **14**:5965-73.

Huber, O., Bierkamp, C., and Kemler, R. (1996). Cadherins and catenins in development. *Curr. Opin. Cell Biol.* **8**:685-691.

Huttenlocher, A., Sandborg, R.R., and Horwitz, A.F. (1995). Adhesion in cell migration. *Curr. Opin .Cell .Biol.* **7**:697-706.

Hynes, R.O. (1992). Specificity of cell adhesion in development: the cadherin superfamily. *Curr. Opin. Genet. Dev.* **2**:621-4.

Hynes, M., Stone ,D.M., Dowd, M., Pitts-Meek, S., Goddard, A., Gurney, A., and Rosenthal, A. (1997). Control of cell pattern in the neural tube by the zinc finger transcription factor and oncogene Gli-1. *Neuron.* **19**:15-26.

Iotsova, V., Caamano, J., Loy, J., Yang, Y., Lewin, A., and Bravo, R. (1997). Osteopetrosis in mice lacking NF-kappaB1 and NF-kappaB2. *Nat. Med.* **3**:1285-9.

Isaacs, H.V., Pownall, M.E., and Slack, J. M. W. (1994). eFGF regulates *Xbra* expression during *Xenopus* gastrulation. *EMBO J.* **19**:4469–4481.

Jackson, A., Freidman, S. Zhan, X., Engleka, K. A., Forough, R., and Maciag T. (1992). Heat shock induces the release of fibroblast growth factor-1 from NIH-3T3 cells. *Proc. Natl. Acad. Sci. USA.* **89:**10691–10695.

Jacobson, M.D., Weil, M., and Raff, M.C. (1997). Programmed cell death in animal development. *Cell.* **88**:347-54.

Jensen, A. M., and Wallace. V. A. (1997). Expression of Sonic hedgehog and its putative role as a precursor cell mitogen in the developing mouse retina. *Development.* **124**:363-371.

Jones, C.M., Lyons, K.M., Lapan, P.M., Wright, C.V.E., and Hogan, B.L.M. (1992). DVR-4 (Bone Morphogenetic Protein-4) as a posterior-ventralizing factor in *Xenopus* mesoderm induction. *Development.* **115:** 639–647.

Jones, M.C., and Smith, J. C. (1999a). An overview of *Xenopus* development. *Methods Mol. Biol.* **97**:331-340.

Jones, M.C., and Smith, J.C. (1999b) Mesoderm induction assays. *Methods Mol. Biol.* **97**:341-349.

Kalyani, A. J., and Rao, M. S. (1998). Cell lineage in the developing neural tube. *Biochem. Cell. Biol.* **76**:1051-1068.

Kanamaru, C., Yasuda, H., Takeda, M., Ueda, N., Suzuki, J., Tsuchida, T., Mashima, H., Ohnishi, H., and Fujita, T. (2001). Smad7 is induced by norepinephrine and protects rat hepatocytes from activin A-induced growth inhibition. *J. Biol. Chem.* **276**:45636-41.

Kanegae, Y., Tavares, A.T., Izpisua Belmonte, J.C., and Verma, I.M. (1998). Role of Rel/NF-kappaB transcription factors during the outgrowth of the vertebrate limb. *Nature.* **392**:611-4.

Kao, K.R., and Elinson, R.P. (1988). The entire mesodermal mantle behaves as Spemann's organizer in dorsoanterior enhanced *Xenopus laevis* embryos. *Dev. Biol.* **127**: 64-77.

Kao, K.R., and Hopwood, N.D. (1991). Expression of a mRNA related to c-rel and dorsal in early *Xenopus laevis* embryos. *Proc. Natl. Acad. Sci. USA.* **88**:2697-7201.

Kao, K, and Danilchik, M. (1991). Generation of body plan phenotypes in early embryogenesis. *Methods Cell Biol.* **36**:271-84.

Kao, K.R., and Lockwood, A. (1996). Negative regulation of dorsal patterning in early embryos by overexpression of *XrelA*, a *Xenopus* homologue of NF-kappa B. *Mech. Dev.* **58**:129-139.

Kaufmann, E., Paul, H., Friedle, H,, Metz, A., Scheucher, M., Clement, J.H., and Knochel, W. (1996). Antagonistic actions of activin A and BMP-2/4 control dorsal lip-specific activation of the early response gene XFD-1' in *Xenopus laevis* embryos. *EMBO J.* **15**:6739-49.

Keller, R.E. (1980). The cellular basis of epiboly: an SEM study of deep-cell rearrangement during gastrulation in *Xenopus laevis*. *J. Embryol. Exp. Morphol.* **60**:201-34.

Keller, R.E. (1986). The cellular basis of amphibian gastrulation. *Dev. Biol.* **2**:241-327.

Keller, R.E. (1991). Early embryonic development of *Xenopus laevis*. *Methods Cell Biology.* **36:**62-109, Academic Press, San Diego.

Keller, R.E., and Danilchik, M. (1988). Regional expression, pattern and timing of convergence and extension during gastrulation of *Xenopus laevis*. *Development.* **103**:193-209.

Kessler, D.S., and Melton, D.A. (1994). Vertebrate embryonic induction: mesodermal and neural patterning. *Science*. **266**:596-604.

Kimelman, D., and Maas, A. (1992), Induction of dorsal and ventral mesoderm by ectopically expressed *Xenopus* basic fibroblast growth factor. *Development*. **114**: 261–269.

Kinzler, K.W., Bigner, S.H., Bigner, D.D., Trent, J.M., Law, M.L., O'Brien, S.J., Wong, A.J., and Vogelstein, B. (1987). Identification of an amplified, highly expressed gene in a human glioma. *Science*. **236**:70-3.

Kispert, A., and Herrmann, B.G. (1993). The Brachyury gene encodes a novel DNA binding protein. *EMBO J.* **12**:3211-20.

Kitajima, I., Nakajima, T., Imamura, T., Takasaki, I., Kawahara, K., Okano, T., Tokioka, T., Soejma, Y., Abeyama, K., and Maruyama, I. (1996). Induction of apoptosis in murine clonal osteoblasts expressed by human T-cell leukemia virus type I tax by NF-κB and TNF- α. *J. Bone Miner. Res*. **11**:200–10.

Klint, P., and Claesson-Welsh, L. (1999). Signal transduction by fibroblast growth factor receptors. *Front. Biosc.* **4**:165-177.

Kouhara, H., Hadari, Y.R., Spivak-Kroizman, T., Schilling, J., Bar-Sagi, D., Lax, I., and Schlessinger, J. (1997). A lipid-anchored Grb2-binding protein that links FGF-receptor activation to the Ras/MAPK signaling pathway. *Cell*. **89**:693-702.

Krieg, P.A., and Melton, D.A. (1987). An enhancer responsible for activating transcription at the midblastula transition in *Xenopus* development. *Proc. Natl. Acad. Sci. USA.* **84**:2331-5.

Krieg, P.A., Varnum, S.M., Wormington, W.M., and Melton, D.A. (1989). The mRNA encoding elongation factor 1-alpha (EF-1 alpha) is a major transcript at the midblastula transition in *Xenopus*. *Dev. Biol.* **133**:93-100.

Ku, M., and Melton, D.A. (1993). *Xwnt-11*, a maternally expressed *Xenopus Wnt* gene. *Development*. **119**:1161–1173.

Kuhl, M., Geis, K., Sheldahl, L.C., Pukrop, T., Moon, R.T., and Wedlich, D. (2001). Antagonistic regulation of convergent extension movements in *Xenopus* by Wnt/beta-catenin and Wnt/Ca^{2+} signaling. *Mech. Dev.* **106**:61-76.

LaBonne, C., and Whitman, M. (1994). Mesoderm induction by activin requires FGF-mediated intracellular signals. *Development.* **120**:463-72.

Lake, B.B., Ford, R., and Kao, K.R. (2001). Xrel3 is required for head formation of *Xenopus laevis*. *Development*. **128**:263-273.

Lamb, T.M., and Harland, R.M. (1995). Fibroblast growth factor is a direct neural inducer, which combined with noggin generates anterior-posterior neural pattern. *Development.* **121**:3627-36.

Lane, M.C., and Smith,W.C. (1999). The origins of primitive blood in *Xenopus*: Implications for axial patterning. *Development.* **126**:423-434.

Latinkic, B.V., Umbhauer, M., Neal, K.A., Lerchner, W., Smith, J.C., and Cunliffe, V. (1997). The *Xenopus* Brachyury promoter is activated by FGF and low concentrations of activin and suppressed by high concentrations of activin and by paired-type homeodomain proteins. *Genes Dev*. **11**:3265-76.

Lemaire, P., and Kodjabachian, L. (1996). The vertebrate organizer: structure and molecules. *Trends Genet*. **12**:525-31.

Lemaire, P., Garrett, N., and Gurdon, J.B. (1995). Expression cloning of Siamois, a *Xenopus* homeobox gene expressed in dorsal-vegetal cells of blastulae and able to induce a complete secondary axis. *Cell.* **81**:85-94.

Leptin, M. (1995). *Drosophila* gastrulation: from pattern formation to morphogenesis. *Annu. Rev. Cell Dev. Biol*. **11**:189-212.

Levine, E. M., Roelink, H., Turner, J., and Reh. T. A. (1997). Sonic hedgehog promotes rod photoreceptor differentiation in mammalian retinal cells *in vitro*. *J. Neurosci.* **17**:6277-6288.

Li, X., and Stark, G.R. (2002). NFkappaB-dependent signaling pathways. *Exp. Hematol.* **30**:285-96.

Lowenstein, E.J., Daly, R.J., Batzer, A.G., Li, W., Margolis, B., Lammers, R., Ullrich, A., Skolnik, E.Y., Bar-Sagi, D., and Schlessinger, J. (1992). The SH2 and SH3 domain-containing protein GRB2 links receptor tyrosine kinases to ras signaling. *Cell.* **70**:431-42.

Luo, X., Budihardjo, I., Zou, H., Slaughter, C., and Wang, X. (1998). Bid, a Bcl2 interacting protein, mediates cytochrome c release from mitochondria in response to activation of cell surface death receptors. *Cell.* **94**:481-490.

Lupo, G., Andreazzoli, M., Gestri, G., Liu, Y., He, R.Q., and Barsacchi ,G. (2000). Homeobox genes in the genetic control of eye development. *Int. J. Dev. Biol.* **44**:627-36.

Maller, J.L., Gross, S.D., Schwab, M.S., Finkielstein, C.V., Taieb, F.E., and Qian, Y.W. (2001). Cell cycle transitions in early *Xenopus* development. *Novartis. Found. Symp.* **237**:58-73.

Marianneau, P., Cardona, A., Edelman, L., Deubel, V., and Despres, P. (1997). Dengue virus replication in human hepatoma cells activates NF-κB which in turn induces apoptotic cell death. *J. Virol.* **71**:3244–9.

Masui, Y., and Wang, P. (1998). Cell cycle transition in early embryonic development of *Xenopus laevis. Biol. Cell.* **90**:537-48.

Matise, M.P., and Joyner, A.L. (1999). *Gli* genes in development and cancer. *Oncogene.* **18**:7852-9.

Mayo, M.W., Wang, C.Y., Cogswell, P.C., Rogers-Graham, K.S., Lowe, S.W., Der, C.J., and Baldwin, A.S. Jr. (1997). Requirement of NF-kappa B activation to suppress p53-independent apoptosis induced by oncogenic Ras. *Science.* **278**:1812-5.

McDowell, N., and Gurdon, J.B. (1999). Activin as a morphogen in *Xenopus* mesoderm induction. *Semin. Cell Dev. Biol.* **10**:311-7.

Mignatti, P., Morimoto, T., and Rifkin, D. B. (1992). Basic fibroblast growth factor, a protein devoid of secretory signal sequence, is released by cells via a pathway independent of the endoplasmic reticulum-Golgi complex. *J. Cell. Physiol.* **151**: 81–93.

Mills, K.R., Kruep,D., and Saha, M.S. (1999). Elucidating the origins of the vascular system: A fate map of the vascular endothelial and red blood cell lineage in *Xenopus laevis*. *Dev. Biol.* **209**:352-368.

Miwa, M., Kushida, S., Maeda, N., Fang, J., Kawamura, T., Kameyama, T., and Uchida, K. (1997). Pathogenesis and prevention of HTLV-1-associated diseases. *Leukemia*. **11**:65–6.

Miyake, A., Konishi, M., Martin, F.H., Hernday, N.A., Ozaki, K., Yamamoto, S., Mikami, T., Arakawa, T., and Ito, N. (1998). Structure and expression of a novel member, FGF-16, on the fibroblast growth factor family. *Biochem. Biophys. Res. Commun.* **243**:148-152.

Mukhopadhyay, T., Roth, J.A., and Maxwell, S.A. (1995). Altered expression of the p50 subunit of the NF-kappa B transcription factor complex in non-small cell lung carcinoma. *Oncogene*. **11**:999-1003.

Muraoka, R.S., Bushdid, P.B., Brantley, D.M., Yull, F.E., and Kerr, L.D. (2000). Mesenchymal expression of nuclear factor-kappa B inhibits epithelial growth and branching in the embryonic chick lung. *Dev. Biol.* **225**:322-38.

Nagarajan, R.P., Chen, F., Li, W., Vig, E., Harrington, M.A., Nakshatri, H., and Chen, Y. (2000). Repression of transforming-growth-factor-beta-mediated transcription by nuclear factor kappa B. *Biochem. J.* **348**:591-6.

Nakao, A., Afrakhte, M., Moren, A., Nakayama, T., Christian, J.L., Heuchel, R., Itoh, S., Kawabata, M., Heldin, N.E., Heldin, C.H., and ten Dijke, P. (1997a). Identification of Smad7, a TGFbeta-inducible antagonist of TGF-beta signalling. *Nature.* **389**:631-5.

Nakao, A., Roijer, E., Imamura, T., Souchelnytskyi, S., Stenman, G., Heldin, C.H., and ten Dijke. P. (1997b). Identification of Smad2, a human Mad-related protein in the transforming growth factor beta-signaling pathway. *J. Biol. Chem.* **272**:2896-900.

Neiman, P.E., Thomas, S.J., and Loring, G. (1991). Induction of apoptosis during normal and neoplastic B-cell development in the bursa of Fabricius. *Proc. Natl. Acad. Sci. USA.* **88**:5857-61.

Newport, J.W., and Kirschner, M.W. (1982a). A major developmental transition in early *Xenopus* embryos: I. Characterization and timing of cellular changes at the midblastula stage. *Cell.* **30**:675–686.

Newport, J.W., and Kirschner, M.W. (1982b). A major developmental transition in early *Xenopus* embryos: II. Control of the onset of transcription. *Cell.* **30**:687–696.

Newport, J.W., and Kirschner, M.W. (1984). Regulation of the cell cycle during early *Xenopus* development. *Cell.* **37**:731-742.

Niehrs, C., Steinbeisser, H., and De Robertis, E.M. (1994). Mesodermal patterning by a gradient of the vertebrate homeobox gene *goosecoid*. *Science*. **263**:817-20.

Nieuwkoop, P.D., and Faber, J. (1994). Normal Table of *Xenopus laevis* (Daudin), Garland Publishing Inc., New York.

Nieuwkoop, P. D. (1969a). The formation of the mesoderm in urodelian amphibians. I. Induction by the endoderm. *Whilhelm. Roux's Arch. Entwicklungsmech. Org.* **162:**341-73.

Nieuwkoop, P. D. (1969b). The formation of the mesoderm in urodelian amphibians. II. The origin of the dorso-ventral polarity of the mesoderm. *Whilhelm. Roux's Arch. Entwicklungsmech. Org.* **163**:298-315.

Nieuwkoop, P. D., and Ubbels, G. A. (1972). The formation of mesoderm in urodelian amphibians. IV. Quantitative evidence for the purely "ectodermal" origin of the entire mesoderm and of the pharyngeal endoderm. *Roux's Arch.* **169**:185-99.

Oberhammer, F.A., Pavelka, M., Sharma, S., Tiefenbacher. R., Purchio, A.F., Bursch, W., and Schulte-Hermann, R. (1992). Induction of apoptosis in cultured hepatocytes and in regressing liver by transforming growth factor beta 1. *Proc. Natl. Acad. Sci. USA.* **89**:5408-12.

Ornitz, D.M., Xu, J., Colvin, J.S., McEwen, D.G., MacArthur, C.A., Coulier, F., Gao, G., and Goldfarb, M. (1996). Receptor specificity of the fibroblast growth factor family. *J. Biol. Chem.* **271**:15292-7.

Palecek, S.P., Loftus, J.C., Ginsberg, M.H., Lauffenburger, D.A., and Horwitz, A.F. (1997). Integrin-ligand binding properties govern cell migration speed through cell-substratum adhesiveness. *Nature*. **385**:537-540.

Papalopulu, N., and Kintner, C.R. (1994). Molecular genetics of neurulation. *Ciba. Found. Symp.* **181**:90-9.

Park, H.L., Bai, C., Platt, K.A., Matise, M.P., Beeghly, A., Hui, C.C., Nakashima, M., and Joyner, A.L. (2000). Mouse *Gli1* mutants are viable but have defects in *Shh* signaling in combination with a *Gli2* mutation. *Development.* **127**:1593-605.

Perkins, N.D., Felzien, L.K., Betts, J.C., Leung, K., Beach, D.H., Nabel, G.J. (1997). Regulation of NF-kappaB by cyclin-dependent kinases associated with the p300 coactivator. *Science*. **275**:523-7.

Popsueva, A.E., Luchinskaya, N.N., Ludwig, A.V., Zinovjeva, O.Y., Poteryaev, D.A., Feigelman, M.M., Ponomarev, M.B., Berekelya, L., and Belyavsky, A.V. (2001). Overexpression of *camello*, a member of a novel protein family, reduces blastomere adhesion and inhibits gastrulation in *Xenopus laevis*. *Dev. Biol.* **234**:483-496.

Pownall, M.E. (1994). More to patterning than Sonic hedgehog. *Bioessays*. **16**:381-3.

Rebbert, M.L., and Dawid, I.B. (1997). Transcriptional regulation of the *Xlim-1* gene by activin is mediated by an element in intron I. *Proc. Natl. Acad. Sci. USA*. **94**:9717-22.

Reifers, F., Bohli, H., Walsh, E.C., Crossley, P.H., Stainier, D.Y., and Brand, M. (1998). Fgf8 is mutated in zebrafish *acerebellar* (ace) mutants and is required for maintenance of midbrain-hindbrain boundary development and somitogenesis. *Development*. **125**:2381-95.

Richardson, J.C., Gatherer, D., and Woodland, H.R. (1995). Developmental effects of over-expression of normal and mutated forms of a *Xenopus* NF-kappa B homologue. *Mech. Dev*. **52**:165-77.

Roberts, W.M., Douglass, E.C., Peiper, S.C., Houghton, P.J., and Look, A.T. (1989). Amplification of the gli gene in childhood sarcomas. *Cancer Res*. **49**:5407-13.

Rowitch, D.H., Jacques, B.S., Lee, S.M., Flax, J. D., Snyder, E. Y., and McMahon. A. P. (1999). Sonic hedgehog regulates proliferation and inhibits differentiation of CNS precursor cells. *J. Neurosci*. **19**:8954-8965.

Salvesen, G., and Dixit, V. (1997). Caspases: intracellular signaling by proteolysis. *Cell*. **91**:443-446.

Sasai, Y., and De Robertis, E.M. (1997). Ectodermal patterning in vertebrate embryos. *Dev. Biol*. **182**:5-20.

Sasai, Y., Lu, B., Steinbeisser, H., Geissert, D., Gont, L.K., and De Robertis, EM. (1994). *Xenopus* chordin: a novel dorsalizing factor activated by organizer-specific homeobox genes. *Cell*. **79**:779-90.

Scharf, S.R., and Gerhart, J.C. (1980).Determination of the dorsal-ventral axis in eggs of *Xenopus laevis*: complete rescue of UV-impaired eggs by oblique orientation before first cleavage. *Dev. Biol.* **79**:181-98.

Schmidt-Ullrich, R., Aebischer, T., Hulsken, J., Birchmeier, W., Klemm, U., and Scheidereit, C. (2001). Requirement of NF-kappaB/Rel for the development of hair follicles and other epidermal appendices. *Development.* **128**:3843-53.

Schulte-Merker, S., Smith, J.C., and Dale, L. (1994). Effects of truncated activin and FGF receptors and of follistatin on the inducing activities of BVg1 and activin: does activin play a role in mesoderm induction? *EMBO J.* **13**:3533-41.

Sen, R., and Baltimore, D. (1986). Inducibility of the k immunoglobulin enhancer-binding protein NF-κB by a posttranslational mechanism. *Cell.* **47**:921–928.

Sha, W.C., Liou, H.C., Tuomanen, E.I., and Baltimore, D. (1995). Targeted disruption of the p50 subunit of NF-kappa B leads to multifocal defects in immune responses. *Cell.* **80**:321-30.

Shih, J., and Keller, R. (1992). Cell motility driving mediolateral intercalation in explants of *Xenopus laevis. Development.* **116**:901-914.

Shiokawa, K., Misumi, Y., Tashiro, K., Nakakura, N., Yamana, K., and Oh-uchida, M. (1989). Changes in the patterns of RNA synthesis in early embryogenesis of *Xenopus laevis. Cell Differ. Dev.* **28**:17-25.

Shiurba, R.A., Jing, N., Sakakura, T., and Godsave, S. F. (1991). Nuclear translocation of fibroblast growth factor during *Xenopus* mesoderm induction. *Development.* **113**: 487–494

Slack, J. M.W. (1984). Regional biosynthetic markers in the early amphibian embryo. *J. Embryol. Exp. Morphol.* **80**:289-319.

Slack, J.M. (1994). Inducing factors in *Xenopus* early embryos. *Curr.Biol. 4*:116-26.

Slack, J. M., and Smith, J. C. (1983). Dorsalization and neural induction: Properties of the organizer in *Xenopus laevis*. *J. Embryol. Exp. Morphol.* **78**, 299–317.

Slack, J.M., Darlington, B.G., Heath, J.K., and Godsave, S.F. (1987). Mesoderm induction in early *Xenopus* embryos by heparin-binding growth factors. *Nature.* **326**:197-200.

Slack, J.M., Isaacs, H.V., and Darlington, B.G. (1988). Inductive effects of fibroblast growth factor and lithium ion on *Xenopus* blastula ectoderm. *Development.* **103**:581-90.

Smith, J.C., Price, B.M., Van Nimmen, K., and Huylebroeck, D. (1990). Identification of a potent *Xenopus* mesoderm-inducing factor as a homologue of activin A. *Nature*. **345**:729-31.

Smith, W.C., and Harland, R.M. (1991). Injected *Xwnt-8* RNA acts early in *Xenopus* embryos to promote formation of a vegetal dorsalizing centre. *Cell*. **67**:753–766.

Smith, W.C., and Harland, R.M. (1992). Expression cloning of *noggin*, a new dorsalizing factor localized to the Spemann organizer in *Xenopus* embryos. *Cell.* **70**:829–840.

Smith, J.C. (1993). Mesoderm-inducing factors in early vertebrate development. *EMBO J.* **12**:4463-4470.

Smith, J.C., Price, B.M., Green, J.B., Weigel, D., and Herrmann, B.G. (1991). Expression of a *Xenopus* homolog of *Brachyury (T)* is an immediate-early response to mesoderm induction. *Cell*. **67**:79-87.

Smith, W.C., McKendry, R., Ribisi, S. Jr., and Harland, R.M. (1995). A *nodal*-related gene defines a physical and functional domain within the Spemann organizer. *Cell.* **82**:37-46.

Smith, W.C., and Kumano, G. (2000). FGF signaling restricts the primary blood islands to ventral mesoderm. *Dev. Biol.* **228**:304–314.

Snoeck, H.W., Weekx, S., Moulijn, A., Lardon, F., Lenjou, M., Nys, G., Van, Ranst. P.C., Van Bockstaele, D.R., and Berneman, Z.N. (1996). Tumour necrosis factor alpha is a potent synergistic factor for the proliferation of primitive human hematopoietic progenitor cells and induces resistance to transforming growth factor beta but not to interferon gamma. *J. Exp. Med.* **183**:705-10.

Sokol, S.Y. (1996). Analysis of *dishevelled* signalling pathways during *Xenopus* development. *Curr. Biol.* **6**:1456-1467.

Song, J., and Slack J. M. W. (1994). Spatial and temporal expression of basic fibroblast growth factor (FGF-2) mRNA and protein in early *Xenopus* development. *Mech. Dev.* **48**:141–151.

Sovak, M.A,, Bellas, R.E., Kim, D.W., Zanieski, G.J., Rogers, A.E., Traish, A.M., and Sonenshein, G.E. (1997). Aberrant NF-κB /Rel expression and the pathogenesis of breast cancer. *J. Clin. Investig.* **100**:2952–60.

Spemann, H., and Mangold, H. (1924). Induktion von Embryonanlagen durch Implantation artfremder Organisatoren. *Roux' Arch. f. Entw. mech.* **100**:599-638.

Stancheva, I., and Meehan, R.R. (2000). Transient depletion of xDnmt1 leads to premature gene activation in *Xenopus* embryos. *Genes Dev.* **14**: 313-327.

Stancheva, I., Hensey, C., and Meehan, R.R. (2001). Loss of the maintenance methyltransferase, xDnmt1, induces apoptosis in *Xenopus* embryos. *EMBO J.* **20**:1963-73.

Stewart, R.M., and Gerhart, J.C. (1990). The anterior extent of dorsal development of the *Xenopus* embryonic axis depends on the quantity of organizer in the late blastula. *Development.* **109**:363-72.

Sternberg, P.W., and Alberola-Ila, J. (1998). Conspiracy theory: RAS and RAF do not act alone. *Cell.* **95**:447-50.

Suzuki, K., Yamamoto, T., and Inoue, J. (1995). Molecular cloning of cDNA encoding the *Xenopus* homolog of mammalian RelB. *Nucleic Acids Res.* **23**:4664-9.

Suzuki, K., Tsuchida, J., Yamamoto, T., and Inoue, J. (1998). Identification and expression of the *Xenopus* homolog of mammalian p100-NFkappaB2. *Gene.* **206**:1-9.

Taira, M., Jamrich, M., Good, P. J., and Dawid, I. B. (1992). The Lim domain containing homeobox Lim1 is expressed specifically in the organizer region of *Xenopus* gastrula embryos. *Genes Dev.* **6**:356–366.

Takeda, K., Takeuchi, O., Tsujimura, T., Itami, S., Adachi, O., Kawai, T., Sanjo, H., Yoshikawa, K., Terada, N., and Akira, S. (1999). Limb and skin abnormalities in mice lacking IKKalpha. *Science.* **284**:313-6.

Tannahill, D., and Wardle, F.C. (1995). Control of axis formation in *Xenopus* by the NF-kappa B-I kappa B system. *Int. J. Dev. Biol.* **39**:549-58.

Thesleff, I., and Sharpe, P. (1997). Signalling networks regulating dental development. *Mech. Dev.* **67**:111-23.

Thompson, J. and Slack, J. M.W. (1992). Overexpression of fibroblast growth factors in *Xenopus* embryos. *Mech. Dev.* **38**: 175–182.

Thomsen. G., Woolf, T., Whitman, M., Sokol, S., Vaughn, J., and Vale, W. (1990) Activins are expressed early in *Xenopus* embryogenesis and can induce axial mesoderm and anterior structures. *Cell*. **63**:485–493.

Thornberry, N., and Lazebnik, Y. (1998). Caspases: enemies within. *Science*. **281**:1312-1316.

Tiedemann, H., Lottspeich, F., Davids, M., Knochel, S., Hoppe, P., and Tiedemann, H. (1992). The vegetalizing factor. A member of the evolutionarily highly conserved activin family. *FEBS Lett*. **300**:123–126.

Veenstra, G.J., Destree, O.H., and Wolffe, A.P. (1999). Translation of maternal TATA-binding protein mRNA potentiates basal but not activated transcription in *Xenopus* embryos at the midblastula transition. *Mol. Cell Biol*. **19**:7972-7982.

Verma, I.M., Stevenson, J.K., Schwarz, E.M., Van Antwerp, D., and Miyamoto, S. (1995). Rel/ NF-κB /IκB family: intimate tales of association and dissociation. *Genes Dev*. **9**:2723–2735.

Vodovotz, Y., Letterio, J.J., Geiser, A.G., Chesler, L., Roberts, A.B., and Sparrow, J. (1996). Control of nitric oxide production by endogenous TGF-beta1 and systemic nitric oxide in retinal pigment epithelial cells and peritoneal macrophages. *J. Leukoc. Biol*. **60**:261-70.

Wallace, V.A. (1999). Purkinje-cell-derived Sonic hedgehog regulates granule neuron precursor cell proliferation in the developing mouse cerebellum. *Curr. Biol*. **9**:445-448.

Wallingford, J.B. (1999). Tumours in tadpoles: the *Xenopus* embryo as a model system for the study of tumorigenesis. *Trends Genet*. **15**:385-8.

Wallingford, J.B., Seufert, D.W., Virta, V.C., and Vize, P.D. (1997). p53 activity is essential for normal development in *Xenopus*. *Curr. Biol*. **7**:747-57.

Wallingford, J.B., Rowning, B.A., Vogeli, K.M., Rothbacher, U., Fraser, S.E., and Harland, R.M. (2000). Dishevelled controls cell polarity during *Xenopus* gastrulation. *Nature*. **405**:81-85.

Wallingford, J.B., Ewald, A.J., Harland, R.M., and Fraser, S.E. (2001). Calcium signaling during convergent extension in *Xenopus*. *Curr. Biol*. **11**:652-61.

Wang, C.-Y., Mayo, M. W., Korneluk, R. C., Goeddel, D. V., and Baldwin, A. S. (1998). NF-kappaB antiapoptosis: induction of TRAF1 and TRAF2 and c-IAP1 and c-IAP2 to suppress caspase-8 activation. *Science*. **281**:1680-1683.

Watabe, T., Kim, S., Candia, A., Rothbacher, U., Hashimoto, C., Inoue, K., and Cho, K.W. (1995). Molecular mechanisms of Spemann's Organizer formation: conserved growth factor synergy between *Xenopus* and mouse. *Genes Dev.* **9**:3038-50.

Watanabe, M., and Whitman, M. (1999). FAST-1 is a key maternal effector of mesoderm inducers in the early *Xenopus* embryo. *Development.* **126**:5621-34.

Weber, H., Holewa, B., Jones, E.A., and Ryffel, G.U. (1996). Mesoderm and endoderm differentiation in animal cap explants: identification of the HNF4-binding site as an activin A responsive element in the *Xenopus* HNF1alpha promoter. *Development.* **122**:1975-84.

Wechsler-Reya, R. J., and Scott, M. P. (1999). Control of neuronal precursor proliferation in the *cerebellum* by Sonic hedgehog. *Neuron.* **22**:103-114.

Weih, F., Carrasco, D., Durham, S.K., Barton, D.S., Rizzo, C.A., Ryseck, R.P., Lira, S.A., and Bravo, R. (1995). Multiorgan inflammation and hematopoietic abnormalities in mice with a targeted disruption of *RelB*, a member of the NF-kappa B/Rel family. *Cell.* **80**:331-40.

Weinstein, D.C., and Hemmati-Brivanlou, A. (1999). Neural induction. *Annu. Rev. Cell Dev. Biol.* **15**:411–33.

Whiteside, S.T., Epinat, J.C. Rice, N.R., and Israel, A. (1997). Ikappa B epsilon, a novel member of the I kappa B family, controls RelA and cRel NF-kappa B activity. *EMBO J.* **16**:1413-1426.

Wilson, P., and Keller, R. (1991). Cell rearrangement during gastrulation of *Xenopus*: direct observation of cultured explants. *Development.* **112**:289-300.

Winklbauer, R. (1990). Mesodermal cell migration during *Xenopus* gastrulation. *Dev. Biol.* **142**:155-68.

Wolda, S.L., Moody, C.J. and Moon, R.T. (1993). Overlapping expression of Xwnt-3 and Xwnt- 1 in neural tissues of *Xenopus laevis* embryos. *Dev. Biol.* **155**:46–57.

Woodland, H.R., and Jones, E.A. (1987). The development of an assay to detect mRNAs that affect early development. *Development.* **101**:925-30.

Wolpert, L., Beddington, R., Brockes, J., Jessell, T., Lawrence, P. and Meyerowitz, E. (1998). Principles of development. Current Biology Ltd., London, U.K.

Wrana, J.L., Attisano, L., Wieser, R., Ventura, F., and Massague, J. (1994). Mechanism of activation of the TGF-beta receptor. *Nature.* **370**:341-7.

Wu, M., and Gerhart, J. (1991). Raising *Xenopus* at the laboratory. *Methods Cell biol.* **36**:3-18.

Wunnenberg-Stapleton, K., Blitz, I.L., Hashimoto, C., Cho, K.W. (1999). Involvement of the small GTPases XRhoA and XRnd1 in cell adhesion and head formation in early *Xenopus* development. *Development.* **126**:5339-5351.

Yang, S., Lockwood, A., Hollett, P., Ford, R., and Kao, K. (1998). Overexpression of a novel *Xenopus* Rel mRNA gene induces tumours in early embryos. *J. Biol. Chem.* **273**:13746-13752.

Yang, J., Tan, C., Darken, R.S., Wilson, P.A., and Klein, P.S. (2002). Beta-catenin/Tcf-regulated transcription prior to the midblastula transition. *Development.* **129**:5743-52.

Yasuda, G., and Schubiger, G. (1992). Temporal regulation in the early embryos: is MBT too good to be true? *Trends Genet.* **8**: 124-127.

Yeo, C.Y., Chen, X., Whitman, M. (1999). The role of FAST-1 and Smads in transcriptional regulation by activin during early *Xenopus* embryogenesis. *J Biol Chem.* **274**:26584-90.

Zandi, E., Rothwarf, D.M., Delhase, M., Hayakawa, M., and Karin, M. (1997). The IκB kinase complex (IKK) contains two kinase subunits, IKKα and IKKβ, necessary for IκB phosphorylation and NF-κB activation. *Cell.* **91**:243–252.

Zhong, Y., Brieher, W.M., and Gumbiner, B.M. (1999). Analysis of C-cadherin regulation during tissue morphogenesis with an activating antibody. *J. Cell Biol.* **144**:351-359.